Taxonomy, Palaeobiology, Palaeobiogeography and –ecology of the Eurasian Cenozoic giant salamanders (Cryptobranchidae, Lissamphibia)

Dissertation

der Mathematisch-Naturwissenschaftlichen Fakultät

der Eberhard Karls Universität Tübingen

zur Erlangung des Grades eines

Doktors der Naturwissenschaften

(Dr. rer. nat.)

vorgelegt von

Dipl. Biol. Davit Vasilyan

aus Eriwan / Armenien

Tübingen

2014

Tag der mündlichen Qualifikation:	30.07.2014
Dekan:	Prof. Dr. Wolfgang Rosenstiel
1. Berichterstatter:	Prof. Dr. Madelaine Böhme
2. Berichterstatter:	Prof. Dr. Hervé Bocherens

Table of contents

Abstract

The present thesis comprises new studies of both Recent and fossil Eurasian giant salamanders Cryptobranchidae, including systematics, different aspects of their biology, their palaeobiogeography and palaeoecology. Three living species and fossil material from over 50 localities from Cenozoic of Eurasia were studied. The dissertation details the osteological and anatomical features of cranial and postcranial skeletal elements of all fossil and Recent species, as well as suggest an osteological nomenclature for the family. Morphological and osteological characters were used to clarify the systematics of the group. Detailed osteological and morphological investigation of giant salamanders proposed a new phylogeny of the group. A new taxon, *Ukrainurus hypsognathus* gen. et sp. nov., has been described. This new taxon and the previously known species of the family Cryptobranchidae are grouped into a new clade, Pancryptobrancha nov. The monophyly of Asiatic and North American forms is demonstrated. The results suggest that Pancryptobrancha originated in Asia and dispersed to North America. The results revealed new data on biology – diet and food consumption, as well as degree of development of skull musculature (biting force). These very large salamanders (up to 2 m) have paedomorphic (*Andrias*, *Cryptobranchus*, *Zaissanurus*, *Ukrainurus*) or peramorphic (*Aviturus*) life history strategies and strictly aquatic or amphibious life style respectively. The development of *Aviturus* documents pronounced peramorphosis for the first time in a crown-group lissamphibian. Furthermore, fossil cryptobranchids are an excellent proxy for palaeoclimatic reconstructions. Their climatic space is best characterized by high humidity with mean annual precipitation values over 900 mm. The patchy stratigraphic distribution of the fossil record is explained by habitat tracking and/or range expansion from higher altitudes into lowland settings during humid periods with increased basinal relief. Here an altitudinal distribution model for dry/wet climates and low/high basinal relief is presented. It suggests that during the late Eocene, respectively late Oligocene to the Early Pliocene the giant salamanders were permanent residents of mountainous habitats of Central Asia and Central Europe (Altay Mountains, Alpine Orogene) but colonized lowland basins only during periods of significantly elevated humidity and groundwater-table, respectively increased basinal relief.

Zusammenfassung

Die vorliegende Arbeit umfasst neue Untersuchungen an rezenten und fossilen Eurasiatischen Riesensalamandern (Cryptobranchidae), insbesondere zu deren Systematik und zu verschiedenen Aspekten ihrer Biologie, Paläobiogeographie und Paläoökologie. Die drei rezente Arten und fossile Cryptobranchidae aus über 50 känozoischen Fundstellen Eurasiens wurden untersucht. Die osteologischen und anatomischen Merkmale der Schädel- und Postkranial-Elemente von allen fossilen und rezenten Arten wurden detailiert beschrieben und eine osteologische Nomenklatur für die Arten der Familie vorgeschlagen. Anhand von morphologischen und osteologischen Merkmalen ließ sich die Systematik der Gruppe klären und die verwandtschaftlichen Beziehungen innerhalb der Cryptobranchidae neu erstellen. *Ukrainurus hypsognathus* gen. et sp. nov. wird in der Arbeit beschrieben. Diese neue Salamander-Gattung wird zusammen mit bereits bekannten Arten der Familie Cryptobranchidae in einem neuen Kladum (*clade*), Pancryptobrancha nov., zusammengefasst. Die phylogenetische Analyse bestätigt die Monophylie der asiatischen und nordamerikanischen Arten. Die Ergebnisse lassen einen asiatischen Ursprung der Pancryptobrancha und ihre spätere Verbreitung nach Nordamerika wahrscheinlich erscheinen. Zusätzlich wurden neue Erkenntnisse zu ihrer Biologie, z.B. Ernährung und Ernährungserwerb, Grad der Entwicklung von Kopfmuskulatur (Schnappkraft), wurden gewonnen. Diese sehr großen Salamander, die 2 m Gesamtlänge erreichen konnten, haben in ihrer Ontogenie pädomorphe (*Andrias*, *Cryptobranchus*, *Zaissanurus*, *Ukrainurus*) oder peramorphe (*Aviturus*) Entwicklungsstrategien eingeschlagen und entsprechend streng aquatische oder amphibische/ semi-terrestrische Lebensweisen besessen. Die Gattung *Aviturus* belegt eine ausgeprägte Peramorphose erstmals innerhalb der Kronengruppe Lissamphibia. Paläo- bzw. bioklimatische Analysen ergaben des Weiteren, dass die Cryptobranchidae hervorragende Proxies für paläoklimatische Rekonstruktionen darstellen. Der klimatischer Bereich, in dem sowohl die rezenten als auch fossilen Vertreter lebten, ist durch höhere Feuchtigkeit mit einem durchschnittlichen Jahresniederschlagwert von minimal 900 mm charakterisiert. Ihre lückenhafte stratigrafische Verbreitung im fossilen Bericht Eurasiens wird durch „habitat tracking“ und / oder Ausbreitung des Areals vom Hochland ins Tiefland während Feuchtphasen mit erhöhtem Grundwasserspiegel erklärt. Es wird ein

Höhenverbreitungmodel für trockene/feuchte Klimate und niedrigem/hohem Grundwasserspiegel vorgeschlagen. Laut dem Model besiedelten die Riesensalamander vom späteren Eozän, resp. späteren Oligozän, bis zum frühen Pliozän permanent die höheren Gebirgsbereiche von Zentralasien und Mitteleuropa (Altai Gebirge, alpines Orogen) und siedelten sich in Tieflandbecken nur während der Perioden mit signifikanten Feuchtigkeitsanstieg und erhöhtem Grundwasserspiegel, bzw. Beckenrelief an.

1. General introduction

Giant salamanders have been known to humankind over many centuries. Since 1 millennium BC the extant salamanders had been mentioned and illustrated in the old Chinese and Japanese scripts and drawings, inspiring human imagination with stories and legends on unnatural creatures (Leu, 1999). The first reference to extinct cryptobranchid by Scheuchzer (1726), a follower of the flood myth, was erroneously considered as a man, a witness of the Deluge “Homo diluvii testis”. Over a century passed before this animal was recognized as a fossil relative of the Recent Asiatic giant salamanders. During this time period it has been assigned to different vertebrates. In 1763 the witness of the Deluge has been considered as a fossil catfish by a Hannoverian pharmacist – Johann Gerard Reinhard Andreae. Later in 1773 a Bernese naturalist – Gottlieb Siegmund Gruner assumed about a shark, in 1790 a Dutch anatomist – Petrus Camper considered it as a lizard. First in 19th century (Leu, 1999) the affinities of this fossils to amphibians has been suggested by a doctor and naturalist from Tübingen – Carl Heinrich Kielmeyer. The famous French palaeontologist George Cuvier using the comparative anatomical method of recognized the giants from Öhningen as salamander genus *Proteus* (Cuvier 1812) and then to axolotl (Cuvier 1817). Holl (1831) has described the Öhningen fossil under its present specific name *Salamandra scheuchzeri*. (Tschudi, 1837) named the fossils by their present generic name *Andrias scheuchzeri*. Noteworthy, the Recent representatives of the family have been discovered by the western scientists in 1802 (Sonnini and Latreille, 1802) – the American *Cryptobranchus* and in 1826 (Fitzinger, 1826) – the Asiatic *Andrias*. This is much later then the fossil giant salamanders had been recovered for scientists. In the beginning of 19th century, the Öhningen fossil and Recent giant salamanders have been finally recognized to belong to one family Cryptobranchidae (Temminck, 1836; Tschudi, 1837; Meyer, 1845).

1.2. Cryptobranchid biology and anatomy

Cryptobranchids represent a clade of the largest extant tailed amphibians that can reach up to 2 m total length. The tailed amphibians Caudata including news and salamanders represent the second largest group of the modern amphibians

Lissamphibia. They principally have holoarctic distribution and they are known since the Jurasic (Duellman and Trueb, 1994). All salamanders share a unique set of characters: maxilla and squamosal are not connected; frontal and parietal are not fused; atlas has a well-pronounced odontoid process, its lateral surfaces are represented by anterior cotyles, laterally from the odontoid process nearly flat anterior condyles build the second pair of the articulation surfaces, hence, the atlas has four articulation surfaces with the skull; transverse process of vertebra is bicapitate. Ontogentic trajectories with Caudata are very complex. During ontogeny from hatchlings to larva and finally adults characters change their states, so larval and adult states of many characters can be defined. Larval characters in caudats are considered presence of teeth and gills; not developed eyelid; curved, paralleling the maxillary row anteriorly shifted vomerine dentition, 3 or more ceratobranchial arcs (Mickoleit, 2004), absence of olfactory region in the cranial vault (Duellman and Trueb, 1994). Adult characters in caudats show the opposite state of these traits, e.g. lack of gills, developed eyelid, posteriorly directed and zickzag-shaped vomerine dentition, 2 ceratobranchial arcs (Mickoleit, 2004), developed olfactory region in the cranial vault (Duellman and Trueb, 1994).

Giant salamanders are closely related to Asiatic salamander Hynobiidae forming with them a suborder Cryptobranchoidea – a phylogenetically basal group among tailed amphibians (Pyron and Wiens, 2011). The monophyly of Cryptobranchoidea is supported by following apomorphies: unicapitate transverse process and ribs, reduction in the number of rib-bearing anterior caudal vertebrae reduced to two or three, hyobranchial und ceratobranchial of the first branchial arc are fused, the spinal nerve foramina in the trunk vertebra is absent (Duellman and Trueb, 1994; Gao and Shubin, 2003; Mickoleit, 2004). The basal position of Cryptobranchoidea within urodels is supported by following plesiomorphic characters: angular is not fused with prearticular; the dorsal process of the premaxillae are short and do not separate nasal medially, the second ceratobranchial and the ypsiloid cartilage are present, vertebra are amphicoelous (Duellman and Trueb, 1994; Mickoleit, 2004). As revealed by phylogenetic analysis of both mitochondrial and nuclear genes (Matsui et al., 2008; Pyron and Wiens, 2011), Cryptobranchidae is a monophyletic group including two separate living genera *Andrias* and *Cryptobranchus*. The family is considered monophyletic based of presence of following synapomorphic characters: lacrimals and septomaxillae are absent and

ontogenetic development is incomplete (including following “larval” characters – the vomerine teeth in a curved row parallel to the maxillary and premaxillary teeth, the eyelid is not developed).

Two species of the genus *Andrias* are found in eastern Asia, the Japanese *Andrias japonicus* (Temminck, 1836) and the Chinese *Andrias davidianus* (Blanchard, 1871). In Northern America only one species *Cryptobranchus alleganiensis* (Daudin, 1803) is known (Fig. 1) (Amphibiaweb, 2012). The Recent species are strictly aquatic amphibians that are today confined to clear, well-oxygenated, cold mountain streams and rivers. As aquatic amphibians, their skin serves as a respiratory organ, since gills are absent (in *Andrias*) and the reduced lungs are largely nonfunctional (Vitt and Caldwell, 2009). Along the lateral margins of the depressed body the skin surface is enlarged by an extensively folded and wrinkled flaps. Short limbs are massive and sturdy. The tail is laterally compressed and finlike. *Andrias* ssp. are thrice as large (total length ~2 m) as *Cr. alleganiensis* (~0.7 m). Giant salamanders are carnivorous (top predators) and feed on large variety of aquatic invertebrates and small vertebrates, by asymmetric suction feeding of the prey (Cundall et al., 1987; Sever, 2003; Vitt and Caldwell, 2009). The eggs are laid in paired, rosary-like strings, one from each oviduct, in depressions beneath stones in streams. Fertilization is external and females lack spermathecae in the cloaca. The males show paternal care by defending the oviposition sites (Nickerson and Mays, 1973; Sever, 2003).

Figure 1. Distribution areas (in red colour) of Recent giant salamanders **A** *Cr. alleganiensis,* **B** *An. davidianus*, and **C** *An. japonicus*

The cryptobranchid skull consists of paired bones, while only parasphenoid is unpaired. The naris is built of premaxilla, maxilla, nasal, and frontal in

Cryptobranchus, whereas in *Andrias* the frontal does not take part in naris. The septomaxillary and lacrimal bones are absent in both genera. The orbitae are large and framed by maxilla, prefrontal, orbitosphenoid, pterygoid, and parasphenoid. The lower jaw consists of three bones; long dentary, coronoid and articular. The upper jaw bears two parallel running anteriorly shifted curved dentition rows. The external row is located on maxilla and premaxilla, the internal on vomer (Fig. 2). The dentary is the only bone of the lower jaw bearing teeth (Estes, 1981; Sever, 2003). The dentition is monostichous, on the labial margins of dentigerous bones. The tooth

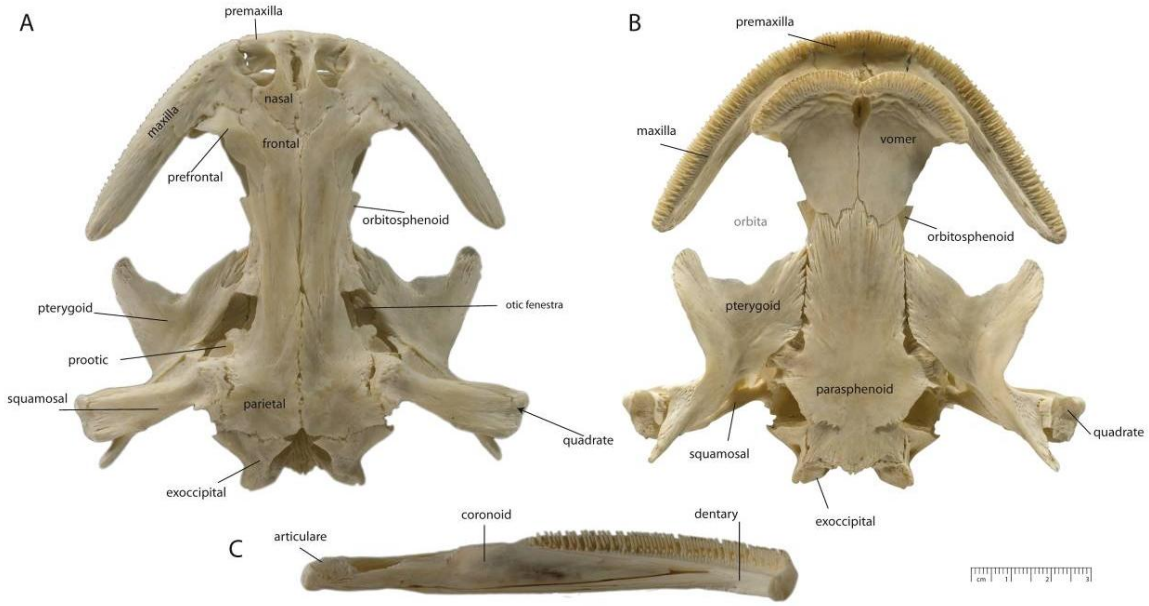

Figure 2. Skull of *An. davidianus* (ZFMK 90469) **A** from dorsal, **B** ventral, and **C** left lower jaw in lingual view. Abbr. ZFMK – Zoologisches Forschungsmuseum Koenig, Bonn, Germany.

pedicles are tall, the tooth crown is bicuspid, low and lingually curved (Greven and Clemen, 2009). The lingual cusp is dominant; it is higher and wider than the labial (secondary) cusp. This difference is less pronounced in *Cryptobranchus* than in *Andrias* (Greven and Clemen, 1980; Greven and Clemen, 2009). In giant salamanders the hyobranchial apparat is mainly cartilaginous. The adults of *Andrias* have two ossified elements – hyobranchial II and ceratobranchial II. In *Cryptobranchus*, in addition to these elements, the distal end of

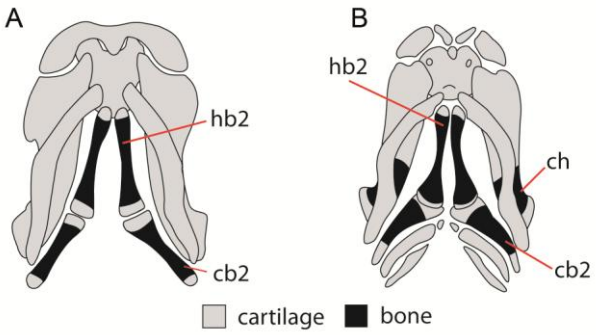

Figure 3. Hyobranchial apparat of adult **A** *An. japonicus* and **B** *Cr. alleganiensis*, redraws from (Rose, 2003). Abbr.: cb2 – ceratobranchial 2, ch – ceratohyal, hb2 – hyobranchial 2.

the ceratohyal is ossified (Rose, 2003). Apparently, the ceratohyals support the internal gills (Fig. 3).

The vertebra column consists of nearly the same number of vertebrae in the precaudal and caudal regions. So, in *An. davidianus* 21-22 precaudal and 20-23 caudal vertebrae (Westphal, 1958), in *An. japonicus* 21 and 24 (Siebold, 1838; according to the fig. 8), in *Cr. alleganiensis* 20 and 19-20 are correspondingly presented (Reese, 1906). The atlas has two elliptical articular condyles reaching the cranial end of one well-developed odontoid process.

Extanct cryptobranchids show paedomorphic characters, e.g. in adults the eyelid are not developed, a pair of gill slits in *Cryptobranchus*, the vomerine teeth lay in a curved row parallel to the praemaxillary and maxillary dentition (Duellman and Trueb, 1994). It is noteworthy, that in *Cryptobranchus* paedomorphic characters (e.g. presence of gills, smaller body size, strongly pronounced labial cusps on tooth crown etc.) are more pronounced than in *Andrias*.

1.3. Phylogeny and stratigraphic distribution of fossil giant salamanders

The clade Cryptobranchoidae (Cryptobranchidae + Hynobiidae) most probably existed since the Middle Jurassic. The divergence time of these sister families has been calibrated at Middle Jurassic with/by the appearance of *Chunerpeton tianyiensis* Gao, Shubin 2003 (Fig. 4) (Middle Jurassic, China; Gao and Shubin, 2003; Marjanović and Laurin, 2007). *Chunerpeton* is recognized as the oldest crown group salamanders and regarded as a member of Cryptobranchidae. However, Matsui et al. (2008; p. 324) suggested that apparently *Chunerpeton* is not a cryptobranchid, but might represent a linage leading to both Cryptobranchidae and Hynobiidae (Matsui et al., 2008; p. 324). The divergence rate within Cryptobranchidae calibrated with *Chunerpeton* ("Estimate II" acc. to Matsui et al., 2008) is as follows splitting of *Andrias* and *Cryptobranchus* at 70 Ma (Late Cretaceous), Japanese *An. japonicus* and Chinese *An. davidianus* at 51.4 Ma.

In Matsui et al. (2008) another (“Estimate 1”) divergence rates for Cryptobranchoidae has been suggested (by null hypothesis). The divergence time for Cryptobranchidae and Hynobiidae is estimated by 20.3 Ma (Early Miocene), Asiatic *Andrias* and American *Cryptobranchus* split at 13.4 Ma (Middle Miocene), Japanese and Chinese *Andrias* in Pliocene (4.3 Ma).

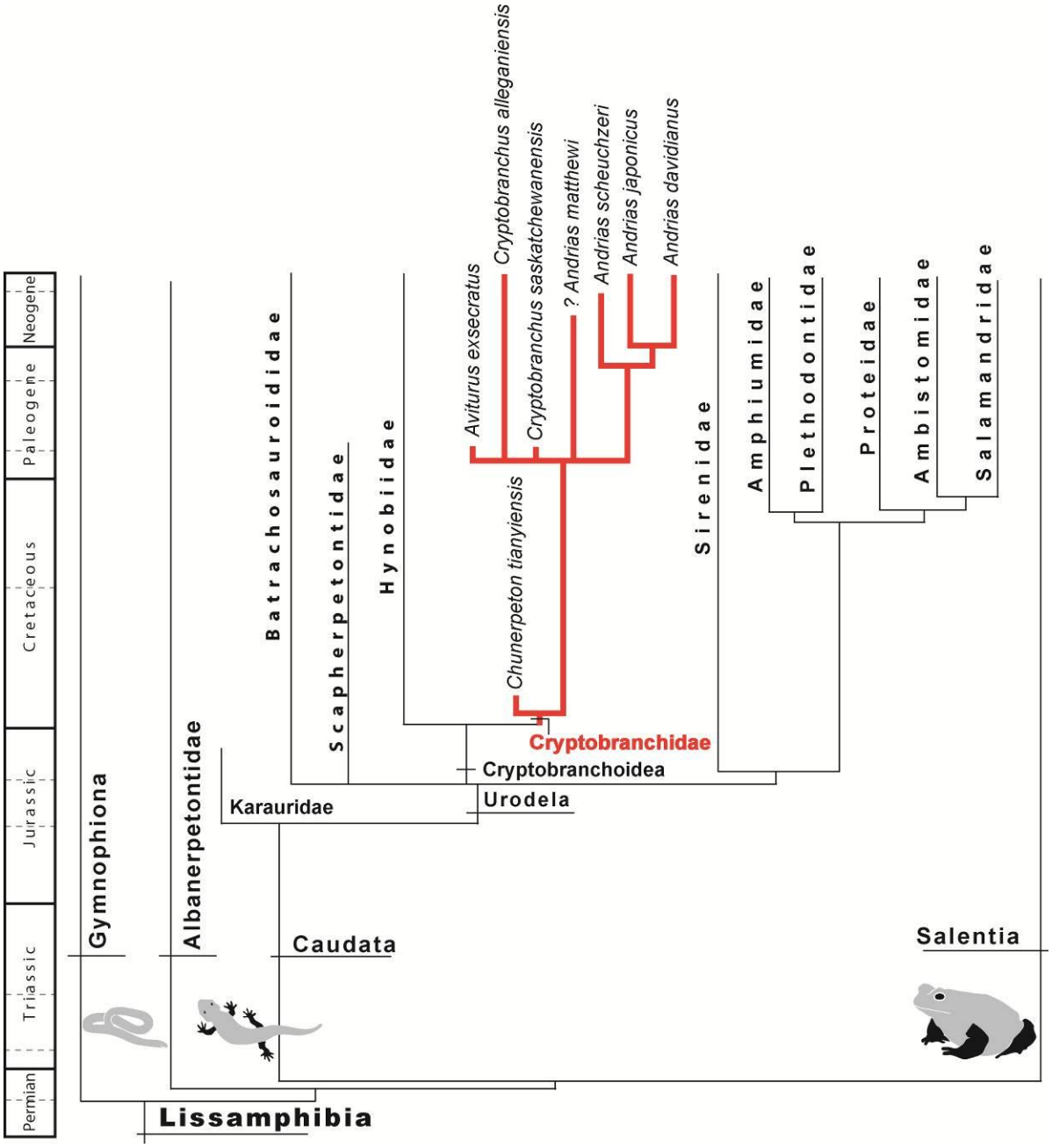

Figure 4. Phylogenetic relationships within lissamphibians with special focus on giant salamander record, redrawn from Marjanović and Laurin (2007).

Beside *Ch. tianyiensis,* two urodel taxa from the Mesozoic of Asia *Eoscaphertepon asiaticum* Nessov, 1981 and *Horezmia gracilis* Nessov, 1981 have also been referred to Cryptobranchidae (Skutschas, 2009). The oldest record of giant salamanders *Ch. tianyiensis* from China suggested that this group originated from Asia (Gao and Shubin, 2003). However, this hypothesis should be tested by the phylogenetic analysis with regard to Eurasian and North American Mesozoic and Cenozoic records as well as taking into consideration the (palaeo)biogeography of their sister family Hynobiidae.

Twelve fossil species ranging throughout the Cenozoic of Eurasia and North America are currently referred to Cryptobranchidae (Westphal, 1958; Chkhikvadze, 1982; Gubin, 1991; Böhme and Ilg, 2003; Gao and Shubin, 2003; Holman, 2006), but the validity of some taxa (e.g. *Zaissanurus beliajevae* Chernov, 1959, *Ulanurus fractus* Gubin, 1991, *Andrias karelcapeki* Chkhikvadze, 1982) is unclear and their phylogenetic affinities are poorly understood. In the fossil record, cryptobranchids are particularly well represented in the Cenozoic of Eurasia and at least 56 fossil localities are currently known (Böhme and Ilg, 2003).

The fossil giant salamander remains (*An. scheuchzeri*) are known since the 18th century from the world-renowned late Middle Miocene locality Öhningen (Upper Freshwater Molasse, North Alpine Foreland Basin [NAFB]) in southwestern Germany (Scheuchzer, 1726) (Fig. 5). The articulated complete or partial skeletons are embedded in laminated limestone. The preservation due to compaction and insufficient preparation of the material did not allow thorough and proper scientific study of 3D skeletal morphology over many decades. Nearly two centuries no other locality worldwide beside the Öhningen-site provided fossil bones of these animals. From the beginning of the 20th century through younger excavations in Central and Eastern Europe, especially in the NAFB disarticulated bone material of giant salamanders have been revealed (Westphal, 1958, 1967, 1970; Zerova, 1985; Böttcher, 1987). During the last decade extensive excavations in the deposites of the NAFB revealed more well-preserved, disarticulated and three dimensionally preserved fossil bone material, allowing detailed study and comparison of the skeletal elements of *An. scheuchzeri*.

Figure 5. *An. scheuchzei* (GPIT 1117/1-7) from the locality Öhningen. Courtesy of Wolfgang Gerber, University Tübingen. Abbr.: GPIT – Paläontologische Sammlung der Universität Tübingen, Tübingen, Germany. Scale bars 5 cm.

The first fossil cryptobranchid from Asian continent is known from the Late Eocene (Aksyr Formation) of the Zaysan Basin, eastern Kazakhstan (Chernov, 1959 [cit. Chkhikvadze, 1982]). The Paleogene record is referred to the species *Z.*

beliajevae, whereas a scarcely described *An. karelcapeki* is know from the sediments of the Akzhar Suite (Miocene), of the same basin (Chkhikvadze, 1982). Aside from the Zaysan Basin, in Asia giant salamander remains are also mentioned from the Late Oligocene of the Aral Basin, western Kazakhstan (Tleuberdina, 2005). Validity of those taxa was debated by (Böttcher, 1987) and Estes (1981). Here, they have been considered (based on description given in Chkhikvadze, 1982) as junior synonyms for *An*. *scheuchzeri*. However, both Kazakhian species need revision, redescription, and emending the diagnoses for validation of their systematic positions.

Further two species of giant salamanders *Aviturus exsecratus* Gubin, 1991 and *U*. *fractus* from Asia have been described by Gubin (1991). They are the oldest fossil cryptobranchids from Eurasia and represent the largest species among both fossil and Recent species. The fossil bones derive from the Naran Bulak Formation, Paleocene-Eocene transition (?), in South-Central Mongolia. Gubin (1991) suggested also new intrafamiliar systematic for Cryptobranchidae, including *Z*. *beliajevae*, *U*. *fractus*, *Av*. *exsecratus*, and North American *Cr. saskatchewanensis* Naylor, 1981, *Andrias matthewi* (Cook, 1917) into the subfamily Aviturinae and *Cr. alleganiensis*, *Andrias* ssp. into Cryptobranchinae.

The cryptobranchid fossil record from their present-day distribution area in East Asia starts at the Early Pliocene and is so far restricted to Japan. Only one species *Andrias* sp. is known from the Pliocene (Tsubusagawa Formation) of Japan and is considered to be specifically distinct from two extant *Andrias* species and may represent a new species (Matsui et al., 2001). Giant salamanders are lacking in the Cenozoic fossil record of China as well as in pre-Pliocene sediments of Japan.

In general, data on palaeobiology and palaeoecology of giant salamanders are scarce or entirely missing. Numerous known features of Recent giant salamanders (e.g. asymmetric mandible movement during food consumption, head musculature, ontogenetic trajectory) are still not documented for fossil species and need further verifications and studies. Since, till now no essential morphological and osteological differences between fossil and Recent species have been documented earlier, it was accepted that fossil cryptobranchids do not differ significantly from the morphology, biology and ecology of their living forms. Tooth morphology (Böttcher, 1987) and hyoid apparat (Westphal, 1958) in *An*. *scheuchzeri* suggested the same degree of ontogenetic development of this species as the Recent *Andrias*. Only for *Av*.

exsecratus a non-typical ecology as “an active periaquatic and shoreline predator” was proposed by Gubin (1991) based on peculiarities of the axial skeleton structure, longer limb, and a higher skull (Gubin, 1991).

Cryptobranchidae, as a phylogenetically basal group among tailed amphibians, represents an exceptional research opportunity with both derived (giant sizes, paedomorphic life history strategy, strict aquatic lifestyle) and ancestral traits (amphicoelous vertebrae, angular in not fused with prearticular) to learn more about the basal salamanders. The understanding of their biology and phylogeny, based on both fossil and Recent records, will enlarge our knowledge on origin, radiation and evolution of the early caudats as well as diversity of ontogeny in early salamanders. This dissertation is trying to fill the gap of this knowledge.

2. Objectives and Output

This thesis addresses questions in current palaeontological research on Eurasian Cenozoic giant salamanders summarized above and with particular focus on study of their systematics, palaeobiology, palaeobiogeography, and –ecology using new available material and research approaches applying first time on this group.

The goals of the present work are:

- Critical revision of giant salamander fossil record. Systematic study of morphology and osteology of both fossil and Recent giant salamanders and verification of species validity based on collection-based studies of newly recovered as well as already described fossil material and literature sources.
- Analysis of phylogenetic relationships among cryptobranchid species and revision the extra- and intrafamiliar relationships proposed by earlier studies. Providing a new insight into the origin and palaeobiogeography of the group.
- Understand stratigraphic distribution during the Eurasian Cenozoic. Proof the palaeoecological adaptations and palaeoclimatic significance of the fossil Cryptobranchidae.
- Enlarging the knowledge regarding biology (e.g. head musculature, food consumption, body kinetics) of fossil cryptobranchids including reconstruction of lifestyle and life history strategies based on bone material.

Structure of the thesis

The research presented within this dissertation covers a wide range of palaeontological studies, including classical description of morphology and osteology, phylogenetic analysis, reconstruction of musculature, feeding, and life history strategies, palaeoclimatic analysis etc. These topics are introduced and organized in the following order:

Paper # 1 presents morphological and osteological description, taxonomic revision and phylogenetic relationships of giant salamanders,

Paper # 2 demonstrates the diversity of their life history strategies and lifestyles,

Paper # 3 presents the palaeoclimatic significance of the group and proposes a model explaining their patchy temporal and spatial distribution during Cenozoic of Eurasia.

3. The papers included in the thesis

3.1. Vasilyan, D., Böhme, M., Chkhikvadze, V. M., Semenov Y. A., Joyce W.G. 2013. A new giant salamander (Urodela, Pancryptobrancha) from the Miocene of Eastern Europe (Grytsiv, Ukraine). Journal of Vertebrate Paleontology 33(2): 301-318, doi:10.1080/02724634.2013.722151

3.2. Vasilyan D., Böhme M. 2012: Pronounced Peramorphosis in Lissamphibians—*Aviturus exsecratus* (Urodela, Cryptobranchidae) from the Paleocene–Eocene Thermal Maximum of Mongolia. PLOSOne 7(9): e40665.

3.3. Böhme M., Vasilyan D., Winklhofer M. 2012. Habitat tracking, range dynamics and palaeoclimatic significance of Eurasian giant salamanders (Cryptobranchidae) — indications for elevated Central Asian humidity during Cenozoic global warm periods. Palaeogeography, Palaeoclimatology, Palaeoecology 342-343: 64-72, doi:10.1016/j.palaeo.2012.04.032.

3.1. Paper # 1: A new giant salamander (Urodela, Pancryptobrancha) from the Miocene of Eastern Europe (Grytsiv, Ukraine)

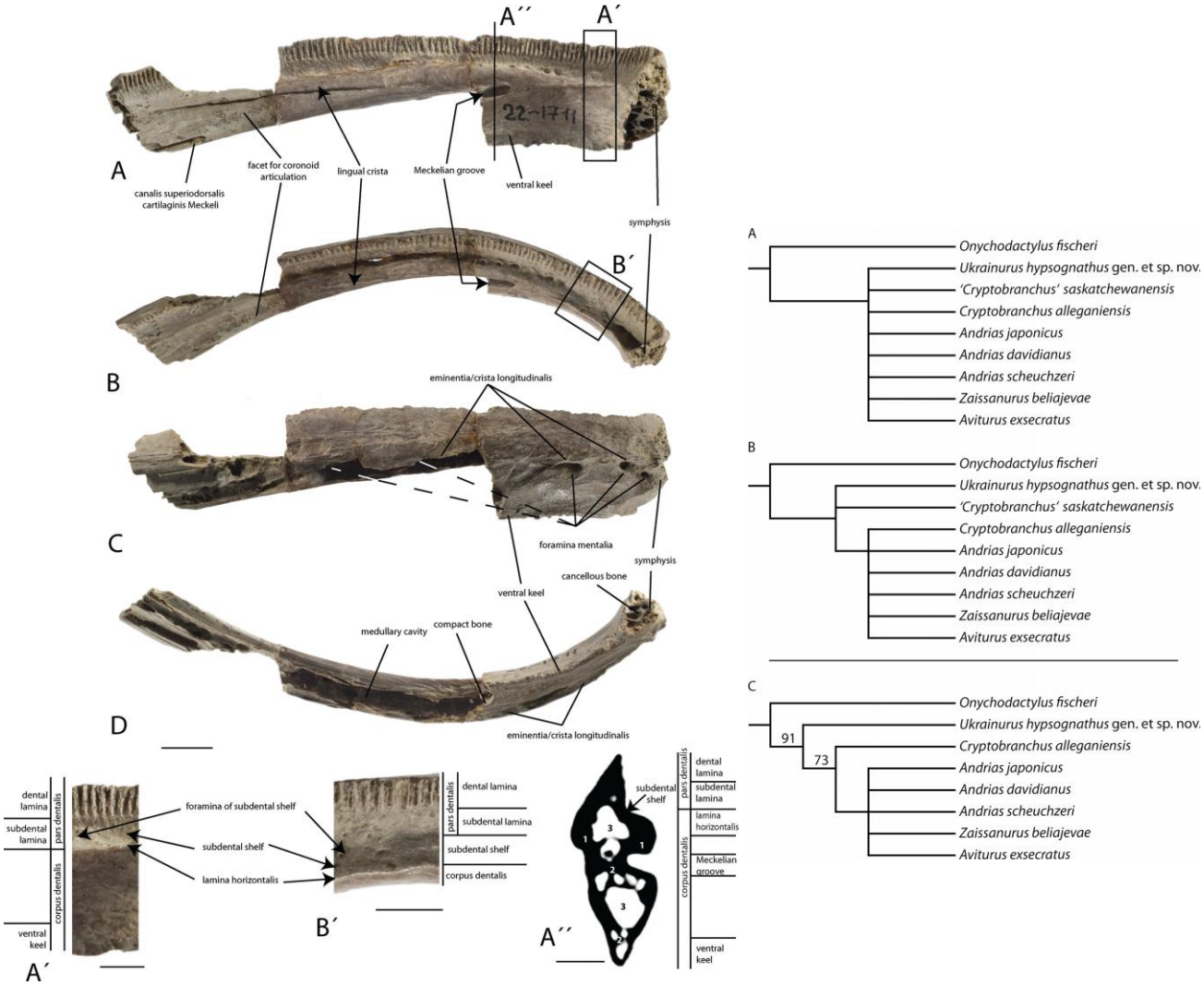

Own contribution:

Scientific ideas (%)	80
Data generation (%)	95
Analysis and Interpretation (%)	85
Paper writing (%)	80

Journal of Vertebrate Paleontology 33(2):301–318, March 2013

ARTICLE

A NEW GIANT SALAMANDER (URODELA, PANCRYPTOBRANCHA) FROM THE MIOCENE OF EASTERN EUROPE (GRYTSIV, UKRAINE)

DAVIT VASILYAN,*[,1] MADELAINE BÖHME,[1,2] VIACHESLAV M. CHKHIKVADZE,[3] YURIY A. SEMENOV,[4] and WALTER G. JOYCE[1]

[1]Department of Geosciences, Eberhard-Karls-University Tübingen, Sigwartstraße 10, 72076 Tübingen, Germany, davit.vasilyan@ifg.uni-tuebingen.de; walter.joyce@uni-tuebingen.de;

[2]Senckenberg Center for Human Evolution and Palaeoecology, Sigwartstraße 10, 72076 Tübingen, Germany, m.boehme@ifg.uni-tuebingen.de;

[3]Institute of Paleobiology, Georgian National Museum, Niagvari str. 4, 0108 Tbilisi, Georgia, chelydrasia@gmail.com;

[4]National Museum of Natural History, National Academy of Sciences of Ukraine, Bogdan Khmelnytski str. 15, 01601, Kiev, Ukraine, yuriy_semenov@mail.ru

ABSTRACT—We present new and well-preserved giant salamander material from the Miocene of the Grytsiv locality, Ukraine. Disarticulated skull and postcranial bones from two individuals are described as a new taxon, *Ukrainurus hypsognathus*, gen. et sp. nov. *U. hypsognathus* is characterized by poorly ossified bone tissues, relatively inflexible mandibles, a high dentary, a crista on the lingual surface of the dentary, a pars dentalis of the dentary that is composed of a dental lamina and a subdental surface, presence of an eminentia dorsalis on the squamosal, a broad pericondylar facet on the occipital, extremely elongated prezygapophyses, and hemal processes with an elongate, oval base. Moreover, *U. hypsognathus* shows evidence of strong mandibular levator muscles that indicate great biting force. A phylogenetic analysis of all well-understood Tertiary and Recent giant salamanders recovers a monophyletic group of Asian and North American cryptobranchids, but places *U. hypsognathus* outside crown group Cryptobranchidae. This result suggests that Cryptobranchidae originated in Asia and dispersed to North America. The oldest representative of crown Cryptobranchidae is *Aviturus exsecratus* from the terminal Paleocene of the Nemegt Basin, Mongolia.

SUPPLEMENTAL DATA—Supplemental materials are available for this article for free at www.tandfonline.com/UJVP

INTRODUCTION

Cryptobranchids (giant salamanders) represent a clade of large salamanders that can reach over 1.5 m in total length. They are strictly aquatic amphibians that are today confined to clear, well-oxygenated, cold mountain streams and rivers (Vitt and Caldwell, 2009). Twelve species ranging throughout the Tertiary are currently referred to Cryptobranchidae (Westphal, 1958; Chkhikvadze, 1982; Gubin, 1991; Böhme and Ilg, 2003; Gao and Shubin, 2003; Holman, 2006), but the taxonomic validity of some taxa (e.g., *Ulanurus fractus* Gubin, 1991) is unclear and their phylogenetic affinities are poorly understood. Three poorly understood taxa from the Mesozoic of Asia (*Chunerpeton tianyiensis* Gao and Shubin, 2003*, Eoscaphertepon asiaticum* Nessov, 1981, and *Horezmia gracilis* Nessov, 1981) have also been referred to Cryptobranchidae, but it is clear that these animals are representatives of the cryptobranchid stem lineage at best (see Discussion). In the fossil record, cryptobranchids are particularly well represented in the Cenozoic of Eurasia and at least 56 fossil localities are currently known (Böhme and Ilg, 2003). All Neogene Eurasian fossils have been attributed to the Recent genus *Andrias*, but only one species, *Andrias scheuchzeri* (Holl, 1831), is well documented (Westphal, 1958). The majority of occurrences are from Central Europe and little is known about cryptobranchids from Eastern Europe. Here we describe a considerable collection of bones of two giant salamander individuals collected by Y. A. Semenov and W. M. Chkhikvadze from the Ukrainian locality Grytsiv. The larger individual was collected during the 1987 field season, the smaller individual during the 1988 field season. The purpose of this contribution is to describe the new material as a new taxon and to analyze, for the first time, the phylogenetic relationships of fossil and Recent giant salamanders.

GEOLOGICAL OVERVIEW

The Grytsiv locality (Fig. 1) is situated in the western part of Ukraine (Shepetovka Rayon), 240 km west of Kiev. The outcrop represents an abandoned limestone quarry along the Khoroma River, 1.5–2 km west of the village of Grytsiv (coordinates: 49.96°N, 27.21°E). The section is up to 12 m thick and comprises a sequence of greenish silts and biogenic algal reef carbonates, situated over a granitic basement (Korotkevich et al., 1985; Topachevskij et al., 1996). Both marine facies contain an early Bessarabian mollusk fauna, including *Sarmatimactra vitaliana*, *Venerupis ponderosus*, and *Obsoletiforma obsoleta vindobonensis* (Korotkevich et al., 1985; Korotkevich, 1988). These sediments represent one of the northernmost outcrops of the early Bessarabian transgression (Novomoskovsky horizon of Didkovsky, 1964) onto the Ukrainian shield (Pevzner and Vangengeim, 1993). The carbonates are overlain in this region by greenish clays that contain the same early Bessarabian mollusk fauna. These clays are also preserved in karstic fissures and holes within the reef carbonate, indicating their formation under terrestrial conditions during a sea-level lowstand. The greenish clays contain an exceptionally well preserved, rich, and diverse vertebrate assemblage, including partial skeletons. On top of

*Corresponding author.

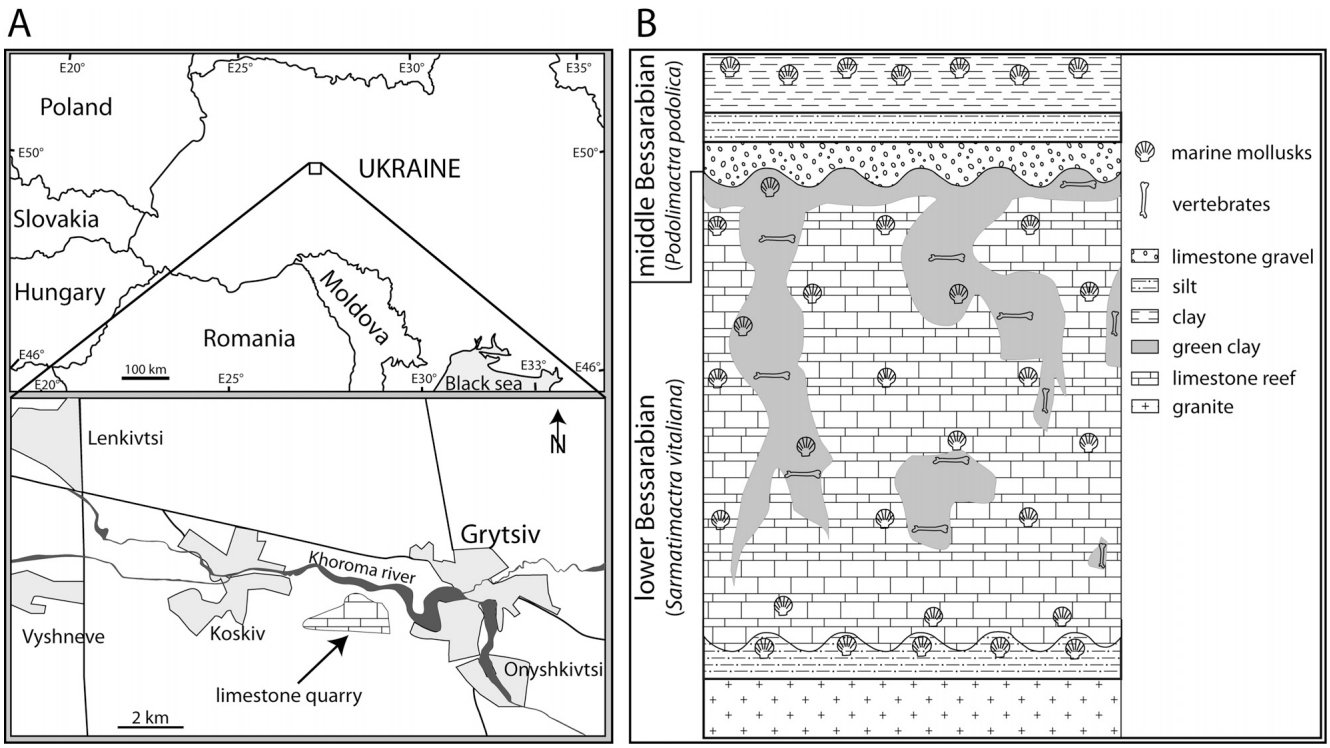

FIGURE 1. **A**, map of Ukraine showing the location of the limestone quarry near Grytsiv; **B**, geological profile at Grytsiv, redrawn from Korotkevich (1988) and Topachevskij et al. (1996).

this level follows a transgressive horizon composed of reworked carbonates, which, in return, is succeeded by more clays and siltstones indicating the next sea-level highstand. The mollusk fauna of this second cycle contain *Podolimactra podolica*, indicative of a middle to late Bessarabian age (Topachevskij et al., 1996).

The sediments that contain the vertebrate fauna are confined to the latest part of the early Bessarabian (*Sarmatimactra vitaliana pallasi* interval zone of Kojumdgieva et al., 1989) near the early–middle Bessarabian boundary. Based on mollusks, the early Bassarabian of the Eastern Paratethys can be correlated to the late Sarmatian of the Central Paratethys (Rögl, 1998; Harzhauser and Piller, 2004), which in return correlates to the late Serravallian (latest middle Miocene). The reverse magnetic polarity of the greenish clay (Chepalyga et al., 1985) furthermore enables a correlation with magnetic chron C5r (12.014 to 11.040 Ma according to Lourens et al., 2004). This agrees with an early Vallesian biostratigraphic age of the fauna, characterized by the first appearance date of the horse *Hippotherium* (in Grytsiv with *H. primigenium* and *H.* sp.; Krakhmalnaya, 1996). The Grytsiv fauna is older than the Moldovan faunas of Kalfa and Buzhor 1 (Nesin and Nadachowski, 2001; contra Vangengeim et al., 2006), which both contain late middle Bessarabian sediments (Vasilievsky horizon of Didkovsky, 1964; below and within horizons with *Plicatiforma fittoni*, *Podolimactra podolica*, and *Sarmatimactra fabreana*; Roshka, 1967; Lungu, 1978, 1981) that correspond to the lower part of the *Plicatiformis fittoni fittoni* range zone of Kojumdgieva et al. (1989).

MATERIALS AND METHODS

The bones of each specimen (a large one and a small one) of *Ukrainurus hypsognathus* described here were found in two separate fossiliferous pockets. In each batch, bones are from animals of comparable size and the bones do not duplicate each other. However, because the bones were not found articulated, we prefer to erect the new species based on the left dentary only.

All Grytsiv fossils are deposited in the National Museum of Natural History (National Academy of Sciences), Kiev, Ukraine. For comparison, the following specimens of Recent cryptobranchoids were considered: *Andrias japonicus* (Temminck, 1836) (NMA, unnumbered specimen; SMNS 7898:1–15; ZIT 240; ZMB 9928), *Andrias davidianus* (Blanchard, 1871) (SMF 89293; ZFMK 76996, 90469), *Andrias* sp. (SMF 69133), *Cryptobranchus alleganiensis* (Daudin, 1803) (ZFMK 5245; SMNK 201; SMNK uncataloged), and *Onychodactylus fischeri* (Boulenger, 1886) (GPIT/RE/7331). Our observations of the fossil taxon *Andrias scheuchzeri* from the North Alpine Foreland Basin of Europe are based on NMA-2009-1/2076-11/2076, NMA-2009-26/2076, NMA-2010-221/2076-232/2050, NMA-2/2076, NMA-346/1633, SMNS 55314, GPIT/AM/717, CGPUJ 201.104, CGPUJ 201.105, SMNK-PAL.6612-6618, PIMUZ A II 1, and PIMUZ A II 2; those of *Zaissanurus beliajevae* Chernov, 1959, from the Paleogene of the Zaisan Basin are based on PIN 416-1, IP ZSN-KKS-2, IP ZSN-K-11, IP ZSN-K-14, IP ZSN-K-15, IP ZSN-Y-9; those of *Ulanurus fractus* from the Paleogene of the Nemegt Basin are based on PIN 4357/27 and PIN 4358/2; and those of *Salamandrella* sp. from the late Miocene of Ertemte 2, China, are based on an unnumbered GPIT specimen. Our observations on *Aviturus exsecratus* Gubin, 1991, from the Paleogene of the Nemegt Basin are based on the description of Gubin (1991) and those of '*Cryptobranchus*' *saskatchewanensis* (Naylor, 1981) are based on the description of Naylor (1981). Because we were not able to observe relevant material of '*C.*' *saskatchewanensis* in person, we regard the generic identity of this species as uncertain.

The terminology used to describe the individual bones and their features is based, where possible, on Osawa (1902), Francis (1934), Cundall et al. (1987), Duellman and Trueb (1994), Elwood and Cundall (1994), Gardner (2003), and Skutschas

(2009). The nomenclature of muscles follows that of Elwood and Cundall (1994).

Dentary cross-sections of *Ukrainurus hypsognathus*, gen. et sp. nov., *An. scheuchzeri*, and *An. davidianus* were made using a Siemens X-ray computer tomography (CT) scanner at the Department of Radiology of the University of Tübingen, Germany. Natural cross-sections of *Z. beliajevae* were drawn using the software Adobe Illustrator. Bone compactness was estimated using the software program Bone Profiler 2010 (Girondot and Laurin, 2003).

Cross-sections of the dentary were studied at the following positions: (1) at the narrowest point between the symphysis and the Meckelian groove; (2) behind the beginning of the Meckelian groove; (3) halfway between the anterior limit of the Meckelian groove and the posterior end of the dental lamina; and (4) at the posterior-most part of the dental lamina.

Institutional Abbreviations—**CGPUJ**, Collection Geology and Palaeontology, Universalmuseum Joanneum, Graz, Austria; **GPIT**, Institut für Geowissenschaften, Universität Tübingen, Tübingen, Germany; **IP**, Institute of Paleobiology, National Museum of Georgia, Tbilisi, Georgia; **NHMUK**, Department of Zoology, Natural History Museum, London, U.K.; **NMA**, Naturmuseum Augsburg, Augsburg, Germany; **NMNHK**, National Museum of Natural History, Kiev, Ukraine; **PIMUZ**, Paläontologisches Institut und Museum der Universtität Zürich, Zurich, Switzerland; **PIN**, Paleontological Institute, Russian Academy of Sciences, Moscow, Russia; **SMF**, Senckenberg Naturmuseum, Frankfurt am Main, Germany; **SMNK**, Staatliches Museum für Naturkunde, Karlsruhe, Germany; **SMNS**, Staatliches Museum für Naturkunde, Stuttgart, Germany; **ZFMK**, Zoologisches Forschungsmuseum Koenig, Bonn, Germany; **ZIT**, Institute of Zoology, University of Tübingen, Tübingen, Germany.

SYSTEMATIC PALEONTOLOGY

AMPHIBIA Linnaeus, 1758
LISSAMPHIBIA Haeckel, 1866
CAUDATA Scopoli, 1777
PANCRYPTOBRANCHA, clade nov.

Diagnosis—Representatives of Pancryptobrancha can be diagnosed by (numbers in parentheses refer to the character matrix used herein): the presence of unicapitate trunk ribs (32); large body size (33); and a contact between the parietal and the squamosal (34).

Currently Hypothesized Content—Pancryptobrancha is currently hypothesized to include *Ukrainurus hypsognathus*, sp. nov., and Cryptobranchidae.

Comments—Our phylogenetic analysis (see below) reveals that the new fossil taxon is sister to the clade formed by extant cryptobranchids and we therefore must distinguish between total group (stem group) and crown group Cryptobranchidae. We herein follow the wide spread convention (Joyce et al., 2004) and use the historical term 'Cryptobranchidae' to refer to the crown group and coin the new term Pancryptobrancha for the total group.

UKRAINURUS, gen. nov.

Type Species—*Ukrainurus hypsognathus*, sp. nov.

Diagnosis—Same as for the type species.

Etymology—The generic name alludes to the country of origin (Ukraine) and '-urus' (ουρά), Greek for tail.

UKRAINURUS HYPSOGNATHUS, sp. nov.
(Figs. 2–8)

Holotype—NMNHK 22-1711, a left dentary.

Paratypes—All bones assigned to the larger of the two available individuals: left and right articulars (NMNHK 22-1711ar-a and NMNHK 22-1711ar-b); right coronoid (NMNHK 22-1711c); left and right squamosals (NMNHK 22-1711sq-a and NMNHK 22-1711sq-b); left and right quadrates (NMNHK 22-1711q-a and NMNHK 22-1711q-b); left orbitosphenoid (NMNHK 22-1711os); left occipital (NMNHK 22-1711oc); right femur (NMNHK 22-1707); six ribs (NMNHK 22-1707a); two terminal phalanges (NMNHK 22-1711f); and six trunk vertebrae (NMNHK 22-1698, NMNHK 22-1699, NMNHK 22-1704, NMNHK 22-1705, NMNHK 22-1706, NMNHK 22-1706a). The smaller of the two available individuals, consisting of nine trunk vertebrae (NMNHK 22-1706b, NMNHK 22-1706c, NMNHK 22-1706d, NMNHK 22-1706-88a, NMNHK 22-1706-88b, NMNHK 22-1706-88c, NMNHK 22-1706-88d, NMNHK 22-1706-88e, NMNHK 22-1706-88f); a pterygapophysis (NMNHK 22-1706f); and one caudal vertebra (NMNHK 22-1706e).

Type Locality—An abandoned quarry 1.5–2 km southeast of the village of Grytsiv (also Gritsev), Shepetivskyi Rayon, Ukraine.

Type Horizon—Karstic fissure fills in early Bessarabian reef limestones.

Stratigraphy—Middle to late Miocene transition (early to late Bessarabian transition), magnetochron C5r, mammal 'zone' MN9 (Topachevskij et al., 1996).

Diagnosis—The new taxon can be diagnosed as a representative of Pancryptobrancha based on the following list of characters (numbers in parentheses refer to the character matrix used herein): trunk ribs unicapitate (32); body size large (33); and parietal and squamosal in contact with one another (34). The following list of characters are unambiguous apomorphies of the new taxon within Pancryptobrancha: symphysis elongated and elliptical (1); triangular ventral space between the dentaries is small (2); sculpture of the dermal ossification on labial side of dentary is rugose to pustular and pointed (3); lingual crista on dentary present (4); ventral keel prolonged (6); pars dentalis subdivided into a dental and subdental lamina (7); mental foramina large, longitudinal flange pronounced (9); labioventral facet of articular broad and sculptured with highly prominent pits and ridges (14); pericondylar facet of occipital broad (19); squamosal robust (20); eminentia dorsalis present (21); paries posterior high (22); paries posterior runs along paries dorsal with an obtuse angle (23); beginning of hemal process oval (27); hemal processes positioned at the posterior portion of vertebral centrum (28); arterial canal in caudal vertebrae broad, with large foramen (29); terminal phalanges slender, with bulbous tips (30); and degree of ossification of the dentary low (bone compactness value >0.8) (31). The new taxon is furthermore diagnosed by one ambiguous apomorphy, which is homoplastic with *Andrias scheuchzeri*: coronoid process broad (17).

Etymology—The specific name derives from a characteristic feature of this animal, its high dentary: in Greek 'hypso' (υψηλός), high, and '-gnathos' (γνάθος), jaw bone.

DESCRIPTION

Skull

Dentary—The dentary (NMNHK 22-1711) is long, high, and strongly compressed labiolingually (Fig. 2). The length of the dentary is 110.8 mm between the posterior and anterior tips and 121.25 mm along the labial surface. The height of the dentary near the symphysis is 21.2 mm. The posteroventral half of the bone, under the Meckelian groove, is absent. The depth of the pars dentalis is less than half of the depth of the corpus dentalis.

The symphysis is not well preserved; only the labial part is present. From what is available, we nevertheless speculate that it was elliptical in outline. The symphyseal surfaces are almost smooth along their margins but become rugose towards their center. The (inter)mandibular joint is formed by the posterior part of the symphysis. The posterior part slopes ventrolaterally

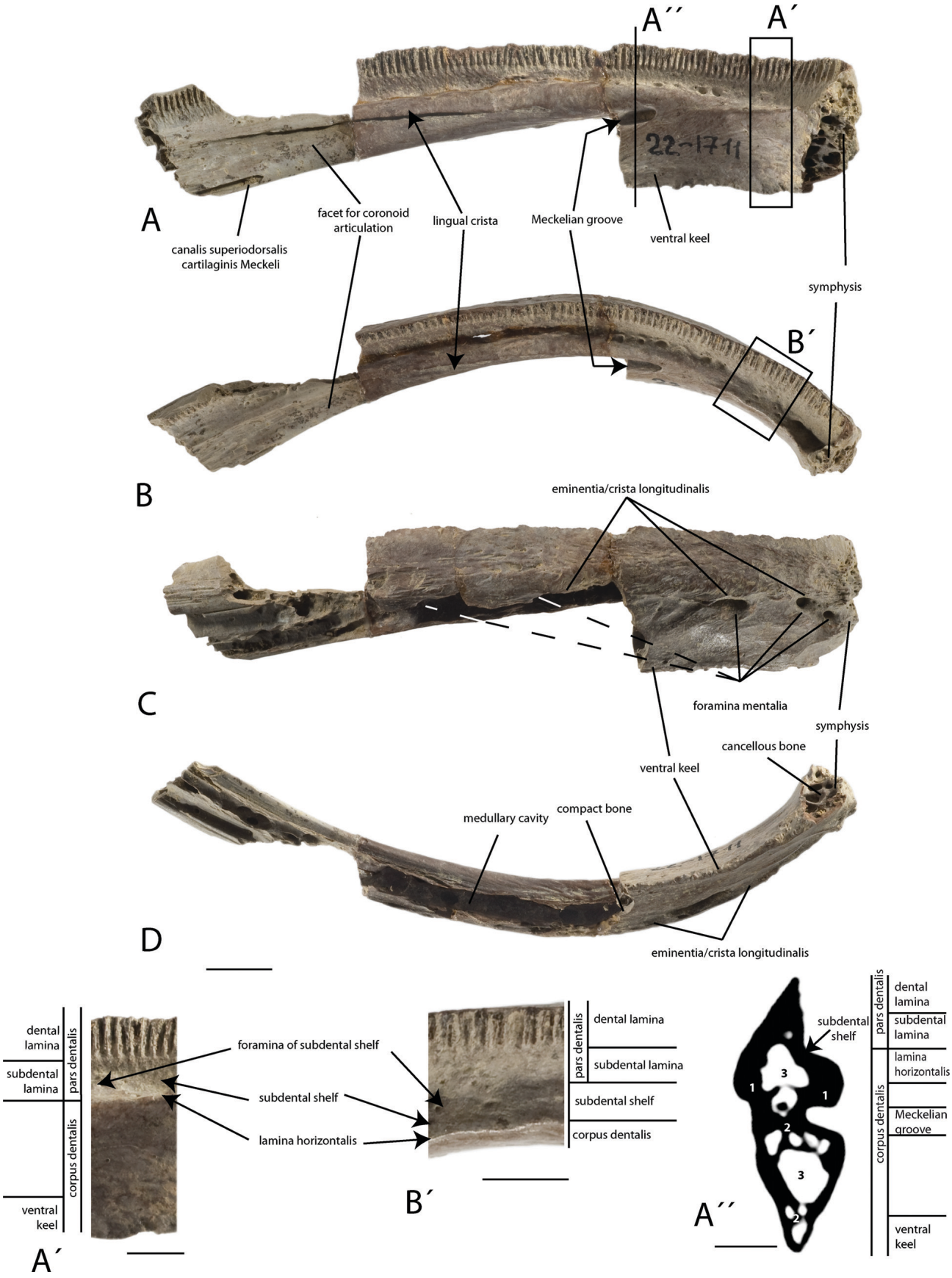

FIGURE 2. Dentary (NMNHK 22-1711) of *Ukrainurus hypsognathus*, gen. et sp. nov. **A**, **A′**, lingual views, **A″**, cross-section behind the anterior limit of the Meckelian groove made by CT (**1**, cortical and **2**, cancellous bones; **3**, medullary cavity]; **B**, **B′**, dorsal, **C**, labial (mirrored), and **D**, ventral views. Scale bars equal 1 cm (**A**–**D**) and 5 mm (**A′**, **B′**, **A″**). (Color figure available online.)

and provides space for the ventral symphyseal cartilage (Cundall et al., 1987).

In lingual view, the pars dentalis lies above the subdental shelf (sulcus dentalis sensu Meszoely, 1966; dental gutter sensu Naylor, 1981) and is composed of dental and subdental laminae of relatively equal depth that are arranged parallel to each other (Fig. 2A). Pedicels of pleurodont teeth are visible along the dental laminae. The surface of the subdental lamina is almost smooth, but slightly pronounced subvertical lines are nevertheless apparent (Fig. 2A, A′).

The dental and subdental laminae are high and narrow near the symphysis, decrease in height and increase in thickness in the middle part, but posteriorly increase in height again. The pars dentalis is nearly twice as high as the dental lamina near the symphysis, 1.2 times in the middle portion of the dentary, and 2.2 times at the posterior-most part of dentary. In the anterior part of the dentary, the pars dentalis is less than half as long as the corpus dentalis (Fig. 2A, A′, B′).

The dentition on the dentary is monostichous. The tooth crowns are missing and the teeth are therefore represented by their pedicellar portions only. The pedicles indicate that the teeth are narrow and numerous. At least 110 teeth must have been present. The dental lamina is 115 mm long.

The subdental shelf is flat in the anterior and posterior portions, but shallow in the middle part. The surface exhibits irregularly placed small foramina and larger pits, which might be piercing the compact bone and connecting the external surface with the medullary cavity (Fig. 3Bi). The anterior-most foramen is the largest and connects with the symphysis.

The anterior part of the dental shelf is broad and accentuated. The margin of the lamina horizontalis is angular. Above the anterior tip of the Meckelian groove, the dental shelf exhibits a marked step, decreasing in width by around 50%, and the ridge of the lamina horizontalis becomes rounded. Posterior to this point, the lamina is angular again (Fig. 2A, B). The anterior portion of the Meckelian groove is deep and narrow and extends 3 mm into the bone. The posterosuperior margin of the Meckelian groove is pierced by a canal (canalis superiodorsalis cartilaginis Meckelii) for the nervus alveolaris und arteria temporalis (sensu Böttcher, 1987). This canal extends 12 mm into the bone (Fig. 2A).

The lingual surface of the corpus dentalis (subdental shelf sensu Gardner and Averianov, 1998) is smooth. Only some small foramina are present. In transverse section, the corpus dentalis is broad superiorly, narrows inferiorly, and ends with a ventral keel. The keel margin is characterized by sparse pustules/warts (Fig. 2A, C, D). The articulation facet with the coronoid on the lingual side of dentary, above the Meckelian groove, forms a sharp lingual crista, which extends subparallel to the inferior margin of dental lamina and fuses posteriorly with the lamina horizontalis (Fig. 2A, B).

The longitudinal axis of the dentary separates the pars dentalis from the corpus dentalis. A longitudinal flange (eminentia longitudinalis) extends labially from this axis. The sculpture of the perichondral ossification on the labial side of the dentary is rugose to pustular. These surface structures are more pronounced directly behind the symphysis and on the ventral margin of the longitudinal flange, which overlies the mental foramina. Two grooves are furthermore present that extend to the center of the symphysis in the labioanterior part of dentary. The superficial symphyseal ligament of the mandibular joint attached at this site (Cundall et al., 1987). Five mental foramina are arranged on the labial side of the dentary along the longitudinal axis. There are also some small foramina on the labial side of the pars dentalis.

Like all of the other bones, the dentary is weakly ossified. It has an extremely thin cortex that surrounds cancellous bone. The medullary cavity is extensive (Figs. 2A″, 3B). In cross-section, two large medullary cavities are apparent dorsal and ventral to the longitudinal flange. Smaller cavities are arranged around these primary cavities. The ventral keel encloses small medullary cavities, which are present in the anterior portion of the dentary. The total medullary cavity of the dentary is not a closed system fully surrounded by bone. Instead, the cavity communicates with the outside via numerous mental foramina, the anterior part of the Meckelian groove, and small foramina along the dental shelf. The medullary cavities extend posteriorly where the two main cavities diffuse into compact bone (Fig. 3). The bone compactness values of the available cross-sections are given in Table 1. There is a general trend in that bone compactness values changes along the dentary. In particular, bone compactness values are comparably higher anteriorly and posteriorly, but lower in the midsection (see Table 1).

TABLE 1. Bone density values of studied giant salamander dentaries at the given positions (see Fig. 3).

		Value			
Taxon	n	i	ii	iii	iv
Zaissanurus beliajevae (IP ZSN-KKS-2)	1	0.837	0.808	?	?
Ukrainurus hypsognathus (NMNHK 22-1711)	1	0.721	0.603	?	?
Andrias scheuchzeri (GPIT/AM/717)	1	0.893	0.728	0.755	0.83

Articular—The articular (angular sensu Osawa, 1902; Reese, 1906; Duellman and Trueb, 1994) is a long, straight, and slender bone. Anteriorly, it narrows and its walls thin (Fig. 4). The posterior end of the articular is massive; on the dorsal side it bears a rounded, slightly elliptical articular condyle (pars condyloidea cartilaginea sensu Hyrtl, 1885). This is the mineralized/ossified posterior portion of the Meckelian cartilage (Buckley et al., 2010).

Much of the labial surface of the articular covers the dentary. The transition between these two bones, however, is nearly invisible. The linguoventral side of the articular has a broad facet (facies coronoideus; Fig. 4A, B) with a highly prominent pit-and-ridge sculpture that narrows anteriorly. The articular covers the articular facet of the coronoid with this facet. Posteriorly, the articular ends with a ventroposteriorly extended elliptical surface, which bears two small pits (Fig. 4A). The posterior fibers of the mandibular depressor muscles attached to this surface.

Coronoid—The flat, wedge-shaped coronoid (prearticular sensu Duellman and Trueb, 1994) lacks its anterior and posterior parts. Labially, the bone is concave and covers the lingual side of the Meckelian cartilage. The bone has a relatively smooth surface. Only the articular and dental facets, dorsal edge of the lingual surface, and the dorsal coronoid process are bumpy to wrinkled. The bone is high at the anterior-most part of the coronoid process and slender posteriorly and anteriorly (Fig. 4). In the middle part, the coronoid ascends dorsolingually to form a fairly pronounced and flattened coronoid process. This large and long process is nearly triangular in dorsal view, wing-like, and protrudes over the lingual surface of the bone. The dental facet of the coronoid starts at the lingual corner of the coronoid process and extends anteroventrally. The preserved part of articular facet is narrow (Fig. 4).

Squamosal—The squamosal (terminology by Delfino et al., 2009) is relatively robust and flattened. The bone consists of two parts: the nearly rectangular caput squamosa and the laterally directed quadrate ramus (Fig. 5B, D). As preserved, the latter part is 2 times longer than the former part. The anterior (zygomatic) and posterior (otic) processes of the squamosal are present. The otic process is about half as long as the zygomatic process. Its

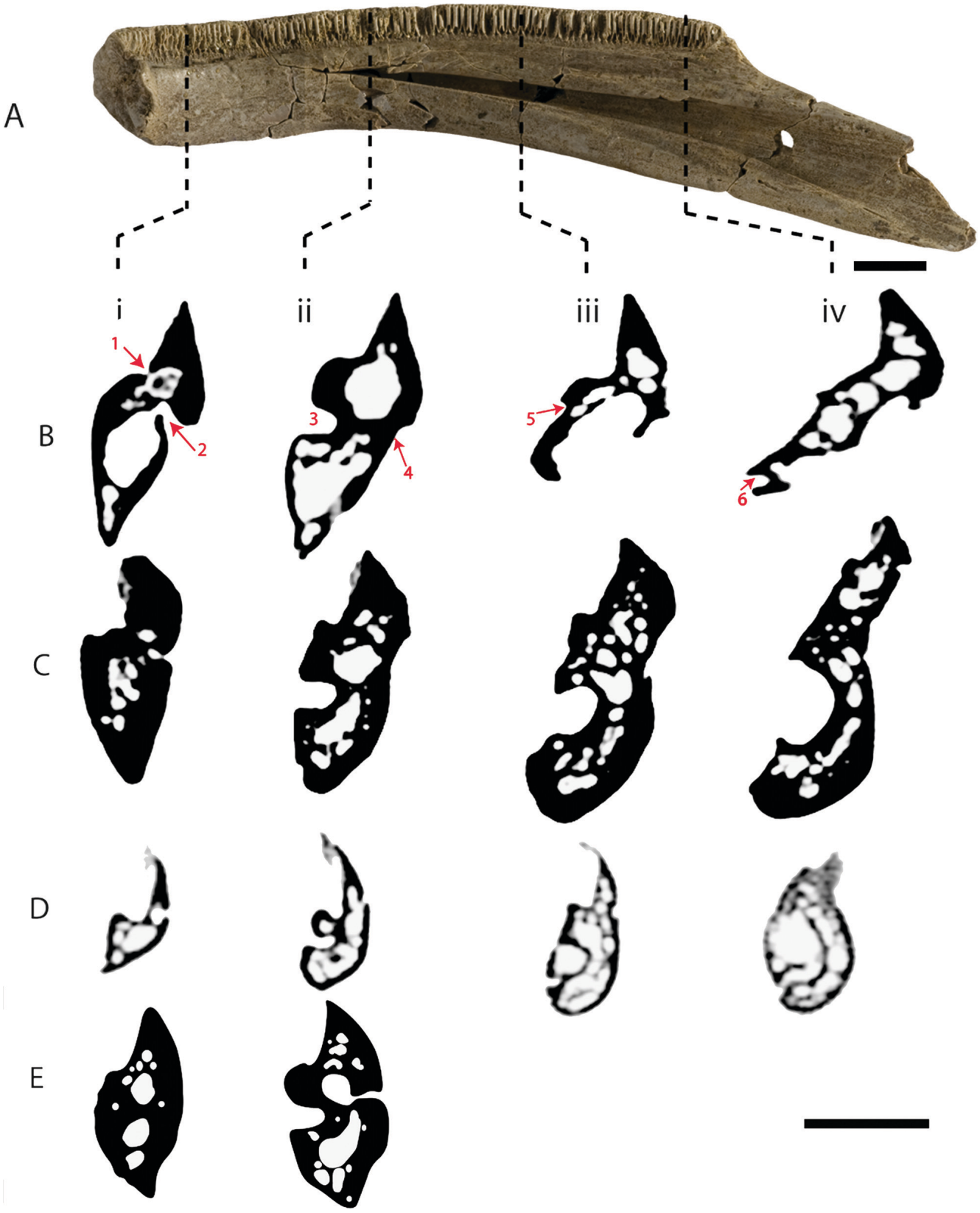

FIGURE 3. Dentary cross-sections of **A**, general view of *Andrias scheuchzeri* dentary (GPIT/AM/717) from the lingual side with the positions of cross-sections; cross-sections of **B**, *Ukrainurus hypsognathus*, gen. et sp. nov. (NMNHK 22-1711); **C**, *An. scheuchzeri* (GPIT/AM/717); **D**, *Andrias davidianus* (ZFMK 90469); and **E**, *Zaissanurus beliajevae* (IP ZSN-KKS-2). **B**, **C**, **D**, were made using CT; **E**, was drawn directly from bones. Cross-section positions: **i**, between symphysis and Meckelian groove; **ii**, behind the beginning of the Meckelian groove; **iii**, in the middle part of the tooth row; **iv**, in the posterior-most part of tooth row. **1**, foramen of the dental shelf; **2**, mental foramen; **3**, Meckelian groove; **4**, eminentia longitudinalis; **5**, labial crista; **6**, canalis superiodorsalis cartilaginis Meckelii. Scale bar equals 1 cm. (Color figure available online.)

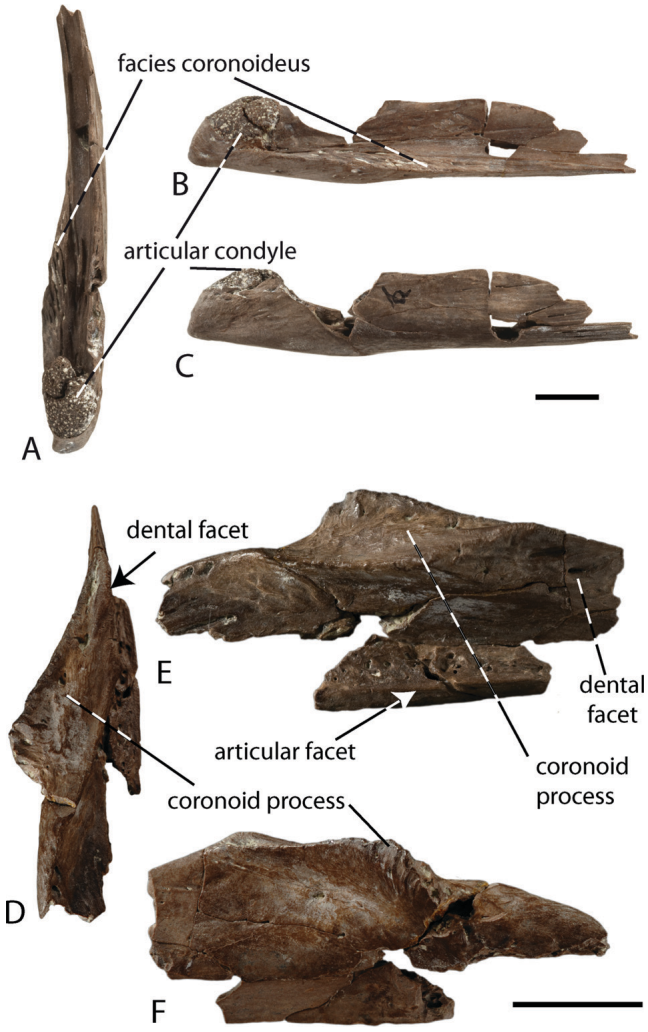

FIGURE 4. Articular and coronoid of *Ukrainurus hypsognathus*, gen. et sp. nov. Articular in **A**, dorsal, **B**, lingual, and **C**, labial views (NMNHK 22-1711ar-a) and coronoid in **D**, labial, **E**, dorsal, and **F**, lingual views (NMNHK 22-1711c). Scale bars equal 1 cm. (Color figure available online.)

ventral surface is robust and directed anterolaterally (Fig. 5A, C). The otic process connects the squamosal with the prootic. The zygomatic process is pointed and directed posteriorly. Its medial surface is robust and the lateral surface is smooth. The medial ridge, ventral surface of the caput squamosa, and the zygomatic process cover the posterolateral part of the parietal.

The dorsal surface of the caput squamosa is almost smooth and exhibits some foramina. There is an anteromedially extending transverse ridge. The ridge begins at the posterodorsal edge of the medial part of the quadrate ramus and ends with an eminence (eminentia dorsalis) near the center of the caput squamosa. The dorsal margin of the caput squamosa ascends slightly and forms a highly robust, pustular surface on the medial side of the bone. The medial portion of the ventral surface of the caput squamosa is robust and bears highly prominent structures (Fig. 5B, E).

The quadrate ramus is 'C'-shaped in anterolateral view. It is composed of three walls (paries): the paries dorsalis, which broadens anteriorly, the paries posterior, which widens laterally, and the paries ventralis, which narrows laterally (Fig. 5). The paries dorsalis and paries posterior overlie the dorsal surface of the squamosal ramus of the quadrate. The proximal portion of the paries ventralis/pterygoideus is broader than the distal portion. This paries covers the ramus posterior of the pterygoid. In the medial part of the quadrate ramus, the paries dorsalis, and paries posterior form a right angle. Laterally, the paries posterior extends ventroposteriorly and the angle becomes obtuse. These paries probably do not form laterally a horizontal bony shelf, as can be seen in extant taxa.

Occipital—The posterior portion of the left occipital is preserved. The occipital bone produces a posterolaterally projecting, horizontally elongated occipital condyle. The facet for the odontoid process of the atlas is not preserved. The external foramen of the jugular canal is situated laterally in the middle part of the bone (foramen postoticum sensu Osawa, 1902, and Francis, 1934; foramen jugulare sensu Delfino et al., 2009). The glossopharyngeus and vagus nerves (Osawa, 1902; Francis, 1934) pass through this canal. On the dorsolateral side of the occipital, a small foramen is preserved for the spinooccipital nerve (Fig. 5F–I). The posterior part of the occipital has a slender ridge that extends subparallel to the margins of the occipital condyle. This ridge builds a pericondylar facet, which is narrow laterally and broadens dorsally and ventrally. The fibers of various neck muscles most likely inserted here (Francis, 1934).

Quadrate—The quadrates are small bones that form almost the entire articulation surface for the lower jaw. Each quadrate is a small, triangular bone that lies at the distal end of the squamosal and is largely covered by it in lateral view. The heavy, basal portion of the quadrate (quadrate caput) projects beyond the ventral margin of the squamosal. The laterodorsal surface of the quadrate caput bears the quadrate condyle, which forms the area mandibularis articularis. The slender squamosal ramus projects laterally, and lies anterior and ventral to the squamosal and dorsal to the pterygoid. In dorsal view, the squamosal ramus forms a prominence (tuber dorsale) (Fig. 5J–L).

Orbitosphenoid—The medial part of the left orbitosphenoid is preserved, but it is fragmentary and bears no morphological information.

Vertebrae

Trunk Vertebrae—The vertebrae belong to two individuals, one of which is relatively small and the other is relatively large. The vertebrae are large and massive, but all are nevertheless partly damaged. The centrum of the largest available specimen (NMNHK 22-1705) measures 32.0 mm in length, that of the smallest (NMNHK 22-1706b) 18.3 mm. The centrum is convex and dumbbell-shaped in lateral view. It is narrow in the middle part, widens towards the cotyles, and forms pericotylar crests along the margins of the cotyles. In all specimens, the centra are deeply amphicoelous and circular and subcircular in cross-section and transverse section, respectively. The central foramen is located dorsally (Fig. 6). The cotyles have a porous surface. The transverse process nearly covers the middle part of the subcentral ridge on the dorsal surface and thereby divides the ridge into the anterior and posterior alar processes (Fig. 6).

The subcentral surface of the centrum is rough and pierced by many smaller and several larger foramina. A single central foramen generally penetrates the bony tissue of the centrum from the ventral side. An additional pair of foramina is positioned lateral to the central one. Shallow and deep anteroposterior grooves adorn the interior surface of the central foramina. In addition to these foramina, the surface of the centrum is pierced by another pair of foramina (ventral foramina for spinal nerve) that are positioned under the ventral wall of the transverse processes in the subcentral groove (Fig. 6).

The neural canal is depressed and wide. Two small processes are situated near the center of the centrum and extend

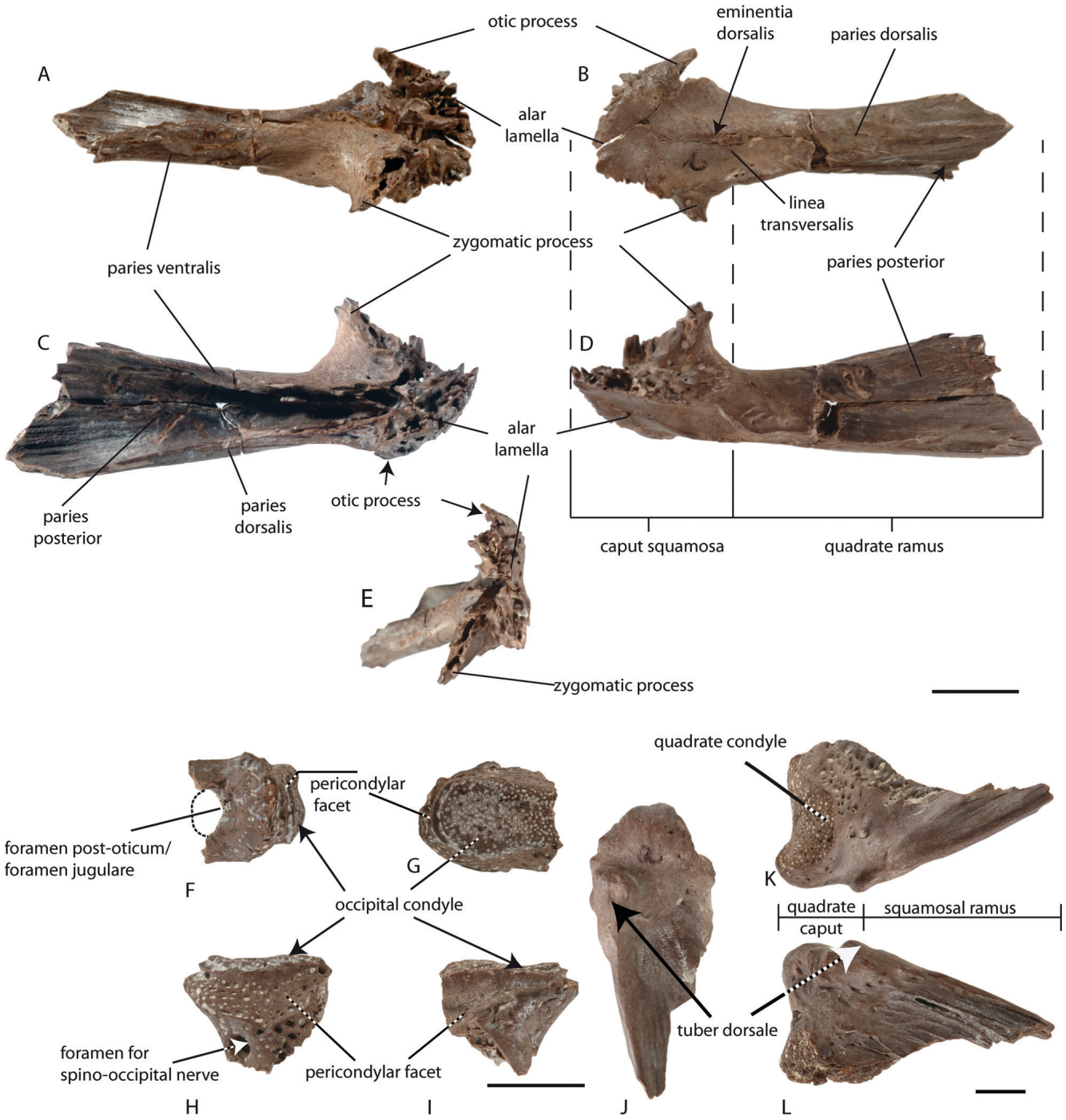

FIGURE 5. Squamosal, occipital, and quadrate of *Ukrainurus hypsognathus*, gen. et sp. nov. Squamosal (NMNHK 22-1711sq-a) in **A**, ventral, **B**, dorsal, **C**, anterior, **D**, posterior, and **E**, medial views; occipital (NMNHK 22-1711oc) in **F**, lateral, **G**, posterior, **H**, ventral, and **I**, dorsal views; quadrate in **J**, anterior, **K**, ventral, and **L**, dorsal views (NMNHK 22-1711q-a). Scale bars equal 1 cm (**A**–**I**) and 5 mm (**J**–**L**). (Color figure available online.)

ventromedially into the neural canal. The dorsal surface of the centrum, under the neural arch and directly below the projecting processes, is pierced by small neural canal foramina. These foramina are connected by canals with the foramina that penetrate the dorsal surface of the arterial canal.

A moderately vaulted neural arch is more or less present in all specimens. Its anterior-most part has a smooth surface and connects the left and right prezygapophyses. Posterior to this surface, the neural arch possesses either no neural spine (on the small vertebrae NMNHK 22-1706-88b, NMNHK 22-1706c) or a poorly developed, low spine with a barbed and wrinkled surface (NMNHK 22-1699, NMNHK 22-1704, NMNHK 22-1705, NMNHK 22-1706). The neural spine arises at the level of the prezygapophyses and extends posteriorly. The posterior portion of the neural arch (pterygapophysis) is broken off in all specimens. There is a single preserved, isolated pterygapophysis that belongs to the

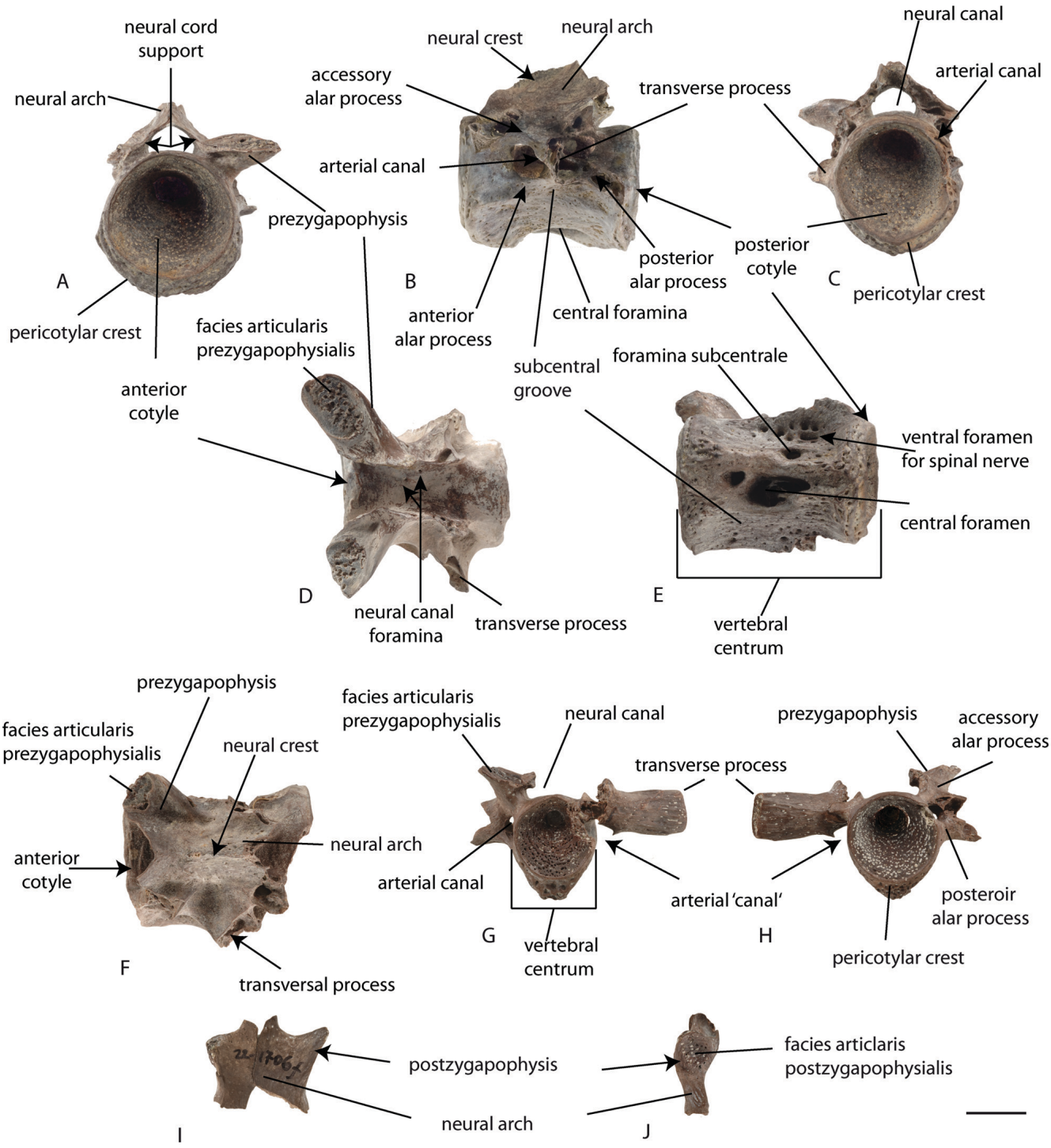

FIGURE 6. Trunk vertebrae of *Ukrainurus hypsognathus*, gen. et sp. nov. **A**, **G**, anterior (NMNHK 22-1105, NMNHK 22-1706b); **B**, lateral (NMNHK 22-1699); **C**, **H**, posterior (NMNHK 22-1105, NMNHK 22-1706b); **D**, **F**, dorsal (NMNHK 22-1698, NMNHK 22-1706), and **E**, ventral (NMNHK 22-1705) views. **I**, anterior and **J**, lateral views of vertebral pterygapophysis (NMNHK 22-1706f). Scale bar equals 1 cm. (Color figure available online.)

smaller individual and that has asymmetric right and left parts. The dorsal surface is smooth and does not possess a neural crest (Fig. 6).

The prezygapophyses are large, strongly elongated, and are anchored between the lateral corners of the neural arch and the centrum. The prezygapophyses possess the facies articularis prezygapophysis on the dorsal side of their anterior portion. This articulation surface has an extremely elongated elliptical form. It is covered with mineralized, strongly porous cartilaginous tissue. The posterior portion of the prezygapophyseal crest joins the lamina (accessory alar process) interconnecting the transverse processes.

The postzygapophyses are preserved only on an isolated pterygapophysis (see above). In this specimen, the postzygapophyses are placed dorsolaterally to the pterygapophysis and project ventromedially. Their articulation facets are irregular circles. The 'interzygapophyseal ridge,' extending between pre- and postzygapophyses, is extremely poorly developed or absent.

The transverse processes in all specimens are completely broken off. There is only one vertebra with a preserved right transverse process, but this specimen is pathologically developed because there is no connection between the transverse process and the subcentral ridge (Fig. 6G, H). The proximal end of the transverse process is triangular in cross-section. Between the medial surfaces of the transverse process and the vertebral centrum the arterial canal for the arteria vertebralis is enlarged (Francis, 1934). It is apparent in anterior view that the transverse processes are directed slightly posteroventrally.

Caudal Vertebra—Only a single caudal vertebra (NMNHK 22-1706e; Fig. 6A–E) is preserved. The hemal processes are broken off. The centrum has a similar structure to that seen in the trunk vertebrae. The neural arch, pre- and postzygapophyses, as well as the transverse processes are broken off. The transverse process seems to have extended posteroventrally, as in Recent species. The proximal end of the transverse process is smaller than those of the trunk vertebrae. The foramina of the arterial canal and the ventral foramina for the spinal nerve are of the same size and are situated near each other. The anteroposterior groove of the vertebral centrum, which passes through the central foramina, is considerably deeper than that of the trunk vertebrae and reaches the middle of the vertebral centrum. The ventral surfaces of the posterior cotyle possess posterodorsally projecting hemal processes that are located posterior to the anteroposterior groove. The bases of the hemal processes have an oval form (Fig. 7E).

Ribs—Six right and left ribs are available from different trunk vertebrae (Fig. 7F–I). The rib morphology is the same as in Recent cryptobranchids, *An. scheuchzeri*, and *Z. beliajevae* (locality Korsak B, IP ZSN-K-14). In particular, the ribs are bent at midlength and the bone surface is generally smooth. However, numerous foramina and small protuberances are visible on the anterior and posterior sides (Fig. 7F, G), which are lacking in other giant salamanders.

In the proximal part, the ribs are anteroposteriorly flattened and the anterior and posterior surfaces are concave. The rib articulation surface with its transverse process is unicapitate and has a dumbbell shape. The upper articulation surface is elongated elliptically, whereas the lower one is oval. Both surfaces are connected by a slender strip (Fig. 7H, I). The distal part of the ribs is slender and slightly dorsoventrally depressed and therefore forms an anteroposteriorly elongated elliptical shape in cross-section.

Long Bones

Femur—The femur is a relatively long (67.3 mm) bone with a broken distal end. In lateral view, the bone is dumbbell-shaped. The femur has a lateromedially compressed distal end and an anteroposteriorly compressed proximal end. The distal end is larger than the proximal end. The femur is cylindrical in the middle part (Fig. 8). The bone compactness value at mid-diaphyseal position (Fig. 8C′) is 0.87 (Table 2).

The distal end of the femur is enlarged to form a rounded, spoon-shaped head. The head is slightly convex on its lateral surface and concave on its medial surface (trochlear groove) (Fig. 8B, B′). In ventral view, the distal end is triangular. The mineralized cartilaginous tissues that cover the distal articulation surfaces are visible. The femur narrows about 2.5 times distally towards the midshaft and becomes cylindrical. Towards the distal end, the femur doubles in width lateromedially. The proximal end is rectangular, has rounded corners, and forms the acetabulofemoral joint. It has an anteriorly slightly concave surface and exhibits a foveal depression (Francis, 1934). The medial surface of the femur possesses a femoral (trochanteric) crest (linea aspera sensu Osawa, 1902). It begins at the middle part of the diaphysis and extends to the anteroventral corner of the proximal end near the highly damaged trochanter. The posterior surface of the bone is wrinkled.

TABLE 2. Bone density values of studied giant salamanders femur femora at the mid-diaphyseal position.

Taxon	n	Value	Reference
Ukrainurus hypsognathus (NMNHK 22-1707)	1	0.87	This study
Andrias japonicus	1	0.979	Laurin et al. (2004)
Cryptobranchus alleganiensis	1	0.966	
Onychodactylus fischeri	1	0.926	

Terminal Phalanges—Two relatively large terminal phalanges are available. The phalanges are slender, relatively long, and have a broad proximal base (3.3 mm) (Fig. 8). They are characterized by a mineralized cartilaginous proximal epiphysis (Fig. 8B). From the base, the terminal phalange becomes less broad toward the rounded tip. The tip possesses a rounded, robust bulb ventrally (Fig. 8B). The base of the phalange from the ventral side is pierced by a laterally stretched 'foramen.' The lateral surface of the phalange bears a lateral ridge, stretching from the basis of bulb to the middle part of phalange.

DISCUSSION

Taxonomic Status of *Ukrainurus hypsognathus*

Ukrainurus hypsognathus, gen. et sp. nov., shares with all crown cryptobranchids several characteristics, such as large body size (0.5–2 m); massive bones; dentaries joined along the ventrocaudal portion of the symphysis; parietal and squamosal in direct contact; trochanter fused with the proximal head of the femur; and trunk ribs and distal end of transverse processes of trunk vertebrae unicapitate. The new taxon differs from *Andrias scheuchzeri*, *An. davidianus*, *Zaissanurus beliajevae*, and *Aviturus exsecratus* by having less bone ossification; i.e., the compact bone is very thin, the cancellous bone is highly porous, and the medullary cavity is extremely extended (Fig. 3; Tables 1, 2). Moreover, *U. hypsognathus* has two pronounced medullary cavities in the anterior region with relatively large 'satellite' cavities. Crown cryptobranchids do not have differentiated medullary cavities, but rather many small- to middle-sized satellite cavities (Fig. 3B).

Ukrainurus hypsognathus, gen. et sp. nov., possesses a number of autapomorphies: (1) the dentary is high and lateromedially compressed; (2) the ventral keel of the dentary is long due to a lateromedial compression of the bone; (3) the pars dentalis is lower than the corpus dentalis in cross-section of the anterior part of the dentary, instead of equal or subequal (Fig. 3); (4) the pars dentalis of the dentary not only produces a dental lamina, bearing the tooth pedicels, but also a smooth subdental lamina; (5) the subdental shelf is plain to very shallow, instead of deep; (6) the longitudinal flange of the labial side of dentary is prominent and has a rugose to pustular and pointed surface, instead of a poorly developed longitudinal flange that is smooth or slightly wrinkled; (7) large mental foramina; (8) lingual crista present on the lingual surface of the dentary; (9) coronoid facet of the articular broad and with highly prominent pit-and-ridge sculpture; (10) nearly invisible, articular-dentary articulation facet at the posterior part of the articular; (11) the prezygapophyses and the facies articularis prezygapophysis extremely elongated and elliptical, instead of round or moderately elongated; (12) eminentia

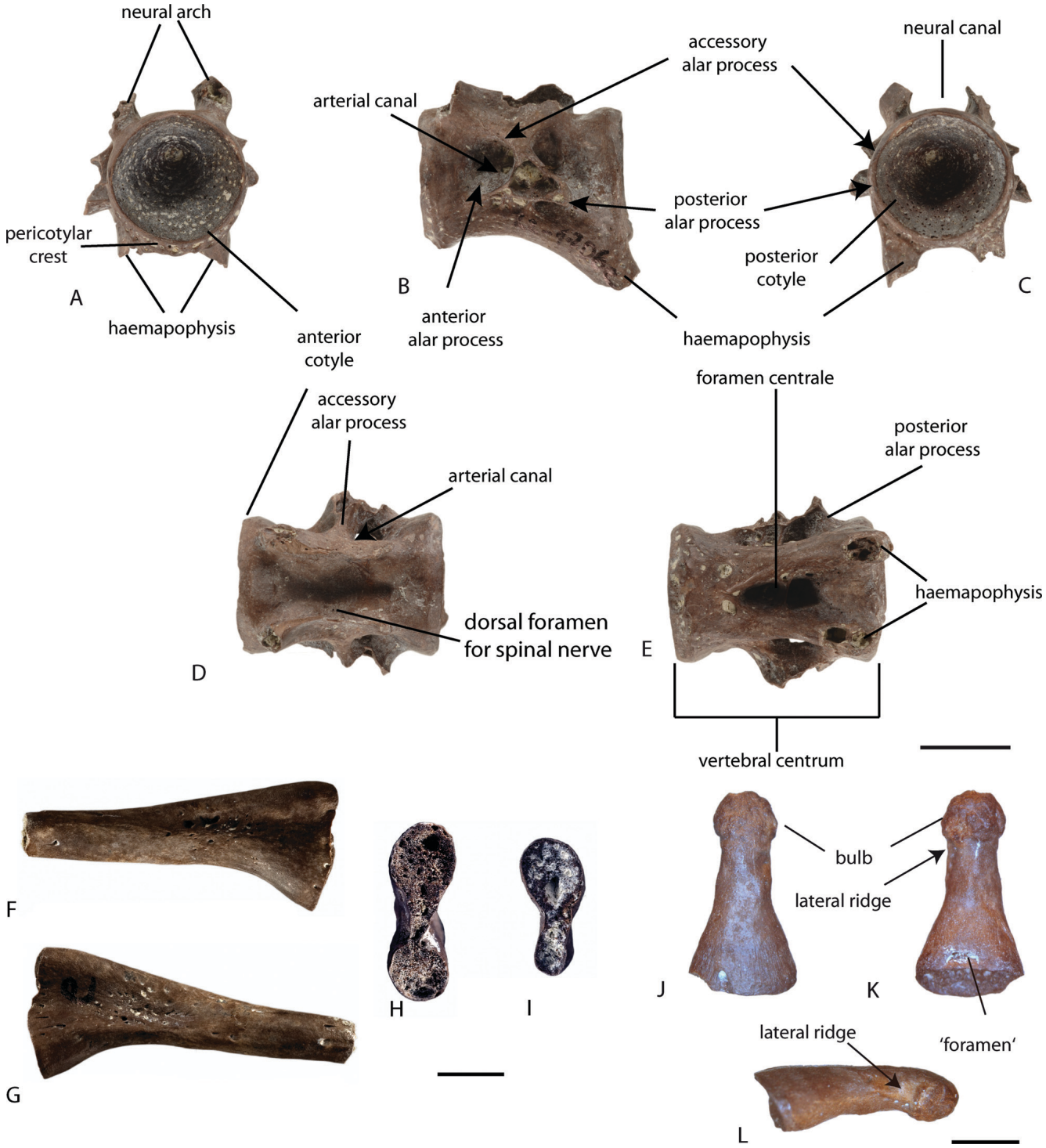

FIGURE 7. Caudal vertebra (NMNHK 22-1706e), ribs, and phalanges of *Ukrainurus hypsognathus*, gen. et sp. nov. Caudal vertebra in **A**, anterior, **B**, lateral, **C**, posterior, **D**, dorsal, and **E**, ventral views; ribs in **F**, anterior and **G**, posterior views (NMNHK 22-1707a_e); rib articulation surface with transverse process of vertebrae (**H**, NMNHK 22-1707a_e and **I**, NMNHK 22-1707a_a); and terminal phalanges (NMNHK 22-1711f_1) in **J**, dorsal, **K**, ventral, and **L**, lateral views. Scale bars equal 1 cm (**A**–**E**), 5 mm (**F**–**I**), and 2 mm (**J**–**L**). (Color figure available online.)

dorsalis present on squamosal; (13) pericondylar facet of occipital broad, instead of slightly pronounced or absent; (14) posterior paries of squamosal high and forming obtuse angle with paries dorsalis, instead of low and parallel to paries dorsalis; (15) paries posterior of squamosal large and zygomatic process directly anterolaterally, instead of anteromedially; (16) dorsal margin of caput squamosal lack marginal lamina; and (17) low bone density values for the dentary (Table 1) and femur (Table 2).

Ukrainurus hypsognathus, gen. et sp. nov., shares a number of homoplastic or symplesiomorphic features with various

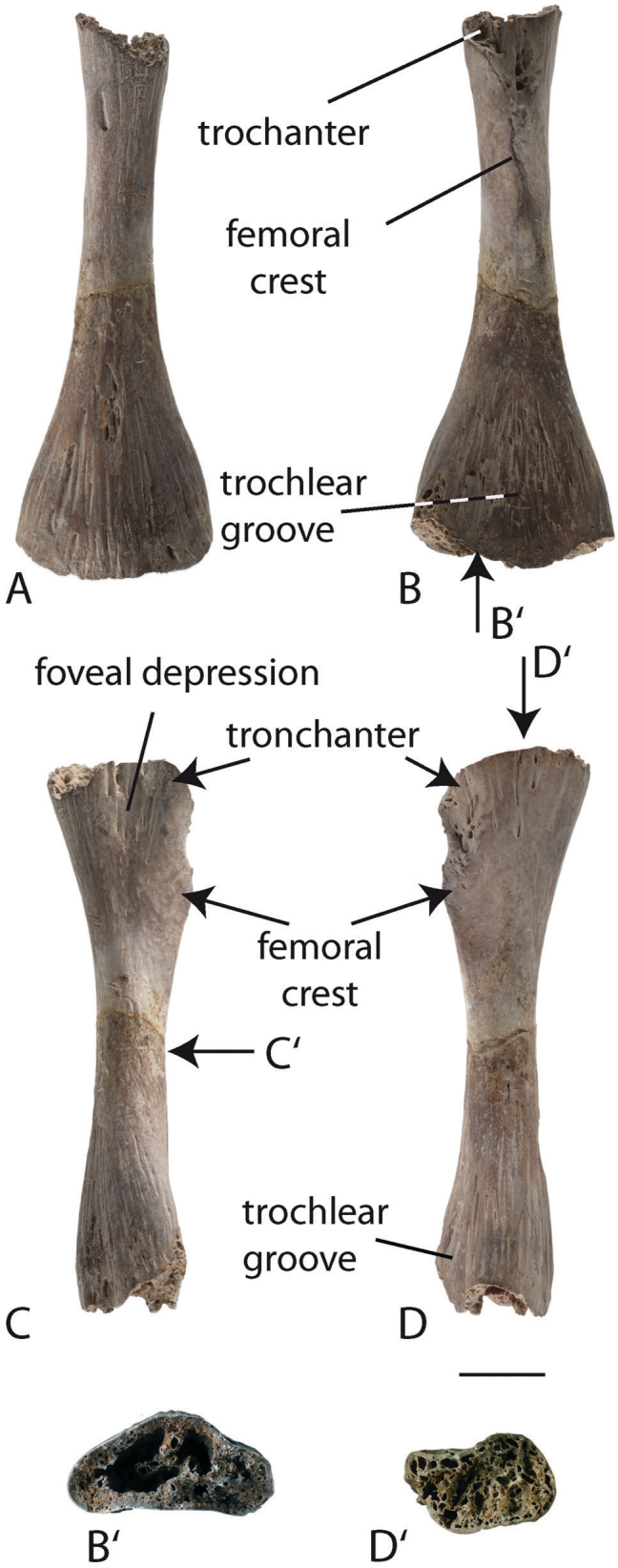

FIGURE 8. Right femur of *Ukrainurus hypsognathus*, gen. et sp. nov. (NMNHK 22-1707) in **A**, dorsal, **B**, ventral, **C**, posterior, and **D**, anterior views; **B′**, distal and **D′**, proximal articulation surface of femur; **C′**, the arrow shows the mid-diaphyseal position of the bone. Scale bar equals 1 cm. (Color figure available online.)

fossil and living pancryptobranchans. The mandibular symphysis is elliptically elongated as in '*Cryptobranchus*' *saskatchewanensis* (Naylor, 1981:fig. 1A), instead of round to slightly elliptical as all other giant salamanders. The ventral symphyseal cartilage is small, as in '*C.*' *saskatchewanensis*, whereas *Andrias* spp. and *Cryptobranchus alleganiensis* have a (~1.5 times) larger cartilage. *Ukrainurus hypsognathus* resembles *Av. exsecratus* in having highly pronounced perichondral ossification on the dentary, the femoral trochanter crest, and neural crest, and by having pierced bone surfaces in the femur, ribs, and vertebrae. The new species and *An. scheuchzeri* have a smooth lingual surface of the corpus dentalis, although an 'S'-shaped concavity is nevertheless apparent in *An. scheuchzeri*. In comparison, *Av. exsecratus* (Gubin, 1991:fig. 6, table 8), *Z. beliajevae* (Chkhikvadze, 1982:figs. 1, 2, pl. 1), and '*C.*' *saskatchewanensis* (Naylor, 1981:fig. 1) have a deep groove (presymphyseal sulcus) on the lingual surface of the corpus dentalis between the symphysis and the anterior limit of the Meckelian cartilage, under the lamina dentalis, and *An. davidianus*, *An. japonicus*, and *C. alleganiensis* have a concave surface in this region.

U. hypsognathus differs from Recent giant salamanders in having a long and broad coronoid process, whereas in the Recent species and *Z. beliajevae* (IP ZSN-K-11) it is long and narrow, and in *An. scheuchzeri* short and broad (for size relation see Appendix 1).

The femur of the fossil species is similar to those of *C. alleganiensis* (ZFMK 5245), *Andrias* spp. (e.g., ZFMK 76996), and *Z. beliajevae* (Chkhikvadze, 1982:fig. 8, pl. 3), but differs from *Av. exsecratus* (Gubin, 1991:fig. 4, table 9), which has the longest femur crista, ending at the left ridge of the trochlear groove. However, *U. hypsognathus* shows the lowest value of femoral bone density at the mid-diaphyseal position (Fig. 8; Table 2)

Two terminal phalanges were found in the fossil remains, which belong to a large amphibian. There are only two large size amphibians from the Grytsiv locality: *Latonia gigantea* (Lartet, 1851) and *Ukrainurus hypsognathus*, gen. et sp. nov. However, the fossil phalanges could be distinguished from *Latonia gigantea* (Discoglossidae) and grouped with Pancryptobrancha by having (1) a lateral ridge between the basis of the bulb and the middle part of phalange (Fig. 7K; this feature is lacking in discoglossids; Kamermans and Vences, 2009); and (2) the phalanges have the same mineralized cartilage tissue at their base as the other long bones of *U. hypsognathus*, gen. et sp. nov. However, despite these similarities, the terminal phalanges differ from those of *An. davidianus*, *An. japonicas*, *An. scheuchzeri*, and *C. alleganiensis* in having a different terminal morphology. The phalanges of the new fossil species are slender, relatively long, and end with a rounded bulb on the ventral surface, whereas in *An. japonicus*, *An. davidianus*, and *An. scheuchzeri* the phalanges are robust, without an expressed bulb on the ventral tip, and in *An. davidianus* and *C. alleganiensis* the lateral ridges can extend to the tip and form a claw-like structure. In *An. japonicus*, *An. scheuchzeri*, *C. alleganiensis*, and *U. hypsognathus*, the lateral ridges are less pronounced than in *An. davidianus*.

The new species can be distinguished from all known pancryptobranchans by the extremely elongated, elliptical prezygapophyses and prezygapophyseal articulation surfaces. Other giant salamander species have short or slightly prolonged, round or elliptical prezygapophyses and prezygapophyseal articulation surfaces, but none of them reach this form. *Ukrainurus hypsognathus* has no interzygapophyseal ridge, a feature common in all other pancryptobranchans with the exception of *Av. exsecratus*, which has a well-developed interzygapophyseal ridge (Gubin, 1991:figs. 2, 3, pl. 9).

The transverse processes of all vertebrae in the new fossil species seem to be directed slightly posteroventrally, as in several trunk vertebrae of *Av. exsecratus* (Gubin, 1991:fig. 2, pl. 9). However, data from the literature (*An. japonicus*, Shikama and

Hesegawa, 1962:figs. 6–9, pl. 29; *Av. exsecratus*, Gubin, 1991; *Andrias* sp., Matsui et al., 2001:fig. 1A–G, pl. 1) and our observations on Recent (*An. davidianus*, *An. japonicus*, *C. alleganiensis*) and fossil (*An. scheuchzeri*, *Z. beliajevae*) species show that transverse process orientation is variable along the vertebral column within individuals. Transverse processes on the anterior trunk vertebrae are generally oriented posteriorly or posterodorsally. The posterior trunk and caudal vertebrae, by contrast, have posteroventrally directed transverse processes. However, more well-preserved specimens would be needed to interpret the systematic significance of this character and its distribution within this species.

The pterygapophyses of the new taxon are asymmetric. However, this is a common feature among fossil and Recent pancryptobranchans. Asymmetry can also be found in other skeletal elements, such as the squamosal, articular, and transverse processes. In addition to asymmetry of individual bones, cryptobranchids can also show pathological development in the skeleton, for example, a skeleton of *An. davidianus* with double left or right postzygapophyses (ZFMK 90469), and *Andrias japonicus* with double left transverse processes on the 19th vertebra (one of two ZNHM unnumbered skeletons; Westphal, 1958:5). Among the trunk vertebrae of *U. hypsognathus*, an abnormal development of the transverse process is present (Fig. 7G, H).

The form and position of the hemal process of the caudal vertebrae in *Ukrainurus hypsognathus* differ from those of all fossil and Recent crown cryptobranchids. The base of the hemal process has an elongated oval form, whereas in Recent forms the process invests on lamella-like structures, forming the lateral walls of the hemal canal. In the Grytsiv species, the processes originate from the posterior portion of the vertebral centrum, whereas the Recent giant salamanders, *An. scheuchzeri*, and *Av. exsecratus*, have hemal processes located in the middle part of the centrum. Moreover, the arterial canal of the Grytsiv form is larger and has a broader opening in comparison to these taxa, which have very narrow arterial canals, with small foramina.

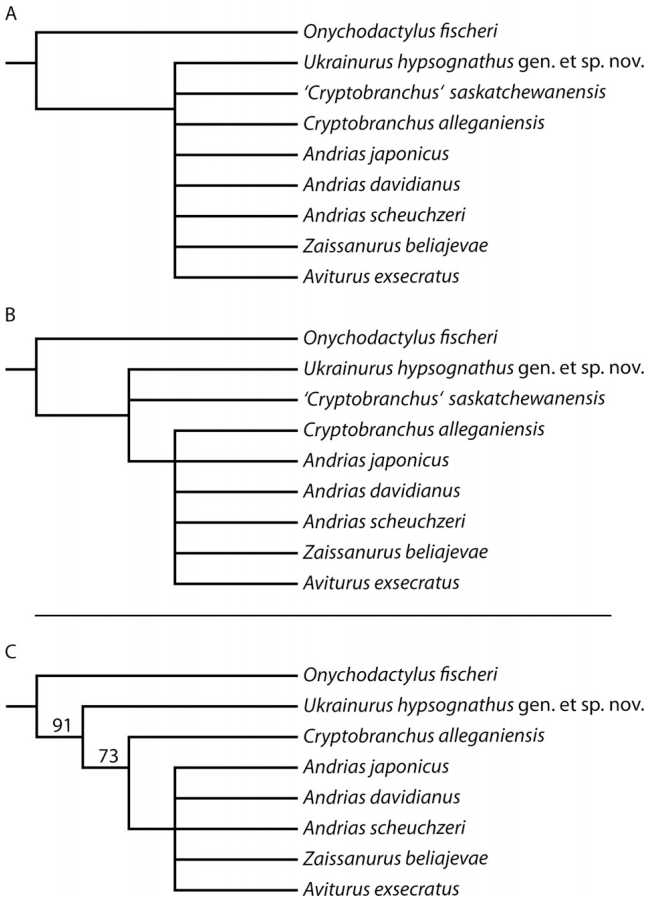

FIGURE 9. Phylogenetic analysis of the interrelationships of cryptobranchids. **A**, strict consensus tree and **B**, Adams consensus tree of the first phylogenetic analysis. **C**, strict consensus, Adams consensus, and 50% majority consensus topology retrieved from the second phylogenetic analysis. Bootstrap support values >50% are shown next to the corresponding node (1000 replicates).

Phylogenetic Considerations

We constructed a data matrix that includes all Tertiary and Recent pancryptobranchans to assess the phylogenetic affinities of *Ukrainurus hypsognathus*, gen. et sp. nov. We purposefully restricted ourselves to Cenozoic taxa, because all putatively related Mesozoic forms (e.g., *Eoscaphertepon asiaticum* and *Horezmia gracilis*) are known from fragmentary material or larvae and/or subadults (*Chunerpeton tianyiensis*) only and lack characters that would allow diagnosing them a priori as being situated close to or within crown group Cryptobranchidae, our clade of interest. Furthermore, we exclude *Andrias karalchepaki* Chkhikvadze, 1982, from the Miocene of Kazakhstan, because this taxon is too poorly known. The monophyly of our ingroup is supported by the following list of characters: trunk ribs unicapitate (character 32); body size large (character 33); and parietal and squamosal in contact with one another (character 34). Our sources for all character observations are listed in Materials and Methods. The final character-taxon matrix consists of 39 characters for eight ingroup taxa and one outgroup taxon. Only 13 characters, however, are parsimony informative. The basal hynobiid salamander *Onychodactylus fischeri* (Zhang et al., 2006) served as the outgroup taxon. The matrix was analyzed using PAUP, version 4.0b10 (Swofford, 2002). The character list is provided in Appendix 1 and the character-taxon matrix in Appendix 2 and the online Supplementary Data.

For the first phylogenetic analysis, all taxa were included, all characters were considered of equal weight, the only available multistate character was left unordered, and branches were set to collapse if their minimum length was zero. An exhaustive search retrieved 40 most parsimonious trees (MPTs) with 46 steps. The consistency index is 0.65 when all parsimony uninformative characters are removed. The strict consensus topology (Fig. 9A) reveals a complete lack of resolution because all ingroup taxa are arranged in a polytomy. The basal placement of '*Cryptobranchus*' *saskatchewanensis* within the Adams consensus topology (Fig. 9B), however, indicates that this taxon causes much of this lack of resolution. This is not surprising, given that we were only able to score this taxon for six parsimony informative characters.

For the second analysis, we used the same parameters as in the first analysis, but omitted '*C.*' *saskatchewanensis* and ran a bootstrap analysis with 1000 randomly seeded replicates. The exhaustive search this time retrieved only four MPTs of 43 steps. The strict, Adams consensus and 50% consensus topologies are identical (Fig. 9C). The consistency index is 0.76 after removal of all parsimony uninformative characters. All four topologies agree by placing *U. hypsognathus* as the sister group to crown Cryptobranchidae and by placing the North American *Cryptobranchus alleganiensis* as the sister group to all Eurasian cryptobranchids. Characters that unite crown Cryptobranchidae to the exclusion of *U. hypsognathus* include the presence of a deep dental shelf (character 8), a pronounced articulation facet between the articular and dentary (character 13), a narrow articular condyle (character 16), and the presence of only slightly elongated

articular surfaces of the prezygapophyses (character 25). The monophyly of Eurasian cryptobranchids is supported by the presence of low enamel caps (character 12) and the presence of only three bones around the nares (character 39). It must be noted, however, that both of these characters cannot be observed among the fossil Eurasian cryptobranchids *Aviturus exsecratus* and *Zaissanurus beliajevae*.

The unclear phylogenetic placement of '*C.*' *saskatchewanensis*, and a number of derived similarities between '*C.*' *saskatchewanensis* and *U. hypsognathus* (i.e., presence of a elongated elliptical symphysis [character 1]; presence of a small triangular space between the dentaries [character 2]), and a lack of shared derived characters between '*C.*' *saskatchewanensis* and *C. alleganiensis* further lead us to conclude that '*C.*' *saskatchewanensis* may be a stem cryptobranchid and, therefore, not closely related to *C. alleganiensis*.

The Mesozoic taxa *Chunerpeton tianyiensis, Eoscaphertepon asiaticum*, and *Horezmia gracilis* have previously been referred to Cryptobranchidae (Gao and Shubin, 2003; Skutschas, 2009). Our phylogenetic analysis allows us to speculate about their placement with respect to Pancryptobrancha. None of these taxa can be scored for the list of characters that unite crown Cryptobranchidae or the clade of Asian cryptobranchids (see above). We therefore do not have any positive or negative evidence that would allow us to exclude them from or include them in these clades. However, it is apparent that characters that unite the relatively derived *U. hypsognathus* clade are absent from these taxa. In particular, *Ch. tianyiensis* lacks a parietal/squamosal contact, *E. asiaticum* lacks a trochanter that is fused with the proximal head of the femur, and *H. gracilis* lacks large body size. All three taxa are therefore most parsimoniously placed outside of the *U. hypsognathus* clade positioned along the cryptobranchid stem lineage and should not be used to calibrate the age of the cryptobranchid crown group. We encourage others to more rigorously test the phylogenetic position of *Ch. tianyiensis*, *E. asiaticum*, and *H. gracilis* using more inclusive character matrices and hope that our analysis will serve as a good starting point.

Our phylogenetic results imply a taxonomy that is substantially different from that of Gubin (1991), who subdivided Cryptobranchidae into the subclades Aviturinae (*Zaissanurus beliajevae*, *Ulanurus fractus*, *Aviturus exsecratus*, and probably '*Cryptobranchus*' *saskatchewanensis* and *Cryptobranchus matthewi*) and Cryptobranchinae (*Cryptobranchus alleganiensis* and *Andrias* spp.). The characters that Gubin (1991) used to support his taxonomy are listed in Table 3.

Many of the characters provided by Gubin (1991) need critical consideration. No size estimates are available for *U. fractus*, '*C.*' *saskatchewanensis*?, and *C. matthewi*?, whereas the largest specimen of genus *Andrias* (both fossil and Recent species) can reach body lengths of more than 170 cm (Estes, 1981; Murphy et al., 2000; Matsui et al., 2008). We therefore cannot support the supposed distribution of this character (see in Table 3) and cannot discover an alternative pattern either.

Long hind limbs are indeed present in *Aviturus exsecratus*, but this character cannot be observed among all other representatives of Aviturinae. Similarly, *Av. exceratus* is the only giant salamander known to have a long parietosquamosal suture. Until more evidence is available, we therefore consider both of these characters to be autapomorphic for *Av. exceratus* and not to be diagnostic of a more inclusive clade.

Gubin (1991) furthermore distinguished his two subfamilies of giant salamanders based on the number of teeth in the dentary tooth row. However, the number of teeth is known to be highly variable even within species and also shows no relationship to size or age of the individual (Böttcher, 1987; pers. observ. of *Andrias davidianus*, *An. japonicus*, *An. scheuchzeri* by D.V.). Until full variation has been documented for each species, it is not possible to draw any phylogenetic conclusions from this character. The same argument can be made for vertebral shapes. Gubin (1991) argued that *Cryptobranchus alleganiensis* and *Andrias* spp. only have rectangular vertebrae, but our observations of the relevant material demonstrate that every individual appears to have a different vertebral shape (also see Böttcher, 1987). It therefore appears that none of the characters listed by Gubin (1991) contradict the phylogenetic analysis that we present herein (Fig. 9).

The Taxonomic Validity of *Ulanurus fractus*

The type locality of *Aviturus exsecratus* has yielded another species of cryptobranchid, *Ulanurus fractus*, and our assessment of character-state distribution and variation in cryptobranchids allows us to reevaluate the validity of the latter species. *Ulanurus fractus* was erected based on two fragmentary dentaries (Gubin, 1991:103, PIN 4357/27, PIN 4358/2) and diagnosed by (1) the presence of a presymphyseal sulcus; (2) the presence of tooth-like crests within the presymphyseal sulcus; and (3) the presence of longitudinal grooves within the presymphyseal sulcus. The type material of *Ulanurus fractus* indeed possesses a presymphyseal sulcus at the corpus dentalis, but this is also present in the holotype of *Av. exsecratus*. Similarly, although tooth-like crests and longitudinal grooves are present in the type material of *U. fractus*, tooth-like crests and longitudinal grooves are also known from some *Av. exsecratus* specimens (PIN 4357/32 and IP ZSN-KKS-1, respectively). It is therefore apparent that *U. fractus* was diagnosed based on characters that are present in the coeval *Av. exsecratus* and we therefore consider *Ulanurus fractus* to be a junior synonym of *Aviturus exsecratus*.

TABLE 3. Characteristic features of the giant salamander subfamilies Aviturinae and Cryptobranchinae according to Gubin (1991).

	Aviturinae Gubin, 1991	Cryptobranchinae Cope, 1889
Taxa included	*Zaissanurus beliajevae*, *Ulanurus fractus*, *Aviturus exsecratus*, '*Cryptobranchus*' *saskatchewanensis*, *Cryptobranchus matthewi*	*Cryptobranchus alleganiensis*, *Andrias* spp.
Features		
1	Very large animals, body length at least 150–170 cm, hind extremities up to 25 cm long	Animals with relatively short extremities (length of femur less than twice the length of centra of trunk vertebrae)
2	Length of parietal-squamosal suture less than two-thirds of parietal length? along the axial line; tubercle absent along the suture line	Suture between parietal and squamosal bones short; bones form a tubercle at point of contact
3	Tooth row of dentary has >100 teeth and is separated from the 'sulcus dentalis' (subdental shelf) by a wide smooth area (subdental lamina?)	Tooth row of dentary has 60–75 teeth; tooth bases lie directly above 'sulcus dentalis' (subdental shelf sensu this study)
4	Vertebrae rectangular, trapezoid, or parallelogram-shaped in profile	Vertebrae always rectangular in lateral view
5	Prezygapophyses do not project above the base of bony processes	Prezygapophyses usually project above bases of bony processes

Biogeographic and Temporal Considerations

The outgroup taxon and the majority of our ingroup taxa originate from Eurasia, with the exception of *Cryptobranchus alleganiensis* and '*C.*' *saskatchewanensis*. If geography is treated as a character and mapped onto the phylogenetic tree, it becomes apparent that the common ancestor of our ingroup lived in Asia and that the ancestor of *C. alleganiensis* and '*C.*' *saskatchewanensis* migrated to North America independently from one another (DELTRAN). The alternative (ACCTRAN) interpretation that the cryptobranchid lineage dispersed to North America, only to later return to Eurasia, appears less likely, because the pancryptobranchan record is rather continuous in Eurasia. The oldest representative of crown Cryptobranchidae is *Aviturus exsecratus* from the terminal Paleocene of the Nemegt Basin, Mongolia. This finding predicts that the basal split of crown Cryptobranchidae must have occur prior to the terminal Paleocene, possibly even as early as the Late Cretaceous, but it remains unclear when the *C. alleganiensis* lineage dispersed into North America.

Diet and Food Consumption

Mandible Movement—During prey capture and prey manipulation, the mandibles of *Cryptobranchus alleganiensis* and *Andrias* spp. sometimes flex around the mandibular symphysis. This movement is permitted by two pads of elastic cartilage that are situated between the dentaries and that are lacking in many other groups of salamanders. This asymmetric movement is largely related to the size of the larger ventral pad, which fills a large, triangular, ventral space between the dentaries (Cundall et al., 1987). *Ukrainurus hypsognathus* has a smaller space for the elastic cartilage relative to all crown cryptobranchids. We therefore assume that it possessed a less flexible mandibular joint and was therefore not able to feed as asymmetrically as Recent cryptobranchids.

Musculature—Using the observations of Buckley et al. (2010), that in plethodontine salamanders the degree of robustness of the squamosal is related to the overall strength of the jaws and the sizes of the mandibular levator muscles and associated otic and squamosal crests, we can made some conclusions about musculature and bite force in fossil giant salamanders. *Ukrainurus hypsognathus* has the most robust squamosal among all known Recent and fossil pancryptobranchans. The coronoid process is particularly long and broad. On the dorsal side, the process partially or completely serves as the site of origin for four groups of mandibular levator muscles (deep mandibular levator, levator mandibulae posterior, levator mandibulae externus, and superficial levator mandibulae anterior; Elwood and Cundall, 1994). Taking into account the size proportions of the process in the Recent species, *Zaissanurus beliajevae*, and *Andrias scheuchzeri*, we conclude that larger and stronger mandibular levator muscles must have been present in the new species. The bone surfaces where the tendons of the large levator mandibulae externus (paries dorsalis of squamosal), small levator mandibulae posterior (anterolateral surface of squamosal), and anterior depressor mandibulae (medial tip and paries posterior of squamosal) attach are also larger than in Recent species. Finally, the pericondylar surfaces of the occipital are greatly enlarged. All of these observations allow us to conclude that the new taxon had a particularly strong biting force and was able to seize large prey with relative ease.

A diverse assortment of vertebrate prey taxa were available for *Ulanurus hypsognathus*. These include adults and larvae of the amphibians *Mioproteus caucasicus*, *Chelotriton paradoxus*, Salamandridae sp., *Palaeobatrachus* sp., *Pelobates* cf. *decheni*, *Pelobates* sp., *Bufo* sp., *Latonia gigantea* (Zerova, 1985; Korotkevich, 1988; Rage and Roček, 2003; Roček, 2005), and *Pelophylax* (*ridibundus*) sp. (pers. observ.), as well as the fishes *Esox* sp., Siluridae indet., and Cyprinidae indet. (pers. observ.). There is no invertebrate fossil record from the Grytsiv locality.

ACKNOWLEDGMENTS

We thank J. Prieto, M. Aiglstorfer, and P. Havlik (Institute for Geosciences, University of Tübingen) for providing comparative material of *Andrias scheuchzeri* (J.P.) and their valuable comments on an earlier version of the manuscript. The photographs in Figures 2–12 were produced by W. Gerber (University of Tübingen). We are indebted to E. Schwaderer (Department of Radiology, University of Tübingen) for computer tomography of fossil and Recent cryptobranchid bones. We are grateful to J. Anderson for editorial comments and to J. Gardner and J.-C. Rage for criticism and constructive reviews. This project was supported by the Deutsche Forschungsgemeinschaft (DFG), grant BO 1550/14 (to M.B.).

LITERATURE CITED

Averianov, A., and L. Tjutkova. 1995. *Ranodon* cf. *sibiricus* (Amphibia, Caudata) from the upper Pliocene of southern Kazakhstan: the first fossil record of the family Hynobiidae. Paläontologische Zeitschrift 69:257–264.

Blanchard, É. 1871. Note sur une nouvelle salamandre gigantesque (*Sieboldia davidiana* Blanch.) de la China occidentale. Comptes Rendus hebdomadaires des Séances de l'Académie des Sciences 73:79–80.

Böhme, M., and A. Ilg. 2003. fosFARbase. Available at www.wahre-staerke.com. Accessed December 1, 2011.

Böttcher, R. 1987. Neue Funde von *Andrias scheuchzeri* (Cryptobranchidae, Amphibia) aus der süddeutschen Molasse (Miozän). Stuttgarter Beiträge für Naturkunde, Serie B 131:1–38.

Boulanger, G. A. 1886. First report on additions to the batrachian collection in the Natural-History Museum. Proceedings of the Zoological Society of London 1886:411–416.

Buckley, D., M. H. Wake, and D. B. Wake. 2010. Comparative skull osteology of *Karsenia koreana* (Amphibia, Caudata, Plethodontidae). Journal of Morphology 271:533–558.

Chepalyga, A. L., V. M. Korotkevich, Trubikhin, V. M., and T. V. Svetliskaya. 1985. Chronology of the eastern Paratethyan regional stages and *Hipparion* faunas according to palaeomagnetic data; pp. 137–139 in F. Rögl (ed.), 7th Congress of the Regional Committee on Mediterranean Neogene Stratigraphy (RCMNS): Abstract Book of Symposium on European Late Cenozoic Mineral Resources. Hungarian Geological Society, 15–22 September 1985, Budapest.

Chernov, S. A. 1959. Fauna of Tadzhikian SSR, Reptiles. Publishing house of Tadzhikian Academy of Sciences, Stalinobad, 204 pp. [Russian]

Chkhikvadze, V. M. 1982. On the findings of fossil Cryptobranchidae in the USSR and Mongolia. Vertebrata Hungarica 21:63–67.

Cope, E. D. 1889. The Batrachia of North America. Bulletin of the United States National Museum 34:1–525.

Cundall, D. J., J. Lorenz-Elwood, and J. D. Grooves. 1987. Asymmetric suction feeding in primitive salamanders. Experientia 43:1229–1231.

Daudin, F. M. 1803. Histoire Naturelle, Générale et Particulière des Reptiles: Ouvrage Faisant suite à l'Histoire Naturelle Générale et Particulieère, Composée par Leclerc de Buffon, et Rédigée par C. S. Sonnini, Membre de Plusieurs Sociétés Savantes. Dufart, Paris, 439 pp.

Delfino, M., S. Doglio, Z. Roček, D. Seglie, and L. Kabiri. 2009. Osteological peculiarities of *Bufo brongersmai* (Anura, Bufonidae) and their possible relation to life in an arid environment. Zoological Studies 48:108–119.

Didkovsky, V. Y. 1964. Biostratigraphy of Neogene deposits on the southern Russian Platform on the basis of the foraminiferal fauna. Ph.D. dissertation, Institute of Geological Sciences, Academy of Sciences of Ukrainian SSR, Kiev, 40 pp. [Russian]

Duellman, W. E., and L. Trueb. 1994. Biology of the Amphibia. The Johns Hopkins University Press, Baltimore and London, 670 pp.

Elwood, J. R. L., and D. Cundall. 1994. Morphology and behavior of the feeding apparatus in *Cryptobranchus alleganiensis* (Amphibia: Caudata). Journal of Morphology 220:47–70.

Estes, R. 1981. Gymnophiona, Caudata; in P. Wellnhofer (ed.), Handbuch der Paläoherpetology–Encyclopedia of Paleoherpetology, Volume 2. Gustav Fischer, Stuttgart and New York, 115 pp.

Francis, E. T. 1934. The Anatomy of the Salamander. Clarendon Press, Oxford, U.K., 381 pp.

Gao, K. Q., and N. H. Shubin. 2003. Earliest known crown-group salamanders. Nature 422:424–428.
Gardner, J. D. 2003. The fossil salamander *Proamphiuma cretacea* Estes (Caudata; Amphiumidae) and relationships within the Amphiumidae. Journal of Vertebrate Paleontology 23:769–782.
Gardner, J. D., and A. O. Averianov. 1998. Albanerpetontid amphibians from the Upper Cretaceous of Middle Asia. Acta Paleontologica Polonica 43:453–467.
Girondot, M., and M. Laurin. 2003. Bone Profiler: a tool to quantify, model, and statistically compare bone-section compactness profiles. Journal of Vertebrate Paleontology 23:458–461.
Greven, H., and G. Clemen. 1980. Morphological dtudies on the mouth cavity of urodeles. Amphibia-Reptilia 1:49–59.
Greven, H., and G. Clemen. 2009. Early tooth transformation in the paedomorphic Hellbender *Cryptobranchus alleganiensis* (Daudi, 1803) (Amphibia: Urodela). Vertebrate Zoology 59:71–79.
Gubin, Y. M. 1991. Paleocene salamanders from Southern Mongolia. Paleontologicheskii Zhurnal 33:96–106. [Russian]
Haeckel, E. 1866. Generelle Morphologie der Organismen. Georg Reimer, Berlin, 574 pp.
Harzhauser, M., and W. Piller. 2004. Integrated stratigraphy of the Sarmatian (upper Middle Miocene) in the western central Paratethys. Stratigraphy 1:65–86.
Holl, F. 1831. Handbuch der Petrefaktenkunde. P.G. Hilscher'sche Buchhandlung, Dresden, 489 pp.
Holman, A. J. 2006. Fossil Salamanders of North America. Indiana University Press, Bloomington and Indianapolis, Indiana, 232 pp.
Hyrtl, J. 1885. *Cryptobranchus japonicus*: schediasma anatomicum, quod almae et antequissimae Universitati Vidonbonensi, ad solennia saecularia quinta, pie celdebranda. Vindobonae, G. Braunmüller, Vindobona, 132 pp.
Joyce, W. G., J. F. Parham, and J. A. Gauthier. 2004. Developing a protocol for the conversion of rank-based taxon names to phylogenetically defined clade names, as exemplified by turtles. Journal of Paleontology 78:989–1013.
Kamermans, M., and M. Vences. 2009. Terminal phalanges in ranoid frogs, morphological diversity and evolutionary correlation with climbing habits. Alytes 26:117–152.
Kojumdgieva, E. I., N. P. Paramonova, L. S. Belokrys, and L. V. Muskhelishvili. 1989. Ecostratigraphic subdivision of the Sarmatian after molluscs. Geologica Carpathica 40:81–84.
Korotkevich, E. L. 1988. History of Eastern European *Hipparion* Fauna Formation. Naukova dumka, Kiev, 164 pp. [Russian]
Korotkevich, E. L., V. N. Kushniruk, Y. A. Semenov, and A. L. Chepaliga. 1985. A new middle Sarmatian vertebrate fauna locality in Ukraine. Vestnik Zoologii 29:81–82. [Russian]
Krakhmalnaya, T. 1996. Hipparions of the Northern Black Sea coast area (Ukraine and Moldova): species composition and stratigraphic distribution. Acta Zoologica Cracoviensia 39:261–267.
Kuzmin, S. L., and B. Thiesmeier. 2001. Mountain salamanders of the genus *Ranodon*. Advances in Amphibian Research in the Former Soviet Union 6:1–200.
Laurin, M., M. Girondot, and M.-M. Loth. 2004. The evolution of long bone microstructure and lifestyle in lissamphibians. Paleobiology 30:589–613.
Linnaeus, C. 1758. Sytema Naturae. L. Salvi, Stockholm, 823 pp.
Lourens, L. J., F. J. Hilgen, J. Laskar, N. J. Shackleton, and D. Wilson. 2004. The Neogene Period; pp. 409–440 in F. M. Gradstein, J. G. Ogg, and A. G. Smith (eds.), A Geologic Time Scale 2004. Cambridge University Press, Cambridge, U.K.
Lungu, A. N. 1978. Hipparion Fauna of Middle Sarmatian of Moldova: Carnivores. Shtintsa, Kishinev, 140 pp. [Russian]
Lungu, A. N. 1981. Hipparion Fauna of Middle Sarmatian of Moldova: Insectivores, Lagomorphs and Rodents. Shtintsa, Kishinev, 135 pp. [Russian]
Matsui, M., E. Kitabayashi, K. Takahashi, and S. Sato. 2001. A fossil giant salamander of the genus *Andrias* from Kyushu, Southern Japan. Research Reports Lake Biwa Museum 18:72–28.
Matsui, M., A. Tominaga, W.-Z. Liu, and T. Tanaka-Ueno. 2008. Reduced genetic variation in the Japanese giant salamander, *Andrias japonicus* (Amphibia: Caudata). Molecular Phylogenetics and Evolution 49:318–326.
Meszoely, C. 1966. North American fossil cryptobranchid salamanders. American Midland Naturalist 75:495–515.
Murphy, R. W., J. Fu, D. E. Upton, T. De Lema, and E.-M. Zhao. 2000. Genetic variability among endangered Chinese giant salamanders, *Andrias davidianus*. Molecular Ecology 9:1539–1547.
Naylor, B. G. 1981. Cryptobranchid salamanders from the Paleocene and Miocene of Saskatchewan. Copeia 1:76–86.
Nesin, V. A., and A. Nadachowski. 2001. Late Miocene and Pliocene small mammal faunas (Insectivora, Lagomorpha, Rodentia) of southeastern Europe. Acta Zoologica Cracoviensia 44:107–135.
Nessov, L. A. 1981. Cretaceous salamanders and frogs of Kyzylkum Desert. Proceedings of the Zoological Institute of Academy of Sciences of the USSR 101:57–88.
Okajima, K. 1908. Die Osteologie des *Onychodactylus japonicus*. Zeitschrift für wissenschaftliche Zoologie A 91:351–381.
Osawa, G. 1902. Beiträge zur Anatomie des japanischen Riesensalamanders. Mitteilungen aus der medicinischen Facultät der Kaiserl.-Japan, Universität zu Tokio 5:1–207.
Pevzner, M. A., and E. A. Vangengeim. 1993. Magnetochronological age assignments of middle and late Sarmatian Mammalian localities of the Eastern Paratethys. Newsletters on Stratigraphy 29:63–75.
Rage, J. C., and Z. Roček. 2003. Evolution of anuran assemblages in the Tertiary and Quaternary of Europe, in the context of palaeoclimate and palaeogeography. Amphibia-Reptilia 24:133–167.
Reese, A. M. 1906. Anatomy of *Cryptobranchus allegheniensis*. The American Naturalist 40:287–326.
Roček, Z. 2005. Late Miocene Amphibia from Rudabánya. Palaeontographia Italica 90:11–29.
Rögl, F. 1998. Paratethys Oligocene-Miocene stratigraphic correlation. Abhandlungen der Senckenbergischen Naturforschenden Gesellschaft 549:3–7.
Roshka, V. K. 1967. Stratigraphic scheme of Sarmatian sediments in Moldova. Proceedings of Academy of Sciences Moldovian SSR 4:72–80. [Russian]
Scopoli, G. A. 1777. Introductio ad Historiam Naturalem, Sistens Genera Lapidum, Plantarum et Animalium Hactenus Detecta, Caracteribus Essentialibus Donata, in Tribus Divisa, Subinde ad Leges Naturae. Apud Wolfgangum Gerle, Prague, 506 pp.
Shikama, T., and Y. Hasegawa. 1962. Discovery of the fossil giant salamander (*Megalobatrachus*) in Japan. Transactions of the Proceedings of the Paleontological Society of Japan, new series 45:197–200.
Skutschas, P. P. 2009. Re-evaluation of *Mynbulakia* Nesov, 1981 (Lissamphibia: Caudata) and description of a new salamander genus from the Late Cretaceous of Uzbekistan. Journal of Vertebrate Paleontology 29:659–664.
Swofford, D. L. 2002. PAUP*: Phylogenetic Analysis Using Parsimony (*And Other Methods), Version 4. Sinauer Associates, Sunderland, Massachusetts.
Temminck, C. J. 1836. Coup d'Oeil sur la Fauna des Îles de la Sonde et de l'Empire du Japon. Discours Préléminaire Destiné à Servir d'Introduction à la Faune du Japon. Müller, Amsterdam, 144 pp.
Topachevskij, V. A., V. A. Nesin, I. V. Topachevskiy, and Y. A. Semenov. 1996. The oldest locality of middle Sarmatian microtheriofauna (Insectivora, Lagomorpha, Rodentia) in the Eastern Europe. Dopovidi NAN Ukrainy 2:107–109. [Russian]
Vangengeim, E. A., A. N. Lungu, and A. S. Tesakov. 2006. Age of the Vallesian lower boundary (Continental Miocene of Europe). Stratigraphy and Geological Correlation 14:655–667.
Venczel, M. 1999. Land salamanders of the family Hynobiidae from the Neogene and Quaternary of Europe. Amphibia-Reptilia 20:401–412.
Vitt, L. J., and J. P. Caldwell. 2009. Herpetology: An Introductory Biology of Amphibians and Reptiles, third edition. Academic Press and Elsevier, London, xiv + 697 pp.
Westphal, F. 1958. Die Tertiären und Rezenten Eurasiatischen Riesensalamander (Genus *Andrias*, Urodela, Amphibia). Palaeontographica, Abteilung A 110:20–92.
Zerova, G. A. 1985. Preliminary results on middle Sarmatian herpteofauna of Ukraine; pp. 78–79 in I. Darevsky (ed.), Abstract Book of 6th All Soviet Herpetological Conference. Nauka, Tashkent, 18–20 September 1985. [Russian]
Zhang, P., Y.-Q. Chen, H. Zhou, Y.-F. Liu, X.-L. Wang, T. J. Papenfuss, D. B. Wake, and L.-H. Qu. 2006. Phylogeny, evolution, and biogeography of Asiatic Salamanders (Hynobiidae). Proceedings of the National Academy Sciences of the United States of America 103:7360–7365.

Submitted December 27, 2011; revisions received August 5, 2012;
accepted August 10, 2012.
Handling editor: Jason Anderson.

APPENDIX 1. List of osteological characters used in the phylogenetic analysis.

Dentary

(1) Shape of symphysis in cross-section: round or oval (0); elongated elliptical (1).
(2) Triangular ventral space between the dentaries: large (0); small (1) (relationship between large and small ~1.5:1).
(3) Sculpture of the dermal ossification on labial side of dentary: smooth or slightly wrinkled (0); rugose to pustular and pointed (1).
(4) Lingual crista on dentary: absent (0); present (1).
(5) Lingual surface of corpus dentalis between symphysis and beginning of Meckelian cartilage, under lamina dentalis is plain (0); has deep groove—presymphyseal sulcus (1). Comment: *Andrias scheuchzeri* has a slight 'S'-shaped depression, which we consider to be plain (0) with respect to the scores used herein.
(6) Ventral keel of dentary: not prolonged (0); prolonged (1).
(7) Pars dentalis: consists of dental lamina only (0); subdivided into a dental and subdental lamina (1).
(8) Dental shelf: plain or shallow (shallowly concave surface) (0); deep (1).
(9) Mental foramina small, longitudinal flange not pronounced or slightly pronounced (0); mental foramina large (more than 1.5 times larger), longitudinal flange pronounced (1).
(10) Lateral and ventral ala of symphysis: large and small (in relation ~2:1), respectively (0); small and large (in relation ~1:2), respectively (1); small and small, respectively (2).
(11) Lateral and ventral ala of symphysis: not fused (0); fused (1).
(12) Dentine shaft of tooth crown: present (0); reduced or absent (1). Comment: Data taken from Böttcher (1987) and Greven and Clemen (1980, 2009).

Articular

(13) Articulation facet of articular-dentary: not pronounced (0); pronounced (1).
(14) Labioventral facet of articular: narrow and relatively rough (0); broad and sculptured with prominent pits and ridges (1).
(15) Articular condyle: elongated (0); short (1) (<1.5:1 relationship).
(16) Articular condyle: broad (0); narrow (1) (<1.5:1 relationship).

Coronoid

(17) Coronoid process: narrow (0); broad (1) (<1:1.5 relationship).
(18) Coronoid process: long (0); short (1) (<1.5:1 relationship).

Occipital

(19) Pericondylar facet of occipital: absent or fragmentarily preserved (0); present (1).

Squamosal

(20) Squamosal: not robust (0); robust (1).
(21) Eminentia dorsalis: absent (0); present (1).
(22) Paries posterior: low (lower than paries anterior) (0); high (higher than paries anterior) (1).
(23) Paries posterior: extends parallel and ventral to the paries dorsalis (0); extends along paries dorsal with an obtuse angle (1).

Femur

(24) Femoral crest: short (terminates at the mid-diaphyseal position) (0); long (terminates at the lateral wall of trochlear groove) (1).

Vertebrae

(25) Prezygapophysis and the facies articularis prezygapophysis: extremely elongated ellipse (0); round or slightly elongated (1).
(26) Interzygapophyseal ridge, running between pre- and postzygapophysis: absent or poorly developed (0); well developed and builds lamella above transverse process (1).
(27) Beginning of hemal process: lamella like (0); oval (1).
(28) Hemal processes positioned: at the middle part of vertebra centrum (0); at the posterior portion of vertebral centrum (1).
(29) Arterial canal in caudal vertebrae: narrow, with small foramen (0); broad, with large foramen (1).

Other Characters

(30) Terminal phalanges: robust, without bulbous tips (0); slender, with bulbous tip (1).
(31) Degree of ossification of the dentary: high (bone compactness value >0.8) (0); low (bone compactness >0.8) (1). Comment: The bone compactness value of *Onychodactylus fischeri* in Laurin et al. (2004) is given for the femur. However, the compactness value of the femur is slightly lower than that of *Andrias japonicus* and *Cryptobranchus alleganiensis*. So, we consider the value for the dentary of *Onychodactylus fischeri* to be more than 0.8.
(32) Trunk ribs: bicapitate (0); unicapitate (1). Comment: The hynobiids were reported to have unicapitate ribs (Duellman and Trueb, 1994). This character was considered as a derived character state of the suborder Cryptobranchoidea (Cryptobranchidae + Hynobiidae) (Duellman and Trueb, 1994). However, there are several species of hynobiids both Recent (*Onychodactylus japonucus*, see Okajima, 1908:fig. 6e–j, table 13; *Onychodactylus fischeri*, GPIT/RE/7331; *Ranodon sibiricus*, see Kuzmin and Thiesmeier, 2001:fig. 35) and fossil (*Parahynobius kordosi, Parahynobius betfianus,* cf. *Parahynobius*, see Venczel, 1999:figs. 1, 3, 4; *Ranodon* cf. *sibiricus*, see Averianov and Tjutkova, 1995:figs. 3, 4; *Salamandrella* sp., GPIT unnumbered specimen), which show bicapitate ribs, as well as two articulation surfaces on the distal end of the transverse processes of the trunk vertebrae. We did not find any hynobiid species that show unicapitate ribs like those reported by Duellman and Trueb (1994).
(33) Adult body size: small (<1 m) (0); large (>1 m) (1).
(34) Parietal and squamosal: partial or not connected (0); completely connected (1).
(35) Processus prefrontalis of maxillae: absent (0); present (1).
(36) Vomerine dentition: curved row parallel to the maxillary and premaxillary teeth, the tooth row lies anteriorly on the vomer (0); vomerine dentition pattern is transverse and does not parallel the maxillary and premaxillary teeth, the tooth row lies posteriorly on the vomer (1). Altered from Duellman and Trueb (1994:464).
(37) Gill slits: absent (0); present (1).
(38) Hyobranchial apparatus: includes ossified ceratobranchial 2 and hyobranchial 2 (0); includes distal part of ceratohyal, ceratobranchial 2, and hyobranchial 2 (1).
(39) Number of bones surrounding external naris: four bones (frontal, nasal, maxilla, and premaxilla) (0); three bones (nasal, maxilla, and premaxilla) (1).

APPENDIX 2. Character-taxon matrix used for phylogenetic analysis. '?' denotes non-preservation and '-' is a non-applicable character state.

An. japonicus	0 0 0 0 0 0 0 1 0 2 1 1 1 0 0 1 0 0 0 0 0 0 0 0 1 0 0 0 0 0 0 1 1 1 0 0 0 0 1
An. davidianus	0 0 0 0 0 0 0 1 0 1 1 1 1 0 0 1 0 0 0 0 0 0 0 0 1 0 0 0 0 0 0 1 1 1 1 0 0 0 1
An. scheuchzeri	0 0 0 0 0 0 0 1 0 0 0 1 1 0 0 1 1 1 0 0 0 0 0 0 1 0 0 0 ? 0 0 1 1 1 0 0 0 0 1
U. hypsognathus	1 1 1 1 0 1 1 0 1 ? ? ? 0 1 0 0 1 0 1 1 1 1 1 0 0 0 1 1 1 1 1 1 1 1 ? ? ? ? ?
Z. beliajevae	0 0 0 0 1 0 0 1 0 1 0 ? 1 0 1 1 0 0 0 0 0 ? ? 0 1 0 ? ? ? ? 0 1 1 1 1 0 ? ? ?
Av. exsecratus	0 0 0 0 1 0 0 1 0 0 0 ? ? ? ? ? ? ? 0 ? ? ? ? 1 1 1 ? 0 ? ? 0 1 1 1 ? ? ? ? ?
C. alleganiensis	0 0 0 0 0 0 0 1 0 1 1 0 1 0 0 1 0 0 0 0 0 0 0 0 1 0 0 0 0 0 0 1 1 1 0 0 1 1 0
'C.' saskatchewanensis	1 1 0 ? 1 0 0 0 0 0 0 ? 1 ? ? ? ? ? ?
O. fischeri	0 - 0 0 0 0 0 0 - - - 0 0 - 0 0 0 0 0 0 0 - - 0 0 0 0 0 0 ? 0 0 0 0 0 1 0 0 0

3.2. Paper # 2: Pronounced Peramorphosis in Lissamphibians—*Aviturus exsecratus* (Urodela, Cryptobranchidae) from the Paleocene–Eocene Thermal Maximum of Mongolia

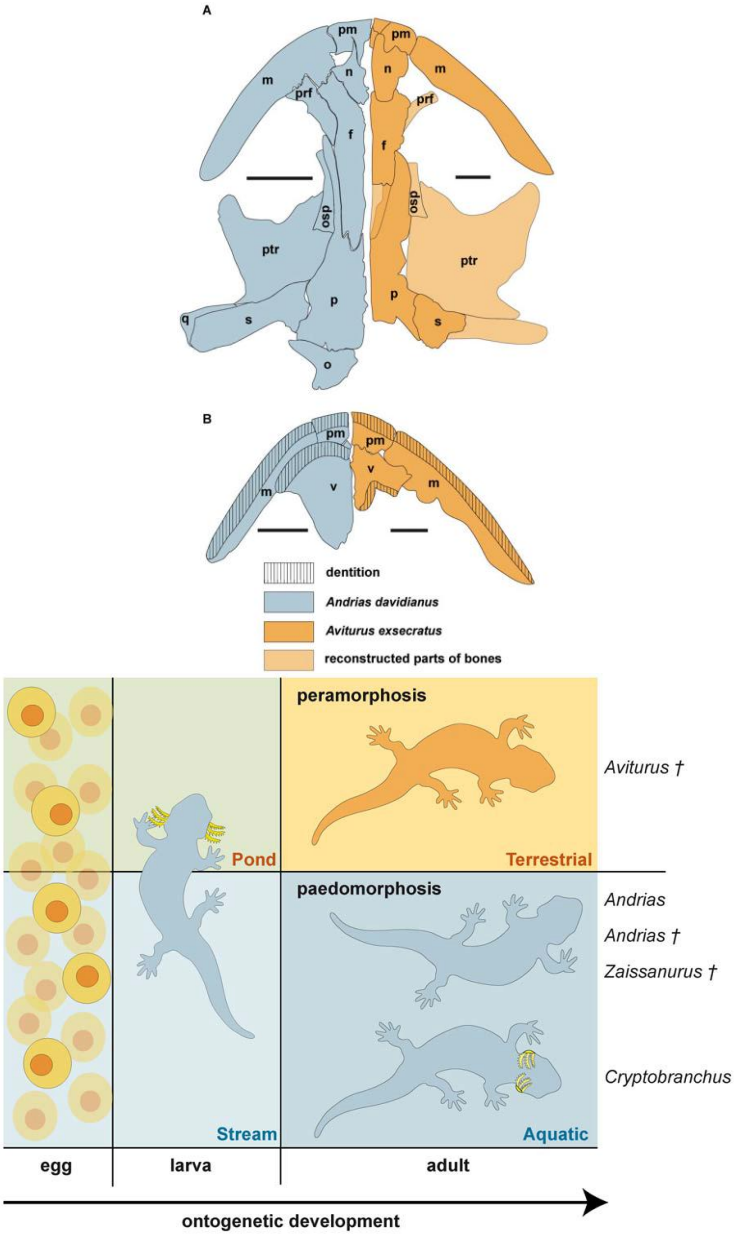

Own contribution:

Scientific ideas (%)	50
Data generation (%)	75
Analysis and Interpretation (%)	85
Paper writing (%)	85

OPEN ACCESS Freely available online

PLOS ONE

Pronounced Peramorphosis in Lissamphibians—*Aviturus exsecratus* (Urodela, Cryptobranchidae) from the Paleocene–Eocene Thermal Maximum of Mongolia

Davit Vasilyan[1]*, Madelaine Böhme[1,2]

1 Department for Geoscience, Eberhard-Karls-University Tübingen, Tübingen, Germany, **2** Senckenberg Center for Human Evolution and Palaeoecology (HEP), Tübingen, Germany

Abstract

Background: The oldest and largest member of giant salamanders (Cryptobranchidae) *Aviturus exsecratus* appears in the latest Paleocene (near the Paleocene–Eocene Thermal Maximum) of Mongolia. Based on femoral and vertebral morphology and metrics, a terrestrial adaptation has been supposed for this species.

Methodology/Principal Findings: A detailed morphological reinvestigation of published as well as unpublished material reveals that this salamander shows a vomerine dentition that is posteriorly shifted and arranged in a zigzag pattern, a strongly developed olfactory region within the cranial cavity, and the highest bone ossification and relatively longest femur among all fossil and recent cryptobranchids.

Conclusions/Significance: The presence of these characteristics indicates a peramorphic developmental pattern for *Aviturus exsecratus*. Our results from *Av. exsecratus* indicate for the first time pronounced peramorphosis within a crown-group lissamphibian. *Av. exsecratus* represents a new developmental trajectory within both fossil and recent lissamphibian clades characterized by extended ontogeny and large body size, resembling the pattern known from late Paleozoic eryopines. Moreover, *Av. exsecratus* is not only a cryptobranchid with distinctive peramorphic characters, but also the first giant salamander with partially terrestrial (amphibious) lifestyle. The morphology of the vomers and dentaries suggests the ability of both underwater and terrestrial feeding.

Citation: Vasilyan D, Böhme M (2012) Pronounced Peramorphosis in Lissamphibians—*Aviturus exsecratus* (Urodela, Cryptobranchidae) from the Paleocene–Eocene Thermal Maximum of Mongolia. PLoS ONE 7(9): e40665. doi:10.1371/journal.pone.0040665

Editor: Casper Breuker, Oxford Brookes University, United Kingdom

Received January 12, 2012; **Accepted** June 11, 2012; **Published** September 19, 2012

Funding: The work was financed by Deutsche Forschungsgemeinschaft, grant nr. BO1550/14-1 to MB. The funders had no role in study design, data collection and analysis, decision to publish, or preparation of the manuscript. No additional external funding received for this study.

Competing Interests: The authors have declared that no competing interests exist.

* E-mail: davit.vasilyan@ifg.uni-tuebingen.de

Introduction

The recent species of the clade Cryptobranchidae are characterized by unicapitate rips, huge body size, obligate paedomorphy, and strict aquatic lifestyle. The adult vomerine teeth are of larval dentition type, i.e., lying in a curved row parallel to the maxillary dentition. The lacrimal and septomatomaxillary bones as well as the eyelids are absent [1–5]. In the present day, one species of giant salamander inhabits North America, China and Japan, respectively [3]. It is accepted that fossil cryptobranchids do not differ significantly from the morphology and biology of living forms [2,4,6,7], although terrestrial adaptations were suggested for *Av. exsecratus* based on the some peculiarities of the axial skeleton, femur, and skull [8].

Aviturus exsecratus is the oldest Cenozoic giant salamander species from Eurasia. It was described by Gubin [8] from the terminal Paleocene Nara-Bulak formation of Mongolia (Paleocene-Eocene Thermal Maximum).

Here we re-examine the material described by Gubin [8] and study additional bones of *Av. exsecratus* from the Naran-Bulak formation. Our results substantiate the suggestion of Gubin [8] that this species exhibit terrestrial adaptations. Moreover, we provide extended information on life style and life history strategy by analyzing skull morphology, the vomerine dentition, the olfactory region of cranial cavity, bone density, as well as the axial and appendicular skeleton. Importantly, we show that *Av. exsecratus* is the first lissamphibian showing a peramorphic life history. Based on our results we are in the position to emend the diagnosis of the family Cryptobranchidae.

Results

Systematic palaeontology

Amphibia Linnaeus, 1758.
Lissamphibia Haeckel, 1866 (sensu Pyron, 2011).
Caudata Scopoli, 1777.
Urodela Duméril, 1806.
Cryptobranchidae Fitzinger, 1826.

Type species. *Andrias scheuchzeri* (Holl, 1831).

Distribution. Possibly in the Late Jurassic of China; Paleocene-Holocene of the Holarctic.

Emended diagnosis. Very large salamanders up to 2 meters, with paedomorphic or peramorphic life history strategy, and aquatic or amphibious life style. Bilateral asymmetric kinetics of

the lower jaw. Parietal and squamosal bones are directly connected and ribs are unicapitate.

***Aviturus* Gubin, 1991.**

Type species. *Aviturus exsecratus* Gubin, 1991.

Distribution. As for the type and only species.

Revised Diagnosis. Same as for the type species and only species.

***Aviturus exsecratus* Gubin, 1991.**

Fig. 1, 2, 3, 4, 5, 6, 7.

Holotype. PIN 4357/27, an almost complete left dentary (Gubin, 1991: fig. 5, tabl.8).

Holotype Locality, Age, and Horizon. Aguy-Dats-Bulak locality, Nemengatin Basin, Ömnögovi Province, Mongolia; Naran member of the Naran Bulak formation, cycle VI [9], latest Paleocene, late Gashatan Asian Land Mammal Age.

Referred Specimens. Four frontals (two pairs): PIN 4357/11, 15; eight parietals (four pairs): PIN 4357/8–10, 12–14, 73; seven premaxillae (three single, two pairs): PIN 4357/1–6; three maxillae: PIN 4357/21, 22, 24; two nasals (one pair): PIN 4357/7; one quadrate: PIN 4357/19; three squamosals: PIN 4357/8, 12, 73; one occipital: PIN 4357/16; five dentaries (three single, one pair): PIN 4357/27, 28, 32, 4358/1, 2; two vomer: PIN 4357/X; three atlases: PIN 4357/34–36; one femur: PIN 4356/1; one ilium: PIN 4357/33; 13 trunk vertebrae: PIN 4356/2–5, 4357/37, 39, 41, 42, 44, 46, 49, 52, 56; one caudal vertebra: (PIN 4357/61); one rib: PIN 4357/62.

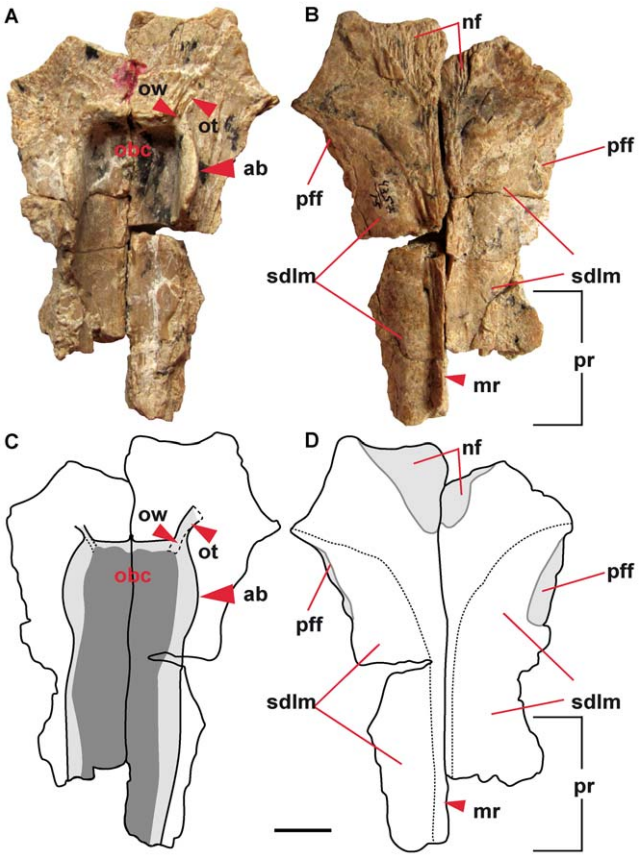

Figure 1. Frontal (PIN 4357/15) of *Aviturus exsecratus* from ventral (A, C) and dorsal (B, D) views. (A), (B) photographs and (C), (D) graphic representations. **Abbreviations**: ab, anterior bump; mr, medial (sagittal) ridge; nf, nasal facet; pff, prefrontal facet; pr, parietal ramus; obc, olfactory region of cranial cavity; ot, olfactory tract; ow, olfactory windows; sdlm, attachment surface of deep levator mandibulae anterior muscle. Scale bar = 1 cm.
doi:10.1371/journal.pone.0040665.g001

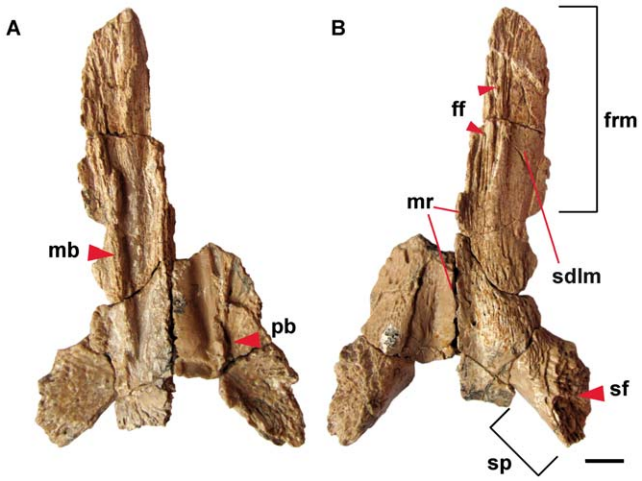

Figure 2. Parietal (PIN 4357/13+73) of *Aviturus exsecratus* in (A) ventral and (B) dorsal views. Abbreviations: ff, frontal facet; frm, frontal ramus; mb, medial bump; mr, medial (sagittal) ridge; pb, posterior bump; sdlm, attachment surface of deep levator mandibulae anterior muscle; sf, squamosal facet; sp, squamosal process. Scale bar = 1 cm.
doi:10.1371/journal.pone.0040665.g002

The eight parietals belong to at least four individuals i. PIN 4357/13+73, ii. PIN 4357/08+12, iii. PIN 4357/9+10, iv. PIN 4357/14. The (right) squamosal PIN 4357/73 belongs to the first and the (left) squamosal PIN 4357/12 to the second individual. Two vomers (PIN 4357/X), a right maxilla PIN 4357/21, a pair of premaxillae (PIN 4357/1), a pair of nasals (one pair) (PIN 4357/7) and a pair of frontals (PIN 4357/15) furthermore belong to the i. indivual (see skull reconstruction Fig. 5).

All material coming from the type locality was within a small surface area (1.5×5 m) and belongs to 3–4 individuals. These individuals do not differ significantly from each other and some bones preserve lifetime articulations [8], which we could not be observe by us on the material.

All bones assigned to i. individual originate from the type locality and can be easily assigned to one individual based on the presence of obvious overlapping articulation surfaces and complementing sutures between neighbouring bones. Two (right [PIN 4357/27] and left [PIN 4357/28]) dentaries can be assigned to the i. individual based on their length and the size of reconstructed skull.

Distribution. Naran member localities, Nemengatin Basin, Ömnögovi Province, Mongolia [8,9].

Revised Diagnosis. Very large salamanders up to 2 meters, with peramorphic life history strategy and amphibious life style; bones massive and strongly ossified; skull relatively high and triangular in outline; skull roof with a sagittal crest for mandibular levator muscles attachment; vomerine dentition shifted posterior and arranged in a zigzag pattern; long premaxillary facet of the vomer; frontals anteriorly broad; parietals slender; substantially modified large and anteriorly closed cranial cavity with high and strong ossified lateral walls; large and deep olfactory grooves and existing olfactory windows and tracts; parietal-squamosal contact oblique to the sagittal axis; caput squamosa long and wide; posterior squamosal lamina strongly developed; trunk vertebrae with pronounced interzygapophyseal ridge, which covers the proximal part of transverse process; large hind limb (femoral index

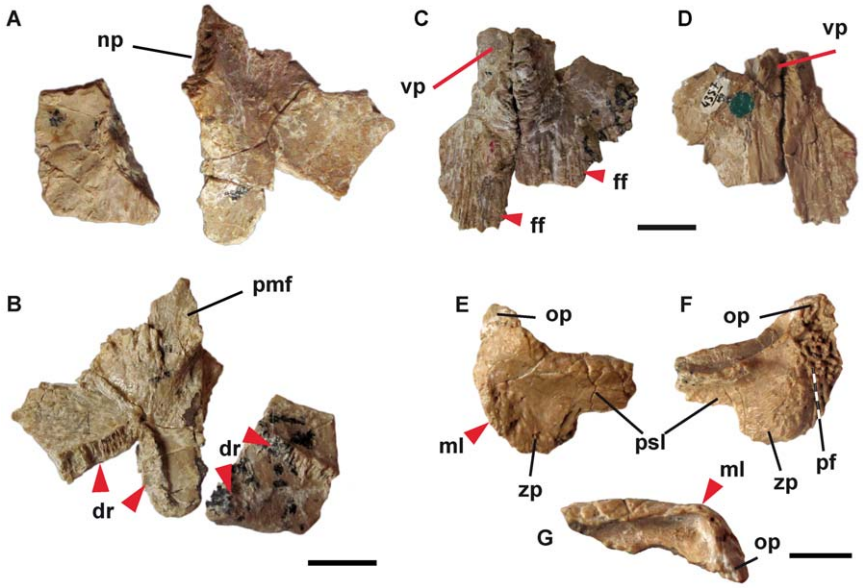

Figure 3. Right and left vomers (PIN 4357/13), nasals (PIN 4357/7), and right squamosal (PIN 4357/73) of *Aviturus exsecratus*. (A) dorsal and (B) ventral views of vomers, (C) ventral and (D) dorsal views of nasals and (E) dorsal, (F) ventral, (G) anterior views of right squamosal. **Abbreviations**: dr, dental row; ff, frontal facet; ml, marginal lamina; np, nasal process; op, otic process; pf, parietal facet; psl, posterior squamosal lamina; pmf, premaxillar facet; vp, vomerine process; zp, zygomatic process. Scale bar = 1 cm.
doi:10.1371/journal.pone.0040665.g003

2.79); large and long trochanteric crest on femur reaching the trochlear groove, broad and large trochanteric groove, proximal end with pretrochanteric fossa and pronounced foveal depression, dorsal side of distal end with "intercondylar" crest and "intercondylar" fossa, distal and proximal ends of femoral shaft are filled with spongious bone.

Description

Skull. The paired frontals are triangular in outline, anteriorly broad and posteriorly narrow. They are connected to each other along their entire length by a suture. The posterior part of the suture is prominent and forms a median (sagittal) ridge, which widens anteriorly into a triangular plain plateau (Fig. 1). Posterolaterally to this plateau the surface of the frontal is convex and forms a large and elongated facet (Fig. 1) for the attachment of the tendinous sheets of the deep levator mandibulae anterior muscle [10]. The frontals overlie with their posterior portions the parietals and built the parietal ramus. The anterior portion of the frontals is covered with a triangular nasal facet. The lateral positioned facets for the prefrontals are slightly curved and narrow (Fig. 1).

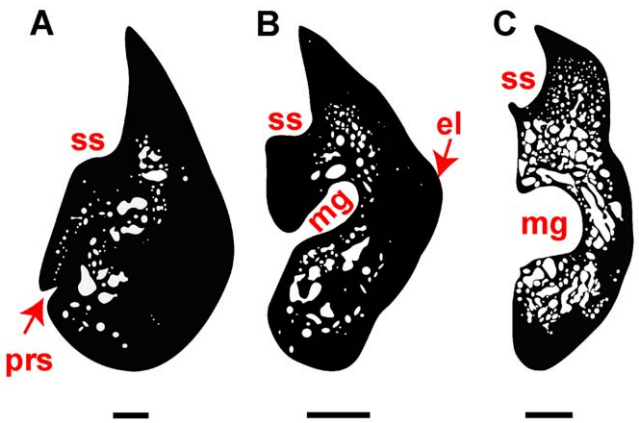

Figure 4. Dentary cross sections of *Aviturus exsecratus*, drawn from natural cross section. (A) position i (PIN 4357/27), (B) pos. ii (PIN 4357/13), and (C) pos. iii (PIN 4357/27). **Abbreviations**: mg, Meckelian groove; el, eminentia longitudinalis; prs, presymphyseal sulcus; ss, subdental shelf. Scale bar = 5 mm.
doi:10.1371/journal.pone.0040665.g004

The parietals are also triangular in outline; posteriorly broad and narrowing anteriorly. The right and left parietals are connected along a medial suture along two-third of their length (Fig. 2). The anterior part of the bone, the frontal ramus, is slightly bent laterally and medially not connected to the opposite parietal (there is a deep antero-sagittal slot on the paired parietals). The lateral portion of frontal ramus is plain and belongs to the facet for the attachment of the deep levator mandibulae anterior muscle. The median (sagittal) ridge that originates from the frontal extents onto the parietal, and becomes lower posteriorly (Fig. 2). In this portion, which represents the posterior third of the parietal, the area between the lower medial (sagittal) ridge and the squamosal process is deeply concave for the attachment of the superficial levator mandibulae anterior muscle [11]. The posterolateral corners of parietals are robust and build the squamosal process with a highly rough squamosal facet. The facet is anteromedially directed and has an elongate, oval-shape surface. On the ventral side of each parietal, at the posterolateral corners of the cranial cavity, a relatively large deepening is visible (Fig. 2).

The ventral surface of the parietals and frontals form the roof of the cranial cavity. The cranial cavity of *Av. exsecratus* has an elongate, oval shape, as in recent giant salamanders, and is bordered by the lateral wall (crista sagitalis sensu [12]). The lateral wall has three bumps (posterior, medial and anterior) to connect the cranial cavity roof to the parasphenoid. The posterior and medial bumps lie on the parietals and the anterior one on the frontal. According to the positions of these bumps, we recognize three portions of the cranial cavity (Fig. 1A, 1C). Accordingly, the anterior portion lies below the frontal, the middle portion below

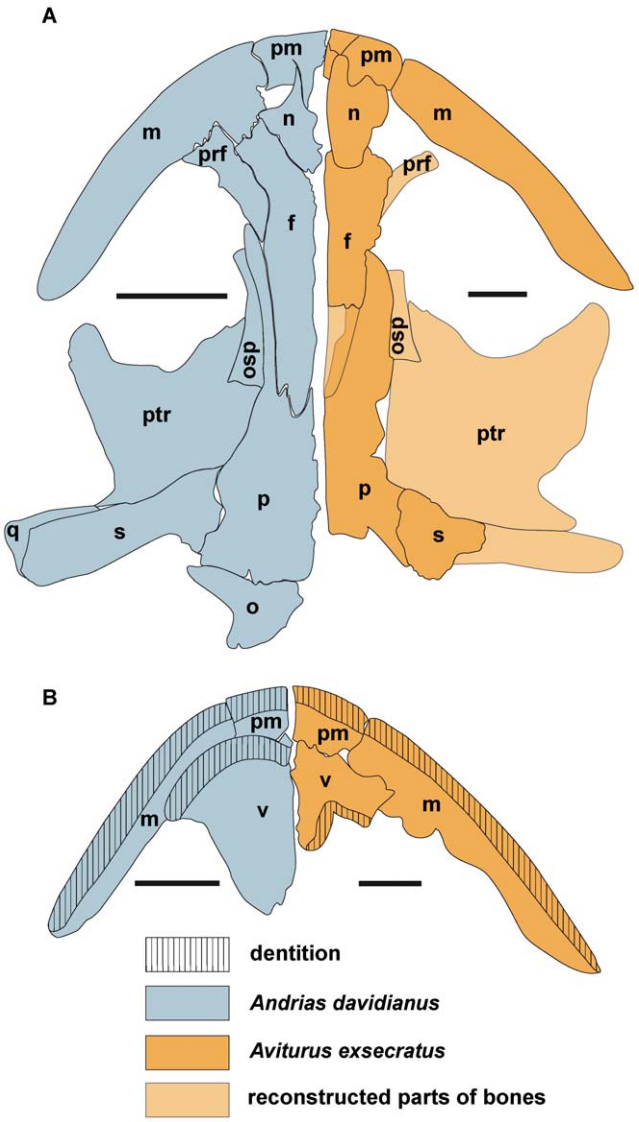

Figure 5. Skull schematic draw of *Andrias davidianus* and skull reconstruction of *Aviturus exsecratus*. (A) in ventral view, showing the dentition pattern on upper jaw and (B) from dorsal view. **Abbreviations**: f, frontal; n, nasal; m, maxillary; o, occipital; p, parietal; osp, orbitosphenoid; pm, premaxillary; prf, prefrontal; ptr, pterygoid; q, quadrate; s, squamosal; v, vomer. Scale bars = 5 mm.
doi:10.1371/journal.pone.0040665.g005

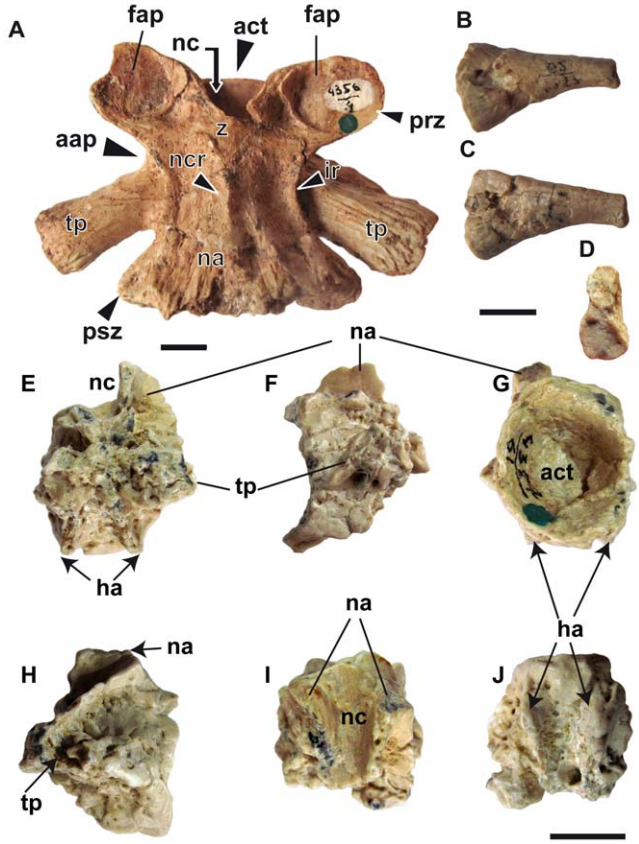

Figure 6. Axial skeleton elements of *Av exsecratus*. (A) PIN 4356/4, a trunk vertebra in dorsal view. (B–D) PIN 4357/62, a rip in anterior (B), posterior (C) and medial (D) views. E–J. PIN 4356/61, a caudal vertebra in posterior (E), left lateral (F), anterior (G), right lateral (H), dorsal (I) and ventral (J) views. **Abbreviations**: aap, anterior alar process; act, anterior cotyle; fap, facies articularis prezygapophysialis; ha, haemapophysis; ir, interzygapophyseal ridge; na, neural arc; nc, neural canal; ncr, neural crest; prz, prezygapophysis; psz, postzygapophysis; tp, transversal process; z, zygosphene. Scale bar = 1 cm.
doi:10.1371/journal.pone.0040665.g006

both the frontal and parietal, and the posterior one only below the parietal. The anterior portion is nearly heart-shaped and forms the olfactory region of the cranial cavity. Here, as in the recent species [1], lies the forebrain, with its olfactory bulbs. The olfactory region of *Av. exsecratus* is very deep and envelops a large volume. In the anterolateral corners of the cranial cavity, the olfactory windows are developed, from which the olfactory tracts run anterolaterally.

The anterior half of the vomers are preserved (PIN 4357/X). On the smooth dorsal side of the bone an oval nasal process ascends at the anteromedial corner. The ventral side bears a long premaxillar facet in the anterior portion. The dental row shows a dentition pattern that is unusual for cryptobranchids vomers: the tooth row is posteriorly shifted and has a zigzag form (Fig. 3B).

The caput squamosa and the proximal part of quadrate ramus of the squamosals (PIN 4357/12, 73) are preserved (Fig. 3E–G). The bones are relatively flattened and broad. The caput squamosa is long and wide. On its dorsal side, nearly subparallel to the parietal facet, a prominent ridge runs – the marginal lamina. The parietal facet is straight and anteromedially directed (oblique to the sagittal plane), moderately rugose and extents anteriorly into the otic process. A robust, horizontal orientated lamina (posterior squamosal lamina) exists on the posterior border of the proximal quadrate ramus (Fig. 3F). The tendon of the strong anterior depressor mandibulae muscle is attached to this lamina.

The dentary is primarily described by Gubin [8], but additional information can be given. *Av. exsecratus* has, as is typical for cryptobranchids, a convex symphysial contact. We furthermore quantified bone compactness values for the dentary. These value were estimated at the positions i, ii and iii (PIN 4357/13, -/27) (see [5]), and are 0.933, 0.906 and 0.736, respectively (Fig. 4). *Av. exsecratus* shows the highest value of bone ossification among studied giant salamanders. The medullary cavity does not form two large cavities above and under the longitudinal flange. Along

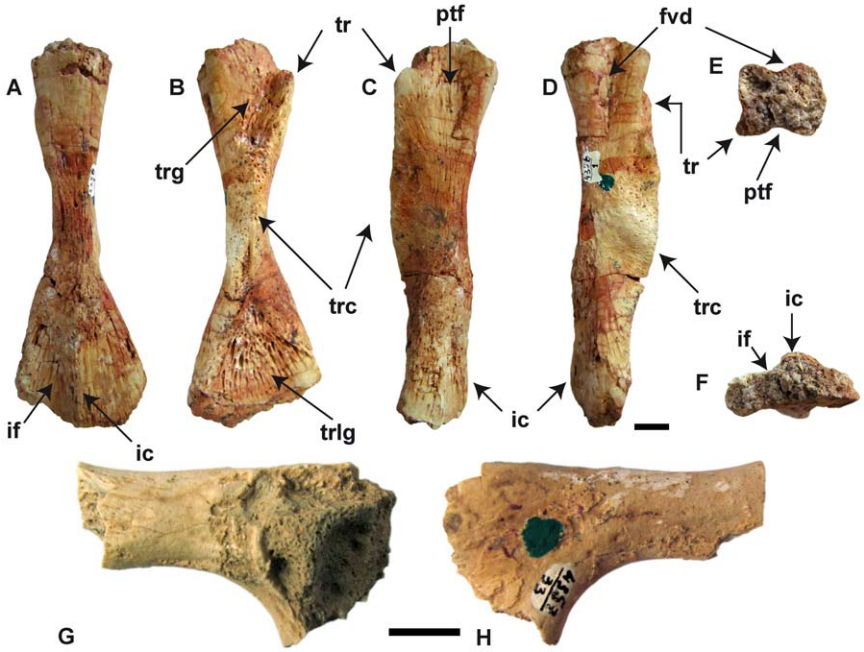

Figure 7. Femur (PIN 4356/1) and ilium (PIN 4357/33) of *Aviturus exsecratus*. Femur in (A) dorsal, (B) ventral, (C) anterior, (D) posterior views and (E) proximal, (F) distal ends. Ilium in (G) lateral and (H) medial sides. **Abbreviations**: fvd, foveal depression; ic, "intercondylar" crest; if, "intercondylar" fossa; ptf, pretrochlear fossa; tr, trochanter; trc, trochanteric crest; trg, trochanteric groove; trlg, trochlear groove. Scale bar = 1 cm.
doi:10.1371/journal.pone.0040665.g007

the dentary medullary cavity extends and posteriorly strongly defuses in the compact bone.

We reconstruct the outline of the skull based on bones from a single individual (skull length from the snout tip to the end of parietals is ≈18 cm). The bone outlines were drawn from photographs and by comparison to recent giant salamanders. These are: right and left premaxillary (PIN 4357/1), a right maxillary (PIN 4357/21), right and left nasal (PIN 4357/7), right and left frontal (PIN 4357/15), as well as a parietal (PIN 4357/13+73), and the right squamosal (PIN 4357/73), right and left vomer (PIN 4357/X). In our reconstruction the general outline of the skull is nearly triangular (Fig. 5). Since the nasal is relatively broad (Figs. 3C, 3D, 5), the frontal was probably excluded from the naris, like in *Andrias japonicus*, *Andrias davidianus*, and *Andrias scheuchzeri* (Fig. 5).

Axial skeleton. The axial skeleton is represented by isolated 17 trunk vertebrae, which are described in Gubin [8]. However, we found some new characters to be described. The vertebrae (PIN 4356/4, 5, etc.) display pronounced interzygapophyseal ridges (Fig. 6A). The accessory alar process is prominent and begins from the anteromedial corner of the transverse process and ends at the ventral surface of prezygapophysis. In some specimens (PIN 4356/2, 3, etc.) the alar process is connected with the interzygapophysal ridge.

The single caudal vertebra is incompletely preserved. Like in other cryptobranchids (but unlike gen. et sp. nov. from the Miocene of Ukraine, see [5]) the bases of the haemapophysis arise in the middle part of centrum (Fig. 6E–J).

The only preserved rib of *Av. exsecratus* (Fig. 6B–D) shows the same morphology as in all other cryptobranchids [5]: an unicapitate articulation surface to the transversal process of trunk vertebra.

Appendicular skeleton. The proximal end of the femur (PIN 4356/1) is sub-quadrate in cross-section and has concave anterior (foveal depression) and posterior (pretrochanteric fossa) surfaces (Fig. 7C–E). The trochanteric (femoral) crest is high and massive, and the trochanteric groove is extended. The distal femoral end shows developed "intercondylar" crest and "intercondylar" fossa (Fig. 7A, C, D, F) and expanded trochlear groove (Fig. 7B). The bone is highly ossified.

A single highly damaged ilium (PIN 4357-33) of *Av. exsecratus* is preserved (Figs. 7G, 7H). Earlier the bone was figured but not described in Gubin (1991). The observable morphology of the bone fully agrees with that of recent crpytobranchids. That concerns specially the smooth bone surface, the large acetabulum and distally ascending acetabular surface, the morphology of the ilial shaft as well as that of the medial aspect of the ilium.

Discussion

Aviturus exsecratus shows characteristics typical for cryptobranchids, such as the large body size, unicapitate ribs, direct parietal – squamosal connection, as well as bilateral asymmetric kinetics of the lower jaw. The caudal vertebra of *Av. exsecratus* also resembles those of all other giant salamanders, with exception of a new genus from the Miocene of Ukraine. The caudal vertebra of the latter is characterised by elongated oval haemal process, lying in the middle part of the centrum. However, *Av. exsecratus* can be easily distinguished from the recent and other fossil cryptobranchids, by the combination of the following characteristics:

1. *Av. exsecratus* has the most ossified bone tissue among all cryptobranchids. The dentary bone compactness value in *Av. exsecratus* shows the highest values among other giant salamanders [5].

2. The vomerine dentition lies on the ventroposterior surface of vomer and has a zigzag arrangement. All other cryptobranchids (*Zaissanurus beliajevae*(Chkhikvadze, 1982, fig. 4, plate II), *Andrias* spp. (SMNS 7898:1–15, ZFMK 90469, SMNK-PAL.6612), *Cryptobranchus* sp. (ZFMK 5245)) show an anteriorly lying row of vomerine teeth that are oriented parallel to the maxillae and premaxillae.
3. The parietal – squamosal contact is completely different from other cryptobranchids. It is straight and oblique to the sagittal plane in *Av. exsecratus*, whereas in other giant salamanders the contact is slightly bended and runs parallel.
4. *Aviturus exsecratus* has larger and wider caput squamosa.
5. The cranial cavity of *Av. exsecratus* is bordered by prominent lateral walls with three elevated bumps. This lateral wall is poorly developed in the recent giant salamanders, generally it is seen only by the bumps. The olfactory region of the cranial cavity of *Av. exsecratus* is the largest and deepest among cryptobranchids. This region in the recent cryptobranchids is a slightly concave surface or a low deepening, but does not form any groove (Fig. 8). Moreover, the olfactory window and olfactory tract are clearly visible in *Av. exsecratus* (Fig. 1A, C). In the recent species these elements are absent or extremely weak developed (Fig. 8). The anterior end of the cranial cavity is not closed in recent salamanders, whereas in *Av. exsecratus* it is closed.
6. *Aviturus exsecratus* displays the strongest cranial musculature (see below) among cryptobranchids.
7. Unlike other cryptobranchids the trunk vertebrae display strong interzygapophyseal ridges and prominent accessory alar process. Both features indicate strong development of intervertebral muscles, responsible for powerful movements (straightening, stretching, rotating, torsion) of the vertebral column [1].
8. The femur of *Av. exsecratus* can be distinguished from other cryptobranchids by the relatively largest and longest trochanteric crest, which reachs the trochlear groove, whereas in all other giant salamanders the crest terminates in the narrowest section of the bone. The distal and proximal ends of femoral shaft are filled with spongious bone, whereas in all other cryptobranchids both are not filled at all. *Aviturus exsecratus* has the broadest and largest trochanteric groove, which in other cryptobranchids is narrow and shallow, and sometimes not developed at all. The distal part of the bone from the dorsal side shows an ''intercondylar'' crest and fossa, which are absent in all cryptobranchids. The proximal end of the bone from anterior and posterior view is concave and forms foveal depression and pretrochanteric fossa accordingly. In all other fossil and recent giant salamanders, the foveal depression is slightly visible and the pretrochanteric fossa is absent. Presence of well pronounced, broad and deep grooves and a high crest are evidence for the strongly developed muscular system of the hind limb of *Av. exsecratus* in comparison to other giant salamanders.
9. *Av. exsecratus* has the largest hind limb relative to body size, which was already suggested by Gubin [8]. His observation (relation of length of femur to the length of largest trunk vertebra) was based on comparison of *Av. exsecratus* with only a single specimen of *Andrias japonicus*. We have estimated femoral index of a larger numbers of specimens (Table 1). *Aviturus exsecratus* has the largest femoral index (2.79) among all cryptobranchids (1.83–2.22), although no value can be calculated for *Zaissanurus beliajevae*, which lack associated femur and trunk vertebra from a single specimen.
10. The skull is triangular in outline, whereas in *Andrias* spp. and *Crytobranchus alleganiensis* the skull has an oval form (Fig. 4). Our skull reconstruction differs from one given in Gubin [8]: fig. 1, p. 98, which shows oval form. Unfortunately, we were not able to verify this skull reconstruction, since not all ref. nr. of the bones used in the reconstruction are clear from the text.

Lifestyle and life history strategy of *Aviturus exsecratus*

In general, data on the ontogeny and lifestyle of fossil giant salamanders is scarce [4]. Only for *Av. exsecratus* a non-typical ecology as ''an active periaquatic and shoreline predator'' was proposed by Gubin [8]: 104 pp., based on peculiarities of the axial skeleton structure, longer limbs, and a higher skull. Our new data confirm this idea. However, due to the detailed analysis of supplementary bones and skeleton parts, e.g., bone ossification, vomer, cranial cavity, as well as skull and axial skeleton, we significantly enlarge our knowledge regarding life style and life history strategy of this oldest Cenozoic cryptobranchid.

Vomerine dentition. The vomerine dentition can be classified in regard to its form and position. According to the position, the dental row can be located along the anterior or the posterior side of vomer, whereas according to form it can be arranged in a zigzag or transverse (i.e., parallel to the maxillary and premaxillary dental rows). The anteriorly lying tooth-row of the vomer is defined as the larval-type (non-metamorphic), the posteriorly lying as the adult-type (metamorphic) [13]. So, the posterior located zigzag vomerine dentition type of *Av. exsecratus* is found in several species of hynobiid salamanders [13]. However, within hynobiids there are also different patterns in the vomerine dentition. Whereas the tooth row lies always on the ventroposterior surface of the vomer, the row can either be arranged in a zigzag (e.g., *Hynobius* and *Salamandrella*) or transverse (e.g., *Ranodon* and *Onychodactylus*) [13].

During the metamorphic remodelling of the vomer in recent salamanders (Hynobiidae, Ambystomidae, Dicamptodontidae, etc.) the larval-type tooth-row is replaced by an adult-type tooth-row [14]. So far, this remodelling was not found in recent or in fossil cryptobranchids.

The zigzag arrangement of the vomerine dentition is characteristic of ''pond-type'' salamanders [13], in which larval development undergoes in still water and the adult feeding is via tongue protraction. ''Pond type'' salamanders live in humid lowlands and have a terrestrial lifestyle. The transverse form of tooth row on vomer characterises ''stream-type'' salamanders [13], in which larval development undergoes in flowing, running water. The adults feed by prehension or suction and live and feed underwater. Transversely oriented vomerine teeth may hinder escape of prey when water is released from the mouth, whereas the ''pond-type'' species mainly feed on small terrestrial invertebrates, which they capture with tongue movements that deliver the prey deep within the mouth, where they are held by the posteriorly directed (zigzag shaped) vomerine tooth row. Similar types of vomerine teeth are present, besides in hynobiids, in plethodontid and salamandrid salamanders, which use the tongue for prey capture [13]. Based on these observations, *Av. exsecratus* is characterized by a peramorphic life history strategy, ''pond-type'' vomerine dentition and amphibious lifestyle.

Terrestrial feeding. *Aviturus exsecratus* has, as typical for cryptobranchids, a convex symphysial contact, which produces a highly mobile mandibular symphysis with two pads of elastic cartilages. The smaller dorsal and larger ventral pads fill triangular spaces between the dentaries and are compressible [11]. This

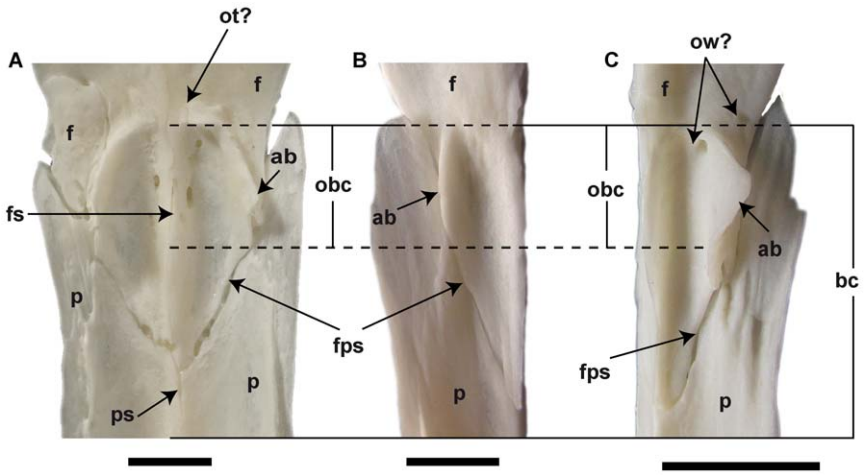

Figure 8. Ventral view of cranial cavity anterior portion in recent cryptobranchids. (A) *Andrias japonicus* (NMA unnumbered specimen). (B) right half of cranial cavity of *An. davidianus* (ZFMK 76996). (C) left half of cranial cavity of *Cryptobranchus alleganiensis* (ZFMK 5245). **Abbreviations**: ab, anterior bump; bc, cranial cavity; f, frontal; fps, frontoparietal sutur; fs, frontal suture; obc, olfactory region of cranial cavity; ot, olfactory tract; ow, olfactory windows; p, parietal; ps, parietal suture. Scale bar = 5 mm.
doi:10.1371/journal.pone.0040665.g008

allows *Aviturus exsecratus* to move the lower jaw during feeding bilaterally asymmetric [11], which provides increased mobility and better manipulation during prey capturing under water.

The morphological investigation of the frontals, parietals, and squamosals reveals a strong development of the mandibular levator and depressor muscles, suggesting substantial force during prey capturing [5,11]. In accordance to increased biting force, the connections of the skull bones are strongly developed, especially the vomerine-premaxillary and the parietal-squamosal contacts. Combining the vomerine dentition type with these lines of evidence, we may suggest that beside the ability of underwater feeding *Aviturus* also possessed a terrestrial mode of feeding.

Olfactory region. *Aviturus exsecratus* is characterised by a well differentiated olfactory region, olfactory tract, and olfactory window of the cranial cavity (Figs. 1A and 1C) in comparison to recent giant salamanders (Fig. 8). For comparison with recent giant salamanders we used both young (skull length 6–8 cm, see Figure 8) and adult individuals (skull length 11 cm [*Andrias davidianus* ZFMK 90469] and 15.5 cm [*Andrias japonicus* PIMUZ A 79]). Both young and adult individuals do not show different degree of developmental of olfactory region of cranial cavity. So, no ontogenetic changes for this character could be observed on the available material. Two existing *Aviturus exsecratus* frontals (PIN 4357/11, 15) are of similar size and also show similar morphology of the olfactory region.

Differentiation of an olfactory lobe, which is located in olfactory region of the cranial cavity, in the anterior part of the cerebral hemisphere occurs in caecilians and anurans [1]. It is poorly developed in most salamanders and is absent in obligate neotenes [1]. The degree of development of the olfactory lobe is positively correlated with development of Jacobson's organ, which is absent in paedomorphic salamanders. There is considerable variation in the complexity of the olfactory organ among salamanders. It is least complex in aquatic taxa, and tends to be more complex in more terrestrial species [1]. The olfactory sense is more important for orientation and seeking prey in terrestrial animals. The well pronounced olfactory region of *Av. exsecratus* is therefore further evidence of its terrestrial lifestyle and non-paedomorphic life history strategy.

Skeleton (bone ossification and femur). Further evidence for a terrestrial lifestyle of *Aviturus exsecratus* is apparent in the skeleton. *Av. exsecratus* has the highest degree of ossification skeleton among giant salamanders, which characterize terrestrial adults in amphibians [15]. As evidenced by the femur, *Av. exsecratus* has the

Table 1. Femoral index (relation of length of femur to the length of largest trunk vertebrae, [8]) in giant salamanders.

Species	n	Femoral index	Specimen or Autor
Aviturus exsecratus	1	2.79	Gubin, 1991
Andrias scheuchzeri	6	1.82–2.22	SMNK-PAL.6612; SMNK-PAL.6613; PIMUZ A/II 1; PIMUZ A/II 2; [4]*
Andrias davidianus	2	1.90–1.96	ZFMK 90469, ZFMK 76996
Andrias japonicus	4	1.95–2.24	SMNS 7898:1–15; PIMUZ A 79; [4,8]*
Andrias sp.	2	2.1–2.2	2 unnumbered specimen in NKMB
Cryptobranchus alleganiensis	2	1.83–1.92	ZFMK 5245; SMNK unnumbered
Cryptobranchidae gen. et sp. nov., Miocene, Ukraine	1	2.18	[5]

*- For 2 specimen of *An. scheuchzeri* (exemplars in collections of Haarlem and London) and 1 specimen (coll. Darmstadt) of *An. japonicas* the figures in [4] is used to estimate the femoral index.
doi:10.1371/journal.pone.0040665.t001

relatively longest hind limbs and well developed process and surfaces for muscle attachment (e.g., trochanteric crest, "intercondylar" crest, "intercondylar" fossa, see Figure 7). These characteristics, including the general femur morphology, are terrestrial adaptations resembling the late Palaeozoic genus *Eryops*, a temnospondyl amphibian. Recent results interpret the lifestyle of *Eryops* either as more terrestrial [16], or more amphibious [15,17]. So, according to Pawley and Warren [16] *Eryops* displays following terrestrial adaptations: highly ossified bones, comparatively large limbs, and well-developed processes for muscle attachments. Whereas, Schoch [15] and Witzmann [17] interpreted the highest degree of ossification of bones, as well as much larger arms and legs as evidences for semi-terrestrial (amphibious) life style of *Eryops*.

Sedimentologic and taphonomic indications. All described *Av. exsecratus* fossils derived from terrestrial, pedogenized overbank sediments [9,18]. These sediments formed the top of alluvial cycles typical for meandering river systems under seasonal climates; starting with cross-stratified sands and ending with white-red mottled palaeosols. None of bones show signs of abrasion. All bones were found as associated, partly articulate skeletons over an area of 1.5×5 meters [18], indicating no post-mortem transport of individual skeleton parts. The palaeosols don't contain any aquatic fossil (e.g., fishes, which are found frequently in the sands). This stratinomic, taphonomic, and lithologic observations point to the suggestion that the burial place in overbank soils near a stream is similar to the living habitat of *Aviturus*.

Conclusions

Metamorphosis and Cryptobranchidae. The three recent cryptobranchids species are strictly aquatic and obligate paedomorphic salamanders. According to our data, the fossil taxa *Andrias scheuchzeri* and *Zaissanurus beliajevae* were also aquatic and paedomorphic. Notable, the recent *Cryptobranchus alleganiensis* is the most paedomorphic, whereas as our studies (data in prep.) showed that recent and fossil species of *Andrias* and *Z. beliajevae* have the same level of paedomorphic development (Fig. 9).

Obligatory paedomorphosis, where the trait is fixed genetically, often at higher taxonomic levels, is associated frequently with environmental adaptation to large, generally permanent bodies of water, including large streams, rivers, lakes, and swamps, as seen in Amphiumidae, Cryptobranchidae, Sirenidae, and (in part) Proteidae [19]. Obligatory paedomorphosis represents an adaptive route to exploiting permanent aquatic habitats in harsh terrestrial environments, including subterranean environments [19]. However, all salamanders excluding cryptobranchids are able to complete their metamorphosis under certain environmental and/or physiological conditions [19], whereas giant salamanders do not undergo metamorphosis even by hormonal treatment [14].

The presence of metamorphic characteristics in *Aviturus* does not necessarily indicate metamorphosis during their ontogeny (i.e., a drastic, short phase of rapid changes, in which a water-living larva transforms into a small-sized land-living adult; see [15]), but rather a peramorphic developmental pattern (Fig. 9). Peramorphosis is the opposite to the pattern of paedomorphosis, during which amphibians create a terrestrial morphology by extending life span, i.e., large intervals between ontogenetic events – resulting in enlargement of body size under permanent ontogenetic development [15]. So far, peramorphic developmental patterns are exclusively known from the early amphibian eryopines [15]. Our results from *Av. exsecratus* indicate for the first time pronounced peramorphosis within a crown-group lissamphibian. Strongly pronounced peramorphic characters within the vomerine dentition, olfactory region, vertebrae morphology, and bone ossification makes *Av. exsecratus* unique among all lissamphibians. Moreover, *Aviturus exsecratus* is not only a cryptobranchid with peramorphic characters, but also the first giant salamander with partially terrestrial (amphibious) lifestyle. Accordingly, its morphology shows the ability both underwater and terrestrial feeding modes.

***Aviturus exsecratus* and the Paleocene–Eocene Thermal Maximum.** The *Av. exsecratus* materials derive from the upper

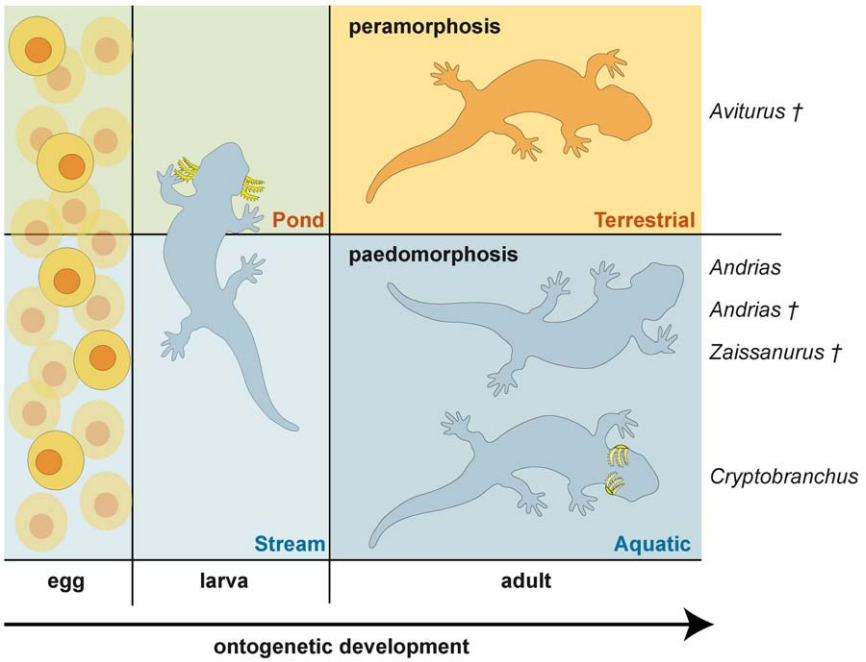

Figure 9. Ontogenetic diversity within Cryptobranchidae.
doi:10.1371/journal.pone.0040665.g009

part of the Naran Member within Naran Bulak Formation in South-Central Mongolia [9,18,20]. The Naran Member can be correlated to the late Gashatan Asian Land Mammal Age and the late Clarkforkian North American Land Mammal Age [21–23]. The *Aviturus*-bearing horizons lying only few meters below the base of the earliest Eocene Bumban Member, thus chronostratigraphically very near to the Paleocene–Eocene Thermal Maximum (PETM; [24]). The PETM is characterized by a transient global temperature rise, probably accompanied by a rise in atmospheric CO_2 [25]. The response of continental ecosystems to this hypothermal event is still poorly known, however, it has been proposed that North American mammals reacted by transient dwarfing [26]. Whether cryptobranchids responded to the PETM by a shift in their ontogenetic trajectories is speculative, in particular so, because high-resolved chronologic dates are missing from the Naran Member. Future investigations are needed to understand the response of amphibian ecology to rapidly increased atmospheric temperatures and CO_2 levels. According to the phylogenetic analysis of Vasilyan et al. [5] *Aviturus exsecratus* is the stratigraphically oldest member of the family Cryptobranchidae. The appearance of cryptobranchids at the Paleocene–Eocene boundary parallels that of several mammalian orders [22,26], which substantiate this time as the main Cenozoic turnover event in terrestrial ecosystems.

Materials and Methods

Anatomical terminology follows Vasilyan et al. [5]. Some of osteological terms are new.

Institutional Abbreviations

NMA, Naturmuseum Augsburg, Augsburg, Germany; PIMUZ, Palaontologisches Institut un Museum der Universitat Zurich; PIN, Paleontological Institute, Russian Academy of Sciences, Moscow, Russia; SMNK, Staatliches Museum für Naturkunde, Karlsruhe, Germany; SMNS, Staatliches Museum für Naturkunde, Stuttgart, Germany; ZFMK, Zoologisches Forschungsmuseum Koenig, Bonn, Germany.

Acknowledgments

We thank Yu. Gubin (Moscow) for making possible the study of the material. R. Schoch (Stuttgart) for constructive comments and fruitful discussion at the earlier stages of the manuscript. We are much indebted to W. Joyce (Tübingen) for the improvement of the English.

Author Contributions

Conceived and designed the experiments: DV MB. Performed the experiments: DV. Analyzed the data: DV MB. Contributed reagents/materials/analysis tools: DV. Wrote the paper: DV MB.

References

1. Duellman WE, Trueb L (1994) Biology of Amphibia. Baltimore, MD: The Johns Hopkins University Press. 670 p.
2. Estes R (1981) Gymnophiona, Caudata. Stuttgart: Gustav Fischer.
3. Zug GR, Vitt LJ, Caldwell JP (2001) Herpetology: an introductory biology of amphibians and reptiles. Waltham, MA: Academic Press. 630 p.
4. Westphal F (1958) Die Tertiären und Rezenten Eurasiatischen Riesensalamander (Genus *Andrias*, Urodela, Amphibia). Palaeontographica A 110: 20–92.
5. Vasilyan D, Böhme M, Chkhikvadze VM, Semenov YA, Joyce W (2012) A new giant salamander (Urodela, Pancryptobrancha) from the Miocene of Eastern Europe (Grytsiv, Ukraine). Journal of Vertebrate Paleontology. In press.
6. Chkhikvadze VM (1982) On the findings of fossil Cryptobranchidae in the USSR and Mongolia. Vertebrata Hungarica 21: 63–67.
7. Böhme M, Vasilyan D, Winklhofer M (2012) Habitat tracking, range dynamics and palaeoclimatic significance of Eurasian giant salamanders (Cryptobranchidae) — indications for elevated Central Asian humidity during Cenozoic global warm periods. Palaeogeography, Palaeoclimatology, Palaeoecology 342–343: 64–72.
8. Gubin YM (1991) Paleocene salamanders from Southern Mongolia. Paleontologicheskij Zhurnal: 96–106.
9. Badamgarev D, Reshetov VJ (1985) Paleontology and Stratigraphy of the Paleogene of the Transaltaic Gobi; Barsbold R, Luvsandanzan B, Tatarinov LP, Trofimov BA, Reshetov VY et al., editors. Moscow: Nauka. 104 p.
10. Elwood JRL, Cundall D (1994) Morphology and behavior of the feeding apparatus in *Cryptobranchus alleganiensis* (Amphibia: Caudata). Journal of Morphology 220: 47–70.
11. Cundal D, Lorenz-Elwood J, Groves JD (1987) Asymmetric suction feeding in primitive salamanders. Experientia 43: 1229–1231.
12. Osawa G (1902) Beiträge zur Anatomie des japanischen Riesensalamanders. Mitteilungen aus der medicinischen Facultät der Kaiserl-Japan Universität zu Tokio 5: 1–207.
13. Zhang P, Chen Y-Q, Zhou H, Liu Y-F, Wang X-L, et al. (2006) Phylogeny, evolution, and biogeography of Asiatic Salamanders (Hynobiidae). Proceedings of the National Academy Sciences U S A 103: 7360–7365.
14. Rose CS (1996) An endocrine–based model for developmental and morphogenetic diversification in metamorphic and paedomorphic urodeles. Journal of Zoology 239: 253–284.
15. Schoch RR (2009) Evolution of Life Cycles in Early Amphibians. Annual Review of Earth and Planetary Sciences 37: 135–162.
16. Pawley K, Warren A (2006) The appendicular skeleton or *Eryops megacephalus* Cope, 1877 (Temnospondyli: Eryopoidea) from the Lower Permian of North America. Journal of Paleontology 80: 561–580.
17. Witzmann F (2009) Comparative histology of sculptured dermal bones in basal tetrapods, and the implications for the soft tissue dermis. Palaeodiversity 2: 233–270.
18. Shishkin MA (1975) Stratigraphy and taphonomy of upper Paleocene vertebrate locality Naran-Bulak (Southern Gobi, Mongolia). In: Kromarenko NN, Luvsandanzan B, Voronin YI, Barsbold R, Pozhdestvenskiy AK, et al., editors. Fossil fauna and flora of Mongolia. Moscow: Nauka. pp. 230–249.
19. Sever DM, editor (2003) Reproductive biology and phylogeny of Urodela. Enfield: Science Publishers. 624 p.
20. Tolstikova NV, Badamgarav D (1976) Freshwater gastropods from the lower Paleogene of Mongolia and southeast Kazakhstan. In: Kramarenko NN, Luvsandansan B, Voronin YI, Barsbold R, Rozhdestvensky AK, et al., editors. Paleontology and biostratigraphy of Mongolia. Moscow: Nauka. pp 145–150.
21. Meng J, McKenna MC (1998) Faunal turnovers of Paleogene mammals from the Mongolian Plateau. Nature 394: 364–367.
22. Luterbacher HP, Ali JR, Brinkhuish H, Gradstein FM, Hooker JJ, et al. (2004) The Paleogene Period. In: Gradstein FM, Ogg JG, Smith AG, editors. A Geological Time Scale 2004. Cambridge: Cambridge University Press. pp 384–408.
23. Secord R, Gingerich PD, Smith ME, Clyde WC, Wilf P, et al. (2006) Geochronology and Mammalian Biostratigraphy of Middle and Upper Paleocene Continental Strata, Bighorn Basin, Wyoming. American Journal of Science 306: 211–245.
24. Ting S, Bowen GJ, Koch PL, Clyde WC, Wang Y, et al. (2003) Biostratigraphy, chemostratigraphic, and magnetostratigraphic study across the Paleocene-Eocene boundary in the Hengyang Basin, Hunan, China. In: Wing SL, Gingerich PD, Schmitz B, Thomas E, editors. Causes and Consequences of Globally Warm Climates in the Early Paleogene. Boulder, CO: The Geological Society of America. pp 521–535.
25. Zachos JC, Dickens GR, Zeebe RE (2008) An early Cenozoic perspective on greenhouse warming and carbon-cycle dynamics. Nature 451: 279–283.
26. Gingerich PD (2003) Mammalian responses to climate change at the Paleocene-Eocene boundary: Polecat Bench record in the northern Bighorn Basin, Wyoming. In: Wing SL, Gingerich PD, Schmitz B, Thomas E, editors. Causes and Consequences of Globally Warm Climates in the Early Paleogene. Boulder, CO: The Geological Society of America. pp 463–478.

3.3. Paper # 3: Habitat tracking, range dynamics and palaeoclimatic significance of Eurasian giant salamanders (Cryptobranchidae) — indications for elevated Central Asian humidity during Cenozoic global warm periods

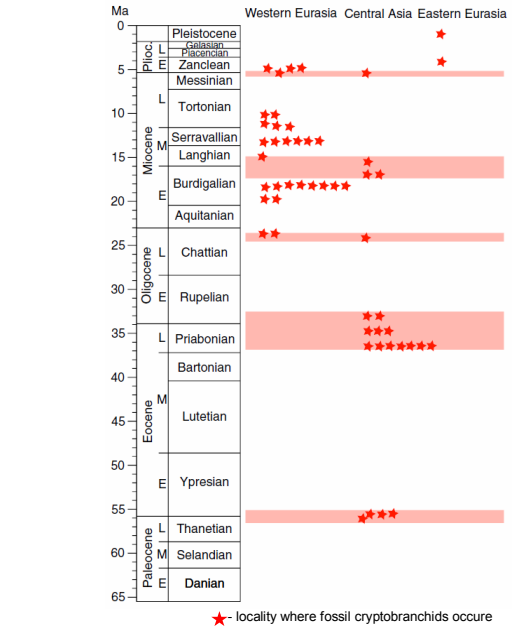

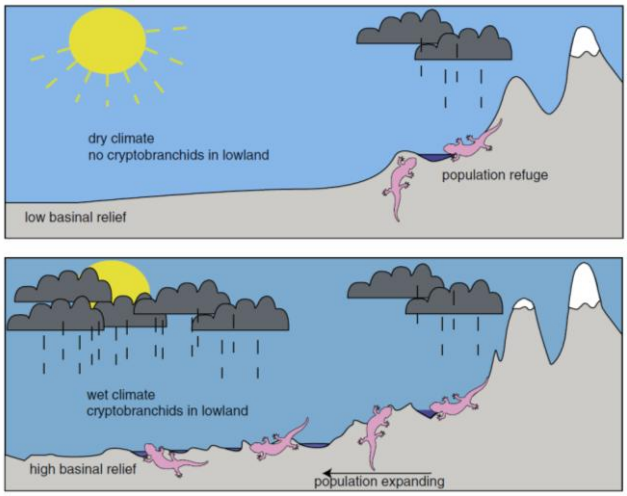

Own contribution:

Scientific ideas (%)	30
Data generation (%)	30
Analysis and Interpretation (%)	30
Paper writing (%)	20

Palaeogeography, Palaeoclimatology, Palaeoecology 342–343 (2012) 64–72

Contents lists available at SciVerse ScienceDirect

Palaeogeography, Palaeoclimatology, Palaeoecology

journal homepage: www.elsevier.com/locate/palaeo

Habitat tracking, range dynamics and palaeoclimatic significance of Eurasian giant salamanders (Cryptobranchidae) — indications for elevated Central Asian humidity during Cenozoic global warm periods

Madelaine Böhme [a,b,*], Davit Vasilyan [b], Michael Winklhofer [c]

[a] Senckenberg Center for Human Evolution and Palaeoecology (HEP), Germany
[b] Eberhard-Karls-University Tuebingen, Department for Geoscience, Sigwartstr. 10, 72076 Tuebingen, Germany
[c] Department of Earth- and Environmental Science, Ludwig-Maximillians-University Munich, Theresienstr. 41, 80333 Munich, Germany

ARTICLE INFO

Article history:
Received 17 December 2010
Received in revised form 23 April 2012
Accepted 26 April 2012
Available online 4 May 2012

Keywords:
Giant salamanders
Environmental stasis
Palaeoprecipitation
Central Asia
Global warm periods

ABSTRACT

Environmental fluctuations are a driving force in vertebrate evolution, but cryptobranchids (giant salamanders) show little morphologic change since the Jurassic. Here we analyze their fossil distribution in the Cenozoic of Eurasia and show that morphologic stasis is also maintained by stable environments, making giant salamanders an ideal proxy-group for environmental and palaeoclimatic studies. The climate space of recent and fossil cryptobranchids is best characterized by high humidity with mean annual precipitation values over 900 mm. The recorded patchiness of their fossil record can be explained by habitat tracking and/or range expansion from higher altitudes into lowland settings during humid periods with increased basinal relief. In Central Asia cryptobranchids are recorded from five intervals, four of them are global warm periods: Paleocene–Eocene Thermal Maximum, Late Oligocene warming, Miocene Climate Optimum, and Mio-Pliocene transition. This distribution suggests that during global warmth the Asian cold high pressure zone during winter months may be weak or absent, thus moist westerly winds penetrate far into the continent. The presence of cryptobranchids also indicates that the aridification across the Eocene–Oligocene boundary as reported from Mongolia and northwestern China, does not occur in the Zaysan Basin, probably due to increased upslope precipitation in the rising Altai Mountains.

1. Introduction

Cryptobranchids represent a group of large sized (up to 1.8 m), paedomorphic basal salamanders known since the Middle Jurassic (Gao and Shubin, 2003; Frost et al., 2006). The group has experienced so little morphological change over the last 160 Myr (Gao and Shubin, 2003) that the two extant genera, the North-American *Cryptobranchus* and the East-Asian *Andrias*, can be regarded as living fossils. This observed morphologic stasis may be attributed to their high degree of behavioral, physiological, and developmental plasticity (Wake et al., 1982; Gao and Shubin, 2003). Here we analyze the fossil cryptobranchid distribution in Eurasia during the last 60 myrs and suggest that morphologic stasis in giant salamanders may also be maintained by relatively stable long-term environmental conditions, which reduce the adaptive plasticity in populations (Masel et al., 2007). We argue that cryptobranchid populations maintained stable environments by habitat tracking or habitat restriction to mountainous refuges during unfavorable conditions in lowland basins. By these, giant salamander fossils can be regarded as very useful palaeoclimatic and palaeoenvironmental proxy organisms.

2. Eurasian cryptobranchids during the Cenozoic

Two extant species of cryptobranchids can be found in eastern Eurasia: *Andrias davidianus* (China) (Fig. 1) and *A. japonicus* (Japan) (Fig. 2). Both are strictly aquatic amphibians and confined to clear, well-oxygenated, cold mountain streams and rivers. They might occur also in lowland rivers earlier in the Holocene (Thenius, 1954), where they are absent now probably due to increased human hunting pressure.

Cenozoic giant salamanders are known from the mid-latitudes of Eurasia with four genera and five or six species from 53 localities, ranging from the Late Paleocene to the Pleistocene (Table 1, Fig. 3). Besides *Aviturus exsecratus* and *Ulanurus fractus* from the latest Paleocene of Mongolia (S-Mongolia, 43°N, 100°E), the Late Eocene species *Zaissanurus beliajevae* is restricted to the Central Asian Zaysan Basin (SE-Kazakhstan, 50°N, 85°E), whereas the Late Oligocene to Early Pliocene species *Andrias scheuchzeri* is widely distributed from

* Corresponding author at: Eberhard-Karls-University Tuebingen, Department for Geoscience, Sigwartstr. 10, 72076 Tuebingen, Germany. Tel.: +49 8921805544; fax: +49 8921806602.
E-mail addresses: m.boehme@ifg.uni-tuebingen.de (M. Böhme), davit.vasilyan@ifg.uni-tuebingen.de (D. Vasilyan), michael@geophysik.uni-muenchen.de (M. Winklhofer).

0031-0182/$ – see front matter © 2012 Elsevier B.V. All rights reserved.
doi:10.1016/j.palaeo.2012.04.032

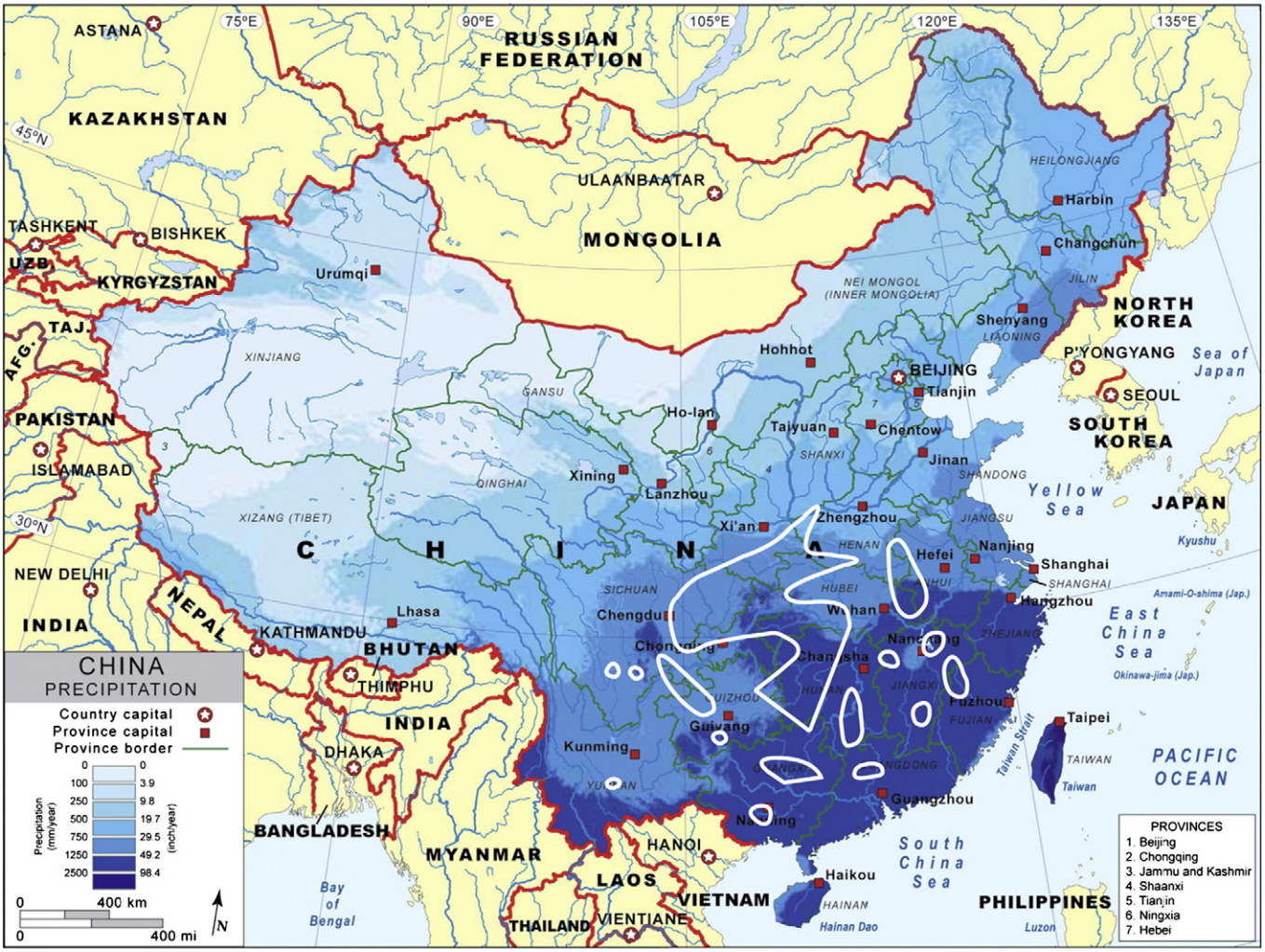

Fig. 1. Current distribution (white lines) of recent *Andrias davidianus* and mean annual precipitation map of China.

Central Europe to Western Siberia and the Zaysan Basin. The fossil record from their present-day distribution area in East Asia starts late (Early Pliocene) and is so far restricted to Japan (Table 1, Fig. 3).

2.1. Palaeoclimatic significance of cryptobranchids

To assess the palaeoclimatic significance of giant salamanders we analyzed climate parameters in their present-day distribution area in East Asia and North America (Table 2) and at selected fossil localities from Europe and Central Asia with an independent palaeoclimate record (Table 3). Humidity turns out to be the key parameter in defining the climate space for cryptobranchids, whereas temperature has a lesser role. All recent and all investigated extinct cryptobranchid species exclusively occur in humid areas, without a distinct dry season and with mean annual precipitation (MAP) exceeding 900 mm (900–1.900 mm), irrespective of the related climatic zone, which ranges from warm subtropical to temperate (Tables 2 and 3). This strongly suggests that fossil cryprobranchids are a useful proxy for significantly elevated levels (MAP > 900 mm) of past humidity. We denote this concordance of ancient and extant humidity requirement as environmental stability, which is remarkable, because recent investigation shows that unlike cryptobranchid salamanders other ectothermic vertebrates display a broad environmental plasticity during their evolution (e.g., the anguin lizard *Pseudopus*, Klembara et al., 2010).

2.2. Explaining the fossil cryptobranchid distribution in Eurasia

In all regions over Eurasia, the fossil distribution is stratigraphically patchy (Fig. 4). In Central Asia cryptobranchids occurred only during five periods; the latest Paleocene, the Late Eocene to earliest Oligocene, the latest Oligocene, the late Early to early Middle Miocene and the Miocene–Pliocene transition (grey bars in Fig. 4). All fossils are found in lowland habitats, within deposits of distal meandric rivers as well as in lake sediments. The occurrence in basinal lacustrine deposits stands in contrast to their recent habitats (Thenius, 1954; Westphal, 1958). However, juvenile individuals have thus far been found only in fluvial sediments, which suggest a habitat shift in ontogeny. To explore their patchiness in stratigraphic distribution, as well as their past habitat extension into lakes in distal basinal settings, the temporal evolution of the palaeoclimate and basin topography can provide key-information.

The Neogene humidity evolution in Central Europe is highly variable (as it was probably also in Central Asia), with frequent changes between humid and semi-arid climates (Böhme et al., 2008, 2011). However, cryptobranchids are not recorded in each and every humid period. The patchiness of their fossil record suggests that elevated humidity is a necessary, but not sufficient condition to explain their past distribution. To understand the dependency relationship between this full-aquatic salamanders and humidity we analyze the hypothesis that relatively cool, oxygenated rivers and rivulets, which are a prerequisite for cryptobranchid larval development and typically occur in mountainous

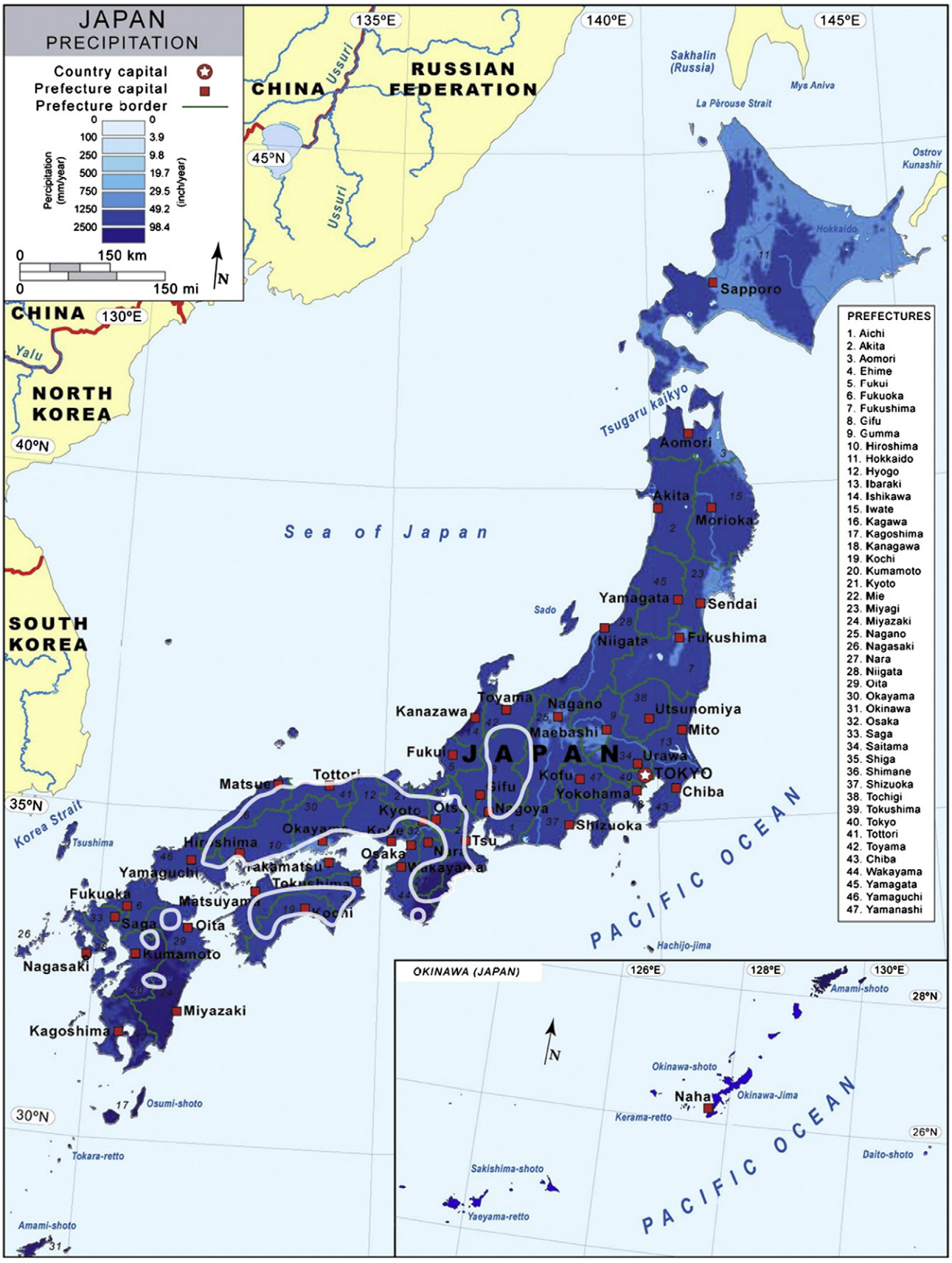

Fig. 2. Current distribution (white lines) of recent *Andrias japonicus* and mean annual precipitation map of Japan.

Table 1
Localities, coordinates, ages, taxon and references for giant salamanders (Cryptobranchidae) from the Cenozoic of Eurasia. Country information of localities are abbreviated and in brackets: Au — Austria, Cz — Czechia, Ge — Germany, Gr — Greece, Jp — Japan, Ka — Kazakhstan, Mo — Mongolia, Ru — Russia, Uk — Ukraine.

	Locality	Coordinates	Stage	Age (Ma)	Taxon	Reference
1	Shikimizu quarry (Jp)	N 33.4667 E 132.717	Late Pleistocene	0.012–0.126	*Andrias japonicus*	Shikama and Hesegawa, 1962
2	Ajimu-Chro (Jp)	N 33.4362 E 131.37	Piacencian	2.80–4.30	*Andrias* sp.	Matsui et al., 2001
3	Willershausen (Ge)	N 51.7833 E 10.10	Zanclean	3.60–5.30	*Andrias scheuchzeri*	Westphal, 1967
4	Kuchurgan (Uk)	N 46.75 E 29.9833	Zanclean	4.85–5.25	*Andrias* sp.	Chkhikvadze, 1982
5	Antipovka (Ru)	N 50.7019 E 40.0167	Zanclean	4.896–4.997	Cryptobranchidae indet.	Averianov, 2001
6	Maramena (Gr)	N 41.1791 E 23.4711	Zanclean	5.25–5.50	Cryptobranchidae indet.	this paper
7	Pavlodar 2A (Ka)	N 52.2759 E 79.9897	Messinian	5.30–5.60	Cryptobranchidae indet.	Chkhikvadze, 1984, this paper
8	Götzendorf (Au)	N 48.0167 E 16.5833	Tortonian	9.78–9.94	*Andrias scheuchzeri*	Miklas, 2002
9	Vösendorf-Brunn (Au)	N 48.20 E 16.36	Tortonian	10.25–10.45	*Andrias scheuchzeri*	Westphal, 1958
10	Hammerschmiede 1 (Ge)	N 47.9258 E 10.5989	Tortonian	11.08–11.28	*Andrias* sp.	this paper
11	Gritsev (Uk)	N 49.975 E 27.16	Tortonian	11.10–11.50	*Andrias scheuchzeri*, Cryptobranchidae gen. et sp. nov.	this paper
12	Mörgen (Ge)	N 48.1521 E 10.5059	Tortonian	11.10–13.30	*Andrias scheuchzeri*	Böhme, 2003
13	Tiefenried (Ge)	N 48.20 E 10.4833	Tortonian	11.10–13.30	*Andrias scheuchzeri*	this paper
14	Derndorf (Ge)	N 48.183 E 10.4717	Tortonian	11.20–12.50	*Andrias scheuchzeri*	Böhme, 2003
15	Eppishausen (Ge)	N 48.1669 E 10.5211	Tortonian	11.20–12.50	*Andrias scheuchzeri*	Böhme, 2003
16	Mataschen (Au)	N 46.903 E 15.9555	Tortonian	11.30–11.45	*Andrias scheuchzeri*	Tempfer, 2004
17	Wartenberg near Erding (Ge)	N 48.4013 E 11.9993	Serravallian	12.00–13.00	*Andrias* sp.	Westphal, 1970
18	Zeilarn (Ge)	N 48.2834 E 12.8942	Serravallian	12.50–12.70	*Andrias scheuchzeri*	this paper
19	Oehningen oberer Bruch (Ge)	N 47.6667 E 8.90	Serravallian	12.50–13.20	*Andrias scheuchzeri*	Westphal, 1958
20	Kirchheim in Schwaben (Ge)	N 48.1833 E 10.4833	Serravallian	13.00–14.00	*Andrias scheuchzeri*	Böttcher, 1987
21	Poltinik (Ka)	N 47.45 E 84.47	Langhian	13.00–15.00	*Andrias karelcapeki*	Chkhikvadze, 1982
22	Hambach 6 C (Ge)	N 50.90 E 6.45	Langhian	14.50–14.90	*Andrias scheuchzeri*	Böhme, 2003
23	Tri Bogatirya (Ka)	N 47.60 E 83.80	Langhian	15.00–18.00	*Andrias karelcapeki*	Chkhikvadze, 1982
24	Vympel (Ka)	N 47.45 E 84.47	Langhian	15.00–18.00	*Andrias karelcapeki*	Chkhikvadze, 1982
25	Illerkirchberg 1 (Ge)	N 48.31 E 10.046	Burdigalian	16.70–17.00	*Andrias scheuchzeri*	Sach and Heinzmann, 2001
26	Illerkirchberg hor. 3a (Ge)	N 48.31 E 10.04	Burdigalian	17.20–17.40	*Andrias scheuchzeri*	Böttcher, 1987
27	Reisensburg near Günzburg (Ge)	N 48.462 E 10.314	Burdigalian	17.30–17.60	*Andrias* sp.	Westphal, 1970
28	Ringingen-Frontal 2 (Ge)	N 48.35 E 9.8167	Burdigalian	17.70–17.80	*Andrias scheuchzeri*	Sach and Heinzmann, 2001
29	Langenau 1 (Ge)	N 48.5003 E 10.1219	Burdigalian	17.75–17.80	*Andrias scheuchzeri*	Böttcher, 1987
30	Hochberg near Jungnau (Ge)	N 48.1513 E 9.24447	Burdigalian	17.75–17.85	*Andrias* sp.	Westphal, 1970
31	Ringingen-Frontal 1 (Ge)	N 48.35 E 9.8167	Burdigalian	17.75–17.85	*Andrias scheuchzeri*	Sach and Heinzmann, 2001
32	Břešťany near Bilina (Cz)	N 50.5667 E 13.75	Burdigalian	18.00–19.00	*Andrias scheuchzeri*	Kvacek et al., 2004
33	Eggingen-Mittelhart (Ge)	N 48.3523 E 9.8598	Burdigalian	17.85–17.90	*Andrias scheuchzeri*	Sach and Heinzmann, 2001
34	Merkur North, Ahnikov (Cz)	N 50.45 E 13.4333	Burdigalian	20.00–20.00	*Andrias* sp.	Böhme, 2003; Kvacek et al., 2004
35	Rott near Hennef (Ge)	N 50.7833 E 7.2833	Chattian	23.80–24.50	*Andrias scheuchzeri*	Westphal, 1958
36	Altyn Shokysu (Ka)	N 47.2724 E 61.025	Chattian	23.80–24.70	*Zaissanurus beliajevae*	this paper
37	Oberleichtersbach (Ge)	N 50.35 E 10.05	Chattian	24.00–24.00	*Andrias scheuchzeri*	Böhme, 2008
38	Pancirny Sloy (Ka)	N 48.2158 E 84.3248	Priabonian	33.80–35.00	*Zaissanurus beliajevae*	Chkhikvadze, 1982
39	Maylibay (Ka)	N 47.4833 E 84.7183	Rupelian	31.00–33.80	Cryptobranchidae indet.	Chkhikvadze, 1984
40	Talagay, Tayzhuzgen section (Ka)	N 47.5984 E 84.00	Rupelian	31.00–33.80	*Zaissanurus beliajevae*	Chkhikvadze, 1982, 1984
41	Korablik (Ka)	N 48.00 E 84.50	Priabonian	33.80–34.60	Cryptobranchidae indet.	this paper
42	Korsak B (Ka)	N 47.4733 E 85.51	Priabonian	35.00–37.00	*Zaissanurus beliajevae*	this paper
43	Sopka obo (Ka)	N 48.2158 E 84.3248	Priabonian	35.00–37.00	*Zaissanurus* sp.	this paper
44	Konur-Kura (Ka)	N 47.4401 E 84.4981	Priabonian	36.20–37.00	*Zaissanurus beliajevae*	Chkhikvadze, 1982
45	Kusto-Kyzylkain section (Ka)	N 47.6137 E 84.1009	Priabonian	35.00–37.00	*Zaissanurus beliajevae*	Chkhikvadze, 1982
46	Lager Biryukova (Ka)	N 48.2158 E 84.3248	Priabonian	35.00–37.00	*Zaissanurus* sp.	this paper
47	Pod Chernim (Ka)	N 48.2158 E 84.3248	Priabonian	35.00–37.00	*Zaissanurus* sp.	this paper
48	Yakor (Ka)	N 48.2158 E 84.3248	Priabonian	33.80–35.00	*Zaissanurus* sp.	this paper
49	Belye Salamandry (Ka)	N 48.2158 E 84.3248	Priabonian	35.00–37.00	*Zaissanurus* sp.	this paper
50	Tsagan-Khushu, Naran member, top (Mo)	N 43.455 E 100.37	Thanetian	55.80–56.00	*Aviturus exsecratus*	Gubin, 1991
51	Aguy-Dats-Bulak, Naran member, top (Mo)	N 43.455 E 100.50	Thanetian	55.80–56.00	*Aviturus exsecratus*	Gubin, 1991
52	Aguy-Dats-Bulak, Naran member, top (Mo)	N 43.455 E 100.50	Thanetian	55.80–56.00	*Ulanurus fractus*	Gubin, 1991
53	Aguy-Dats-Bulak, Naran member, layer 6 (Mo)	N 43.4667 E 100.445	Thanetian	56.02–56.04	*Aviturus exsecratus*	Gubin, 1991

habitats, developed in basinal settings only during periods of increased basinal relief and/or very humid climates. Elevated ground-water levels and increased uplift and erosion will strengthen alluvial springs, whose discharge is regulated mainly by precipitation. This hypothesis can be tested in two well-studied and sampled Cenozoic basins: the European North Alpine Foreland Basin (NAFB) bounded by the Alpine orogene in the south, and the Central Asian Zaysan Basin in southeastern Kazakhstan, bounded by the Altai Mountains in the northeast and the Tian Shan, respectively Tarbagatai Mountains in the south (Fig. 3).

In the NAFB, *Andrias* fossils are known from 16 localities (Table 1, Fig. 4; Böttcher, 1987; Böhme and Ilg, 2003) within two narrow time periods: between 17.8 and 17.4 Ma (8 localities from the Brackishwater Molasse and the earliest part of the Upper Freshwater Molasse — UFM), and between ~13 and ~11.5 Ma (8 localities from the Younger Series of the UFM, including the famous site of Oehningen, the type locality of *Andrias scheuchzeri*). In hundreds of fossil localities analyzed, not a single cryptobranchid was found in the time-interval between the two periods (Böhme, 2010). The cryptobranchid-bearing intervals of the NAFB differ significantly in respect to temperature and vegetation (paratropical evergreen forests versus subtropical/warm temperate deciduous forests, Böhme et al., 2007), but show analogies in terms of basinal relief. Both times are characterized by erosion and hiatuses at the basin margin (Grimm, 1957), moderate alpine topography (Kuhlemann, 2007) and the incision of major valleys (e.g., Graupensand valley, Reichenbacher et al., 1998; Palaeo-Inn valley, Frisch et al., 1998) to which most cryptobranchid localities are bounded (Fig. 5).

From the Zaysan Basin, cryptobranchid salamanders are also known from two time periods only (Fig. 4). From the older period, ten localities derive from the Late Eocene (Late Aksyr and Kusto Formations) and two localities from the earliest Oligocene (Buran

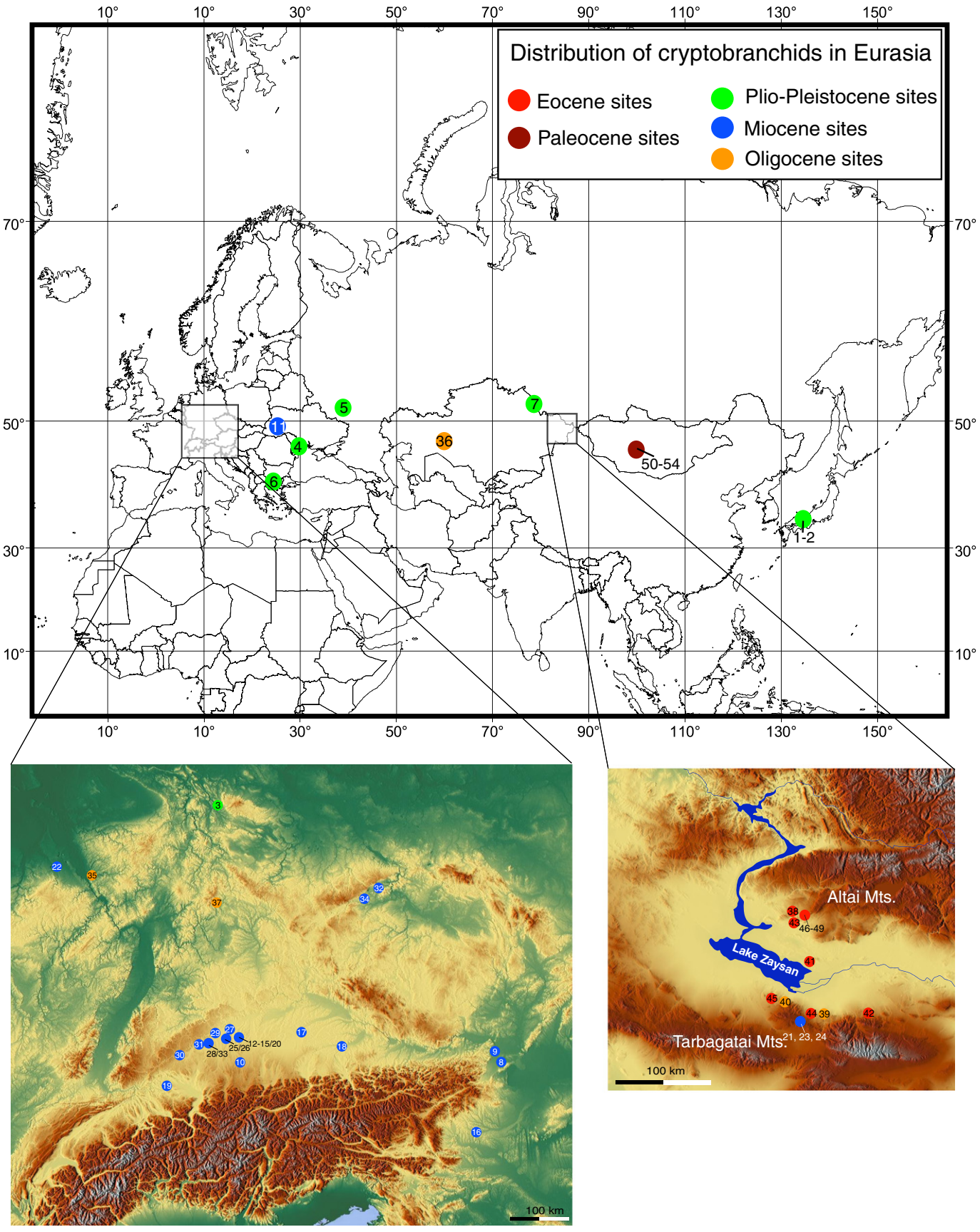

Fig. 3. Map of Eurasia showing the Cenozoic localities of giant salamanders. The dense record in Central Europe and the Zaysan Basin is shown in separate topographic maps. Numbers refer to localities in Table 1.

Table 2
Mean annual precipitation (MAP) from climate stations within the distribution area of extant Eurasian and North American cryptobranchids.

Climate station	Species	MAP	Reference
Hiroshima	*A. japonicus*	1.597	Müller and Hennings, 2000
Osaka	*A. japonicus*	1.360	Müller and Hennings, 2000
Kyoto	*A. japonicus*	1.585	www.weather.com, 2010
Matsue	*A. japonicus*	1.895	www.wunderground.com, 2010
Tottori	*A. japonicus*	1.950	www.wunderground.com, 2010
Kobe	*A. japonicus*	1.314	www.wunderground.com, 2010
Yamaguchi	*A. japonicus*	1.844	www.wunderground.com, 2010
Chongqing	*A. davidianus*	1.090	Müller and Hennings, 2000
Guilin	*A. davidianus*	1.967	Müller and Hennings, 2000
Chengdu	*A. davidianus*	1.146	Müller and Hennings, 2000
Changsha	*A. davidianus*	1.531	Müller and Hennings, 2000
Nanchang	*A. davidianus*	1.864	Müller and Hennings, 2000
Wuhan	*A. davidianus*	1.194	Müller and Hennings, 2000
Savannah River (GA, SC)	*C. a. alleganiensis*	1.220	www.wrcc.dri.edu, 2010
Tennessee River (VA, TN, KY)	*C. a. alleganiensis*	1.170–1.420	www.wrcc.dri.edu, 2010
Ohio River (PA, OH, IN)	*C. a. alleganiensis*	990–1.200	www.wrcc.dri.edu, 2010
Black River (MO)	*C. a. bishopi*	1.140	www.wrcc.dri.edu, 2010
White River (AR)	*C. a. bishopi*	1.140	www.wrcc.dri.edu, 2010

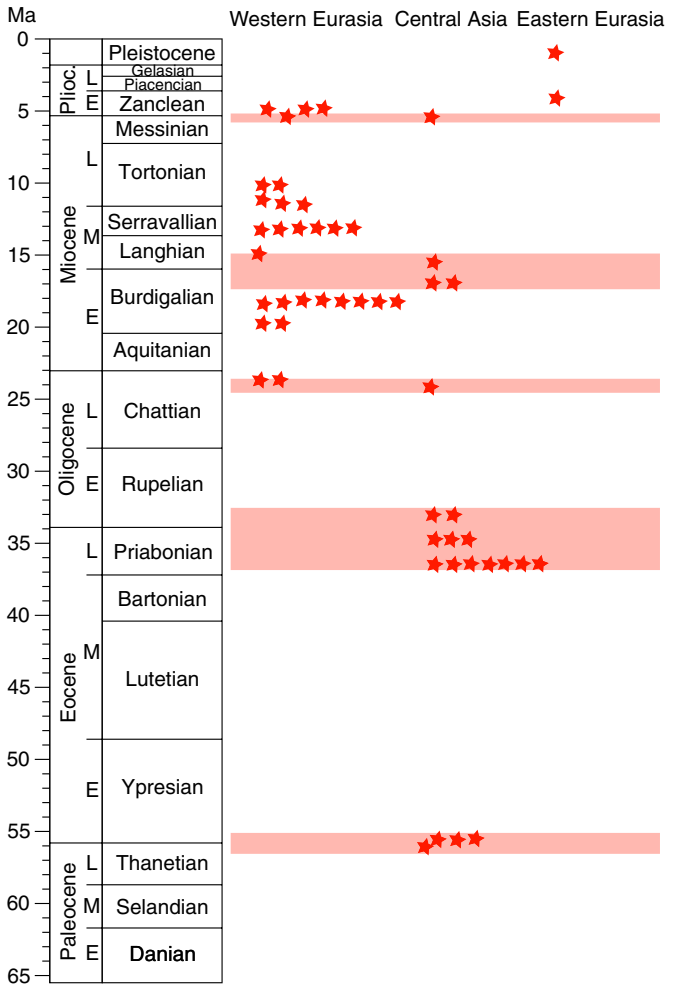

Fig. 4. Stratigraphic distribution of cryptobranchids in Eurasia during the Cenozoic. Western Eurasia covers Europe and the European part of Russia, Central Asia covers Kazakhstan, the Asian part of Russia and Mongolia, and East Asia document Japanese localities. The five periods when cryptobranchids are present in Central Asia are highlighted in grey.

Formation), suggesting that giant salamanders were present in the basin over a significant time span (Late Aksyr to Buran Formations) between 37 and 33 Ma. The second period (17 to 15 Ma) includes three localities crossing the Early to Middle Miocene boundary (Shamangora and Zaysan Formations). The regional tectonic evolution suggests that after a period of stability and regional peneplainization during the late Cretaceous to Paleocene a first period of tectonic deformation occurred in the Zaysan basin during the Late Eocene to Early Oligocene, including a regional uplift of the Altai Mountains (Buslov, 2004). A second period of tectonic movements along reactivated accretion–collision zones and faults is documented from the Middle Miocene (Buslov, 2004; DeGrave et al., 2007).

Therefore, the fossil distribution and tectonic data from both basins support the hypothesis that, besides elevated humidity increased basinal relief is necessary to provide spawning habitats for giant salamanders in lowland settings. Given these circumstances it is reasonable to assume that Central European giant salamanders lived permanently during the Neogene in mountain habitats of the Alpine orogene and colonized lowland basins only during periods of significantly elevated humidity and increased basinal relief (Fig. 6). We hypothesize the same for cryptobranchids of Central Asia where the Altai Mountains may act as a refuge for giant salamander populations. In both cases, environmental stability will be maintained by habitat restriction to mountainous refuges during dry climates, and/or periods without suitable spawning habitats in the lowland basins. This model explains the high patchiness of giant salamander distribution in densely sampled basins and illustrates

Table 3
Mean annual precipitation (MAP) values of giant salamander localities from the Oligocene and Neogene of Europe and Asia.

Locality	Country	Age (in Ma)	Stage	Species	MAP (in mm)	Reference
Willershausen	Germany	5.3–3.6	Zanclean	*A. scheuchzeri*	897–1.151	Thiel et al., 2012*
Kuchurgan	Ukraine	5.25–4.85	Early Zanclean	*Andrias* sp.	1.425 ± 273	Böhme, pers. comm.**
Maramena	Greece	5.5–5.25	Messinian/Zanclean	*Andrias* sp.	994 ± 257	Böhme, pers. comm.**
Götzendorf	Austria	9.94–9.78	Early Tortonian	*A. scheuchzeri*	1.303 ± 267	Böhme et al., 2008**
Vösendorf	Austria	10.45–10.25	Early Tortonian	*A. scheuchzeri*	918 ± 255	Böhme et al., 2008**
Hammerschiede 1	Germany	11.28–11.08	Earliest Tortonian	*Andrias* sp.	974 ± 256	Böhme et al., 2008**
Oehningen	Germany	13.5–13.0	Early Serravallian	*A. scheuchzeri*	1.159–1.237	Mosbrugger et al., 2005*
Hambach 6 C	Germany	15.0–14.5	Late Langhian	*A. scheuchzeri*	1.174 ± 262	Böhme, pers. comm.**
Reisensburg	Germany	17.5–17.3	Late Burdigalian	*A. scheuchzeri*	1.648 ± 285	Böhme et al., 2011**
Langenau	Germany	17.9–17.75	Late Burdigalian	*A. scheuchzeri*	1.112 ± 260	Böhme et al., 2011**
Oberleichtersbach	Germany	23.5–23.0	Latest Chattian	*A. scheuchzeri*	1.131 ± 261	Böhme, 2008**
Rott	Germany	23.5–23.0	Latest Chattian	*A. scheuchzeri*	843–1.281	Utescher et al., 2000*
Altyn Shokysu	Kazakhstan	23.8–24.7	Late Chattian	*Z. beliajevae*	897–1.028	Bruch and Zhilin, 2007*

* Estimated by botanical proxy-method (Coexistence Approach, Mosbrugger and Utescher, 1997).
** Estimated by herpetofaunal proxy-method (Böhme et al., 2006).

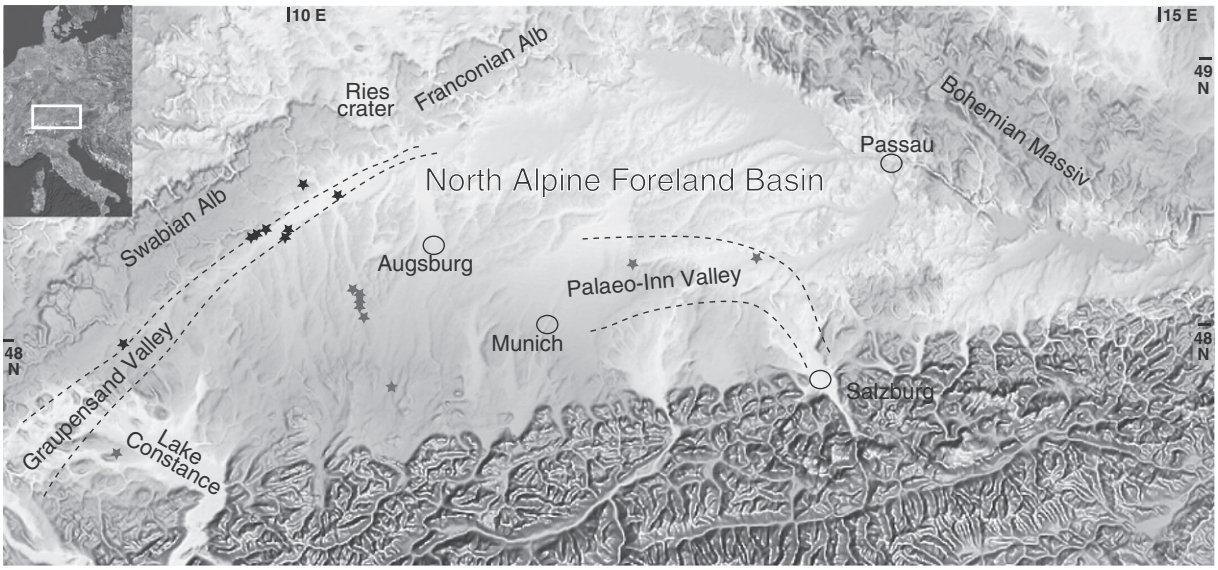

Fig. 5. Digital elevation model of Southern Germany (from Kuhlemann et al., 2006, 2007) showing the location of all crypobranchid occurrences in the North Alpine Foreland Basin (black stars — Burdigalian localities; grey stars — Serravallian localities) in relation to the two main incised valleys of the Upper Freshwater Molasse: the Burdigalian Graupensand valley (according to Reichenbacher et al., 1998) and the Serravallian Palaeo-Inn valley (according to Frisch et al., 1998).

biogeographic patterns during 20 million years of cryptobranchid residence in Central Europe and Central Asia.

3. Implications for Cenozoic palaeoclimatology of Central Asia

Applying the relationship between giant salamander occurrences and humidity indicates that the five Central Asian cryptobranchid intervals (Fig. 4) are characterized by humid to very humid climates, with MAP above 900 mm. Interestingly all but one interval represent global warm periods. Cryptobranchids from the oldest interval derive from the top of the Naran Member of the Naran Bulak Formation in south-central Mongolia (Tolstikova and Badamgarav, 1976: Fig. 4), which can be correlated to the late Gashatan Asian Land Mammal Age and the late Clarkforkian North American Land Mammal Age (Meng and McKenna, 1998; Luterbacher et al., 2004; Secord et al., 2006), very near or contemporary with the Paleocene–Eocene Thermal Maximum. For both the Naran Member and the contemporary nearby Chinese Nomogen Formation humid environments have been already suggested (Tolstikova and Badamgarav, 1976; Van Itterbeeck et al., 2007). The second Central Asian cryptobranchid period covers not only the Late Eocene warming, but also the latest Eocene and the earliest Oligocene cooling periods (see Villa et al., 2008: Fig. 9). The third Central Asian cryptobranchid period is documented in latest Oligocene strata near the present-day Lake Aral (Aral Formation) and may correspond to the Late Oligocene warming, whereas the fourth cryptobranchid period is documented in the Zaysan basin again (Shamangora and Zaysan Formations). This period falls within the Miocene Climatic Optimum (Flower and Kennett, 1994; Böhme,

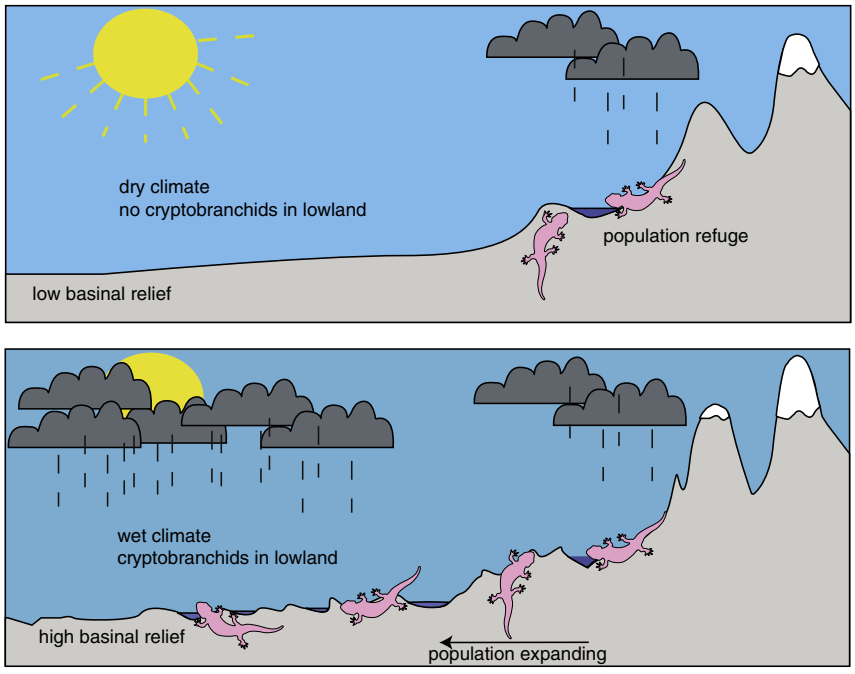

Fig. 6. Altitudinal distribution model of giant salamanders during dry climate and low basinal relief (above) and wet climate and high basinal relief (below).

2003). The last Central Asian cryptobranchid populations are found at the Miocene/Pliocene transition, when giant salamanders are recorded from bio-magnetostratigraphically dated (5.6 to 5.3 Ma) sediments near Pavlodar (West Siberia).

4. Conclusion

Based on their environmental stability fossil cryptobranchids are excellent palaeoclimate proxies, indicating humid to very humid climates with MAP exceeding 900 mm. Their fossil distribution in Eurasia is shown to be highly patchy and we hypothesize that they occur in basinal habitats only during humid periods of increased regional uplift. In Central Asia giant salamanders occur during five intervals, four of them are characterized as global warm periods (Paleocene–Eocene Thermal Maximum, Late Oligocene warming, Miocene Climate Optimum, Mio-Pliocene transition), suggesting a direct (positive) relationship between global temperature and Central Asian humidity evolution. The elevated and probably less seasonal humidity in Central Asia during global warm periods may be explained by a weak or absent Asian cold high pressure zone during winter months, allowing moist westerly winds (low-pressure systems) to penetrate far into the continent. The presence of cryptobranchids in the Zaysan Basin across the Eocene–Oligocene transition indicates that, unlike in Mongolia and northwest China where an intense aridification is recorded at this time (Böhme, 2007; Dupont-Nivet et al., 2007; Xiao et al., 2010), the Zaysan Basin exhibits a humid climate during this stepwise global cooling period. This may be explained by the contemporary uplift of the easterly bordering Altai Mountains and an increase in upslope precipitation.

Acknowledgment

We thank Dr. V. V. Chkhikvadze for making possible the study of Central Asian fossil cryptobranchids. We are grateful to editor Dr. Kershaw, as well as Dr. J. – C. Rage and anonymous reviewer for constructive comments. Financial support was provided by the Deutsche Forschungsgemeinschaft (grant number BO 1550/14).

References

Averianov, A., 2001. New record of proteid salamanders (Amphibia, Caudata) from the Pliocene of Ukraine and lower Pleistocene of Moldavia. Vestnik Zoologii 35, 43–46.
Böhme, M., 2003. Miocene climatic optimum: evidence from lower vertebrates of central Europe. Palaeogeography, Palaeoclimatology, Palaeoecology 195, 389–401.
Böhme, M., 2007. Oligocene-Miocene Vertebrates from the Valley of Lakes (Central Mongolia): Morphology, phylogenetic and stratigraphic implications. 3. Herpetofauna (Anura, Squamata) and palaeoclimatic implications: preliminary results. Annalen des Naturhistorischen Museums in Wien 108 A, 43–52.
Böhme, M., 2008. Ectothermic vertebrates (Teleostei, Allocaudata, Urodela, Anura, Testudines, Choristodera, Crocodylia, Squamata) from the Upper Oligocene of Oberleichtersbach (Northern Bavaria, Germany). Courier Forschungsinstitut Senckenberg 260, 161–183.
Böhme, M., 2010. Ectothermic vertebrates (Osteichthyes, Allocaudata, Urodela, Anura, Crocodylia, Squamata) from the Miocene of Sandelzhausen (Germany, Bavaria): their implication for environmental reconstruction and palaeoclimate. Paläontologische Zeitschrift 84, 3–41.
Böhme, M., Ilg, A., 2003. fosFARbase. www.wahre-staerke.com2003(accessed April 2012).
Böhme, M., Ilg, A., Ossig, A., Küchenhoff, H., 2006. A new method to estimate paleoprecipitation using fossil amphibians and reptiles and the Middle and Late Miocene precipitation gradients in Europe. Geology 34, 425–428.
Böhme, M., Bruch, A., Selmeier, A., 2007. The reconstruction of the Early and Middle Miocene climate and vegetation in the North Alpine Foreland Basin as determined from the fossil wood flora. Palaeogeography, Palaeoclimatology, Palaeoecology 253, 91–114.
Böhme, M., Ilg, A., Winkelhofer, M., 2008. Late Miocene "washhouse" climate in Europe. Earth Planetary Science Letters 275, 393–401.
Böhme, M., Winklhofer, M., Ilg, A., 2011. Miocene precipitation in Europe: temporal trends and spatial gradients. Palaeogeography, Palaeoclimatology, Palaeoecology 304, 212–218.
Böttcher, R., 1987. Neue Funde von *Andrias scheuchzeri* (Cryptobranchidae, Amphibia) aus der süddeutschen Molasse. Stuttgarter Beiträge zur Naturkunde B 131, 1–38.
Bruch, A.A., Zhilin, S.G., 2007. Early Miocene climate of Central Eurasia — evidence from Aquitanian floras of Kazakhstan. Palaeogeography, Palaeoclimatology, Palaeoecology 248, 32–48.
Buslov, M.M., 2004. Cenozoic tectonics of central Asia: basement control. Himalayan Journal of Science 2, 104–105.
Chkhikvadze, V.M., 1982. On the finding of fossil Cryptobranchidae in the USSR and Mongolia. Vertebrata Hungarica 21, 63–67.
Chkhikvadze, V.M., 1984. Survey of the fossil urodelan and anuran amphibians from the USSR. Izvestia Akademii Nauk Gruzinska SSR, Seria Biologitcheskaya 10, 5–13 [in Russian].
DeGrave, J., Buslov, M.M., Van Den Haute, P., Dehandschutter, B., Delvaux, D., 2007. Meso-Cenozoic evolution of mountain range — intramontan basin system in the Southern Siberian Altai Mountains by apatite fission-track thermochronology. In: Lacombe, O., Roure, F., Lavé, J., Vergés, J. (Eds.), Thrust belts and foreland basins: from fold kinematics to hydrocarbon systems. Springer-Verlag Berlin Heidelberg, Berlin, Heidelberg, pp. 457–469.
Dupont-Nivet, G., Krijgsman, W., Langereis, C.G., Abels, H.A., Dai, S., Fang, X., 2007. Tibetan plateau aridification linked to global cooling at the Eocene–Oligocene transition. Nature 445, 635–638.
Flower, B., Kennett, J.P., 1994. The middle Miocene climatic transistion: east Antarctic ice sheet development, deep ocean circulation and global carbon cycling. Palaeogeography, Palaeoclimatology, Palaeoecology 108, 537–555.
Frisch, W., Kuhlemann, J., Dunkl, I., Brügel, A., 1998. Palinspastic reconstruction and topographic evolution of the Eastern Alps during the late Tertiary extrusion. Tectonphysics 297, 1–15.
Frost, D.R., Grant, T., Faivovich, J., Bain, R.H., Haas, A., Haddad, C.F.B., de Sá, R.O., Channing, A., Wilkinson, M., Donnellan, S.C., Raxworthy, C., Campbell, J.A., Blotto, B.L., Moler, P., Dreswes, R.C., Nussbaum, R.A., Lynch, J.D., Green, D.M., Wheeler, W.C., 2006. The amphibian tree of life. Bulletin of the American Museum of Natural History 297, 1–370.
Gao, K.-Q., Shubin, N.H., 2003. Earliest known crown-group Salamanders. Nature 422, 424–428.
Grimm, W.D., 1957. Stratigraphische und Sedimentpetrographische Untersuchungen in der Oberen Süßwassermolasse zwischen Inn und Rott (Niederbayern). Geologisches Jahrbuch, Beihefte 26, 97–199.
Gubin, Y.M., 1991. Paleocene salamanders from Southern Mongolia. Paleontologicheskij Zhurnal 1, 96–106 [in Russian].
Klembara, J., Böhme, M., Rummel, M., 2010. Revision of the anguine lizard *Pseudopus laurillardi* (Squamata, Anguidae) from the Miocene of Europe, with comments on paleoecology. Journal of Paleontology 84 (2), 159–196.
Kuhlemann, J., Dunkl, I., Brügel, A., Spiegel, C., Frisch, W., 2006. From source terrains of the Eastern Alps to the Molasse basin: detrital record of non-steady state exhumation. Tectonophysics 413, 301–316.
Kuhlemann, J., 2007. Paleogeographic and paleotopographic evolution of the Swiss and Eastern Alps since the Oligocene. Global and Planetary Change 58, 224–236.
Kvacek, Z., Böhme, M., Dvorak, Z., Konzalova, M., Mach, K., Prokop, J., Rajchl, M., 2004. Early Miocene freshwater and swamp ecosystems of the Most Basin (northern Bohemia) with particular reference to the Bilina Mine section. Journal of the Czech Geological Society 49 (1–2), 1–40.
Luterbacher, H.P., Ali, J.R., Brinkhuish, H., Gradstein, F.M., Hooker, J.J., Monechi, S., Ogg, J.G., Powell, J., Rohl, U., Sanfilippo, A., Schmitz, B., 2004. The Paleogene period. In: Gradstein, F., Ogg, J.G., Smith, A. (Eds.), A Geologic Time Scale. Cambridge University Press, Cambridge, pp. 384–408.
Masel, J., King, O.D., Maugham, H., 2007. The loss of adaptive plasticity during long periods of environmental stasis. The American Naturalist 169, 38–46.
Matsui, M., Kitabayashi, E., Takahashi, K., Sato, S., 2001. A fossil giant salamander of the genus Andrias from Kyushu, Southern Japan. Research Reports Lake Biwa Museum 18 72–28 [in Japanese].
Meng, J., McKenna, M.C., 1998. Faunal turnovers of Paleogene mammals from the Mongolian Plateau. Nature 394, 364–367.
Miklas, P.M., 2002. Die Amphibienfauna (Amphibia: Caudata, Anura) der obermiozänen Fundstelle Götzendorf an der Leitha (südliches Wiener Becken, Niederösterreich). Annalen des Naturhistorischen Museums in Wien 103A, 161–211.
Mosbrugger, V., Utescher, T., 1997. The coexistence approach — a method for quantitative reconstructions of Tertiary terrestrial palaeoclimate data using plant fossils. Palaeogeography, Palaeoclimatology, Palaeoecology 134, 61–86.
Mosbrugger, V., Uterscher, T., Dilcher, D.L., 2005. Cenozoic continental climate evolution of Central Europe. Proceedings of the National Academy of Science 102 (42), 14964–14969.
Müller, M.J., Hennings, D., 2000. The Global Climate Data Atlas on CD-Rom. Flensburg and Köln.
Reichenbacher, B., Böttcher, R., Bracher, H., Doppler, G., von Engelhardt, W., Gregor, H.J., Heissig, K., Heizmann, E.P.J., Hofmann, F., Kälin, D., Lemcke, K., Luterbacher, H., Martini, E., Pfeil, F., Reiff, W., Schreiner, A., Steininger, F.F., 1998. Graupensandrinne — Ries-Impakt: Zur Stratigraphie der Grimmelfinger Schichten, Kirchberger Schichten

und Oberen Süßwassermolasse. Zeitschrift Deutsche Geologische Gesellschaft 149, 127–161.

Sach, V.J., Heinzmann, P.J., 2001. Stratigraphie und Säugetierfaunen der Brackwassermolasse in der Umgebung von Ulm (Südwestdeutschland). Stuttgarter Beiträge zur Naturkunde. Serie B — Geologie und Paläontologie 310, 1–95.

Secord, R., Gingerich, P.D., Smith, M.E., Clyde, W.C., Wilf, P., Singer, B.S., 2006. Geochronology and mammalian biostratigraphy of Middle and Upper Paleocene continental strata, Bighorn Basin, Wyoming. American Journal of Science 306, 211–245.

Shikama, T., Hesegawa, Y., 1962. Discovery of the fossil giant salamander (*Megalobatrachus*) in Japan. Transactions of the Proceedings of the Paleontological Society of Japan, new series 45, 197–200.

Tempfer, M.A., 2004. *Andrias scheuchzeri* (Caudata: Cryptobranchidae) aus der obermiozänen (MN7/8) Fundstelle Mataschen/Steiermark. Joannea — Geologie und Paläontologie 5, 257–268.

Thenius, E., 1954. Über das Vorkommen von Riesensalamandern (Cryptobranchidae, Amphibia) im Unterpliozän (Pannon) des Wiener Beckens. Paläontologische Zeitschrift 28 (3/4), 172–177.

Thiel, C., Klotz, S., Uhl, D., 2012. Palaeoclimate estimates for selected leaf floras from the Late Pliocene (Reuverian) of Central Europe based on different palaeobotanical techniques. Turkish Journal of Earth Sciences 21, 263–287.

Tolstikova, N.V., Badamgarav, D., 1976. Freshwater gastropods from the lower Paleogene of Mongolia and southeast Kazakhstan. In: Kramarenko, N.N., Luvsandansan, B., Voronin, Yu.I., Barsbold, R., Rozhdestvensky, A.K., Trofimov, B.A., Reshetov, Yu, V. (Eds.), Palaeontology and Biostratigraphy of Mongolia (The Joint Soviet-Mongolian Paleontological Expedition, transaction vol. 3). Nauka, Moscow, pp. 145–150.

Utescher, T., Mosbrugger, V., Ashraf, A.R., 2000. Terrestrial climate evolution in Northwest Germany over the last 25 million years. Palaios 15, 430–449.

Van Itterbeeck, J., Missiaen, P., Folie, A., Markevich, V.S., Van Damme, D., Guo, D.-Y., Smith, T., 2007. Woodland in a fluvio—lacustrine environment on the dry Mongolian Plateau during the late Paleocene: evidence from the mammal bearing Subeng section (Inner Mongolia, P.R. China). Palaeogeography, Palaeoclimatology, Palaeoecology 243, 55–78.

Villa, G., Fioroni, C., Pea, L., Bohaty, S., Persico, D., 2008. Middle Eocene–late Oligocene climate variability: calcareous nannofossil response at Kerguelen Plateau, Site 748. Marine Micropaleontology 69, 173–192.

Wake, D.B., Roth, G., Wake, M.H., 1982. On the problem of stasis in organismal evolution. Journal of theoretical Biology 101, 211–224.

Westphal, F., 1958. Die Tertiären und rezenten Eurasiatischen Riesensalamander. Palaeontolographica Abt. A 110, 20–92.

Westphal, F., 1967. Erster Nachweis des Riesensalamanders (*Andrias*, Urodela, Amphibia) im europäischen Jungpliozän. Neues Jahrbuch für Geologie und Paläontologie — Monatshefte 67–73.

Westphal, F., 1970. Neue Riesensalamander-Funde (*Andrias*, Amphibia) aus der Oberen Süßwassermolasse von Wartenberg in Bayern. Mitteilungen der Bayerischen Staatssammlung für Paläontologie und historische Geologie 10, 253–260.

www.weather.com National and local weather forecast, hurricane, radar and Report. (accessed April 2010).

www.wrcc.dri.edu Western Regional Climate Center (accessed October 2010).

www.wunderground.com Weather underground. (accessed April 2010).

Xiao, G.Q., Abels, H.A., Yao, Z.Q., Dupont-Nivet, G., Hilgen, F.J., 2010. Asian aridification linked to the first step of the Eocene–Oligocene climate Transition (EOT) in obliquity-dominated terrestrial records (Xining Basin, China). Climate of the Past 6, 501–513.

4. Conclusions

This thesis explores the biology, biogeography, ecology, and systematics of both fossil and Recent giant salamanders (crown-clade Cryptobranchidae) using a broad range of approaches and methods. In the following, the main conclusions of the present investigations are summarized.

- A new osteological nomenclature for cranial and postcranial skeletal elements for the group has been proposed. Detailed study, description and comparison of the available osteological material of nearly all known fossil species shows that all cryptobranchid genera and species can be distinguished clearly based on osteological characters. Eurasian fossil and Recent giant salamanders are represented by 4 genera and at least 6 species. Those genera include *Aviturus* from the Paleocene of Mongolia, *Zaissanurus* from the Eocene and Oligocene of Kazakhstan, *Ukrainurus* gen. et sp. nov. from the Miocene of Ukraine, fossil *Andrias* from the Oligocene and Neogene of Western Eurasia and the Recent *Andrias* from Eastern Asia.
- Phylogenetic analysis of all well-understood Cenozoic and Recent giant salamanders recovers a monophyletic group of Asian and North American cryptobranchids. The phylogenetic analysis does not support the previously proposed intrafamiliar taxonomy (subfam. Aviturinae and Cryptobranchinae). The phylogenetic analysis places *Ukrainurus* gen. et sp. nov. outside crown Cryptobranchidae, they can be included into a clade Pancryptobrancha. The results suggest that Cryptobranchidae originated in Asia and dispersed to North America. The Mesozoic forms (*Chunerpeton*, *Eoscapherpeton*, *Horzemia*), previously referred to crown Cryptobranchidae, should be placed outside of Pancryptobrancha along the cryptobranchid stem lineage. *Ulanurus fractus* from Paleocene of Mongolia is considered to be a junior synonym of *Aviturus exsecratus*.
- The majority of fossil giant salamanders (*Zaissanurus*, *Andrias*, *Ukrainurus*) have strictly aquatic lifestyle and obligate paedomorphic life history strategy. Characters such as rates of bone ossification, vomerine dentition pattern, developmental grade of the cranial vault, femur and vertebrae morphology etc., allow to draw conclusion about the life history strategy and lifestyle of this group. *Aviturus*

from the Paleocene-Eocene Thermal Maximum of Mongolia shows a non-typical ecology and biology within Cryptobranchidae: peramorphic life history strategy and partially terrestrial (amphibious) lifestyle. It shows numerous adaptations for a terrestrial lifestyle but retains also aquatic adaptations. *Aviturus* in not only the sole example of pronounced peramorphosis among giant salamanders but also among crown-group lissamphibians. Giant salamander genera feed by prehension or suction whereas only *Aviturus* was able to feed by tongue protraction. Movement of the lower jaw during feeding in cryptobranchids is bilaterally asymmetric. *Aviturus* and *Ukrainurus* show strongest development of skull musculature, i.e. increased biting force in comparison with other genera.

- Giant salamanders are recorded in a total of 53 Cenozoic localities ranging from Central Europe to Central Asia. Their fossil record is mainly restricted to two basins – the North Alpine Foreland Basin (17 loc.) and the Zaisan Basin (15 loc.). Due to stability of their climatic space, fossil cryptobranchids can be used as an excellent palaeoclimatic proxy, indicating humid to very humid climates, with MAP ≥ 900 mm. The patchy stratigraphic distribution of the fossil record can be explain by habitat tracking and/or range expansion from higher altitudes into lowland settings during humid periods (increase in precipitation) with increased basinal relief (tectonic activities). Taking this into account we assume that Central European and Central Asian giant salamanders lived permanently in mountain habitats of the Alpine Orogene (during the Neogene) and Altay Mountains (Eocene to Miocene), respectively. They colonized lowland basins only during periods of significantly elevated humidity and increased basinal relief.

5. Outlook

Cryptobranchids have been an object of research for nearly three centuries. Numerous studies have documented their anatomy, osteology, and biology, but also raised new questions. Thus, my work is not the first and will not be the last effort to understand the fossil giant salamanders. Of course, the present study finds answers to many questions left open in previous studies but also raises new ones. Some of the most salient and contemporary questions rising from the present study are detailed below.

Fossil material of the Neogene giant salamander taxon from Kazakhstan *Andrias karalchepaki* was not available for the present study. It plausibly represents the descendants of the Paleogene genus *Zaissanurus* and, at the same time (assuming that the generic assignment is correct), would be the oldest Asiatic ancestors of the genus *Andrias*. It could be an important fossil for interpreting the origin of the Recent *Andrias* ssp. in Eastern Asia. Giant salamanders have no fossil record in the areas of their present distribution in Eastern Asia (China and Japan). The fossil relatives and ancestors of the Recent *Andrias* spp. are still unknown from the Cenozoic deposits. Most probably the cause is to be found in taphonomic or sampling biases.

Further enlargement of our knowledge regarding the developmental strategy and lifestyle of some fossil giant salamanders (e.g., *Andrias*, *Zaissanurus*) can be achieved by recovering and studying more bone material, like cranial vault bones, complete specimens with vertebral column and appendicular skeleton etc., as well as isotopic analysis. The latter will be also applicable for *Aviturus*, to ascertain the degree of terrestrialization of this taxon.

The current study focuses on Eurasian giant salamanders, whereas the treatment of the North American record was very cursory. A next important step would be the systematic study of the latter. This would reveal the Cenozoic diversity of the group outside of Eurasia as well as allow better understanding of the phylogenetic relationships, affiliations and origin of the Northern American and Asiatic clades, as well as ecological and biological adaptations of those forms.

A further issue requiring detailed investigation is the pre-Paleogene fossil record of the group. As mentioned in the conclusions, *Chunerpeton* and other Mesozoic salamanders should be placed outside of Pancryptobrancha. Thus, new fossil finds of this group will shed light on the time and place of origin of the stem giant salamanders, as well as split of Cryptobranchidae and Hynobiidae. This fossils should be found in the pre-Paleogene sediments, as this split most probably occurred in the Mesozoic. Evidence for this hypothesis is the occurrence of both families in the early Cenozoic: the late Paleocene record of *Aviturus* (this work) and a probable hynobiid (author's unpub. data.) find from the late Paleogene of Inner Mongolia, China (Itterbeeck et al., 2007, fig. 9.8-10).

6. Acknowledgement

First I want like to thank Prof. Dr. Madelaine Böhme and Prof. Dr. Hervé Bocherens for supervising and support during my work on the thesis, inspiring and encouraging me with this topic, as well as patience and spending endless hours for constrictive discussions, interpreting the data, which increase not only the quality of my work but also my professional competence.

I am grateful to Prof. Dr. Walter Joyce, Dr. Viacheslav Chkhikvadze, Dr. Yurij Semenov and Dr. Michael Winklhofer for collaboration and their valuable contributions to the research. The special thanks to Prof. Dr. Frank Westpahl and Dr. Rainer Schoch for constructive comments and productive discussions about the ontogeny of salamanders. I thank Dr. V. Chkhikvadze for making possible the study of the unpublished collection material on *Zaissanurus beliajevae*, Dr. Yurij Gubin for the material on *Aviturus exsecratus*, Dr. Michael Rummel and Dr. Jérôme Prieto for the material on *Andrias scheuchzeri*. I am indebted to Riederle brothers and Thomas Hiller for the cooperation and the access to study the exceptional fossil material of giant salamander from NAFB from their collections.

Many thanks to the master craftsmen – Hans Luginsland for the preparation of the fossil material; Wolfgang Gerger for his time and production of the perfect photographs of the fossil bones; Per Jeisecke for producing the cross-sections of the fossil bones, as well as Erwin Schwaderer for computer tomography of fossil and Recent cryptobranchid bones. I am much indebted to Prof. Dr. W. Joyce and Dr. Krister Smith for the linguistic revisions. Further I want to thank my friends and colleagues, especially all colleagues of our working group “Terrestrial palaeoclimatology” encouragement and support, discussions and help in research.

I am most grateful to my parents and my brother for helping to realize my own potential and showing another – non-scientific sides of the life.

ՇՆՈՐՀԱԿԱԼՈՒԹՅՈՒՆ

7. References

Amphibiaweb. Amphibiaweb: Information on amphibian biology and conservation. AmphibiaWeb, Berkeley, California. Retrieved Aug 08.

Böhme, M., and A. Ilg. fosFARbase. Available at www.wahre-staerke.com. Retrieved December 1, 2011.

Böttcher, R. 1987. Neue Funde von Andrias scheuchzeri (Cryptobranchidae, Amphibia) aus der süddeutschen Molasse (Miozän). Stuttgarter Beiträge Naturkunde Serie B 131:38.

Chernov, S. A. 1959. Reptiles, Volume 18. Academy of Sciences Tajik SSR, Stalinbad, 202 pp.

Chkhikvadze, V. M. 1982. On the findings of fossil Cryptobranchidae in the USSR and Mongolia. Vertebrata hungarica 21:63-67.

Cundall, D. J., J. Lorenz-Elwood, and J. D. Grooves. 1987. Asymmetric suction feeding in primitive salamanders. Experientia 43:1229-1231.

Duellman, W. E., and L. Trueb. 1994. Biology of Amphibia. The Johns Hopkins University Press, Baltimor, London, 670 pp.

Estes, R. 1981. Gymnophiona, Caudata, Handbuch der Paläoherpetology – Encyclopedia of Paleoherpetology. Gustav Fischer, Stuttgart, New York.

Fitzinger, L. 1826. Neue Classification der Reptilien nach ihrer natürlichen Verwandtschaft. J. G. Heubner Wien, 66 pp.

Gao, K. Q., and N. H. Shubin. 2003. Earliest known crown-group salamanders. Nature 422:424-428.

Greven, H., and G. Clemen. 1980. Morphological Studies on the Mouth Cavity of Urodeles. Amphibia-Reptilia 1:49-59.

Greven, H., and G. Clemen. 2009. Early tooth transformation in the paedomorphic Hellbender Cryptobranchus alleganiensis (Daudi, 1803) (Amphibia: Urodela). Vertebrate Zoology 59:71-79.

Gubin, Y. M. 1991. Paleocene salamanders from Southern Mongolia. Paleontologicheskij Zhurnal:96-106.

Holl, F. 1831. Handbuch der Petrefaktenkunde. P.G. Hilscher'sche Buchhandlung, Dresden, 489 pp.

Holman, A. J. 2006. Fossil salamanders of North America. Indiana University Press, Bloomington, Indianapolis, 232 pp.

Leu, U. 1999. Geschichte der Paläontologie in Zürich; pp. 11-76, Paläontologie in Zürich. Fossilien und ihre Erforschung in Geschichte und Gegenwart. Zoologisches Museum der Universität Zürich, Zürich.

Marjanović, D., and M. Laurin. 2007. Fossils, Molecules, Divergence Times, and the Origin of Lissamphibians. Systematic Biology 56:369-388.

Matsui, M., E. Kitabayashi, K. Takahashi, and S. Sato. 2001. A fossil giant salamander of the genus Andrias from Kyushu, Southern Japan. Research Reports Lake Biwa Museum 18:72-28.

Matsui, M., A. Tominaga, W.-z. Liu, and T. Tanaka-Ueno. 2008. Reduced genetic variation in the Japanese giant salamander, Andrias japonicus (Amphibia: Caudata). Molecular Phylogenetics and Evolution 49:318-326.

Meyer, H. v. 1845. Zur Fauna der Vorwelt: Fossile Saeugethiere, Voegel und Reptilien aus dem Molasse-Mergel von Oeningen. Schmerber & Keller, Frankfurt am Main, [1] Bl., VI pp.

Mickoleit, G. 2004. Phylogenetische Systematik der Wirbeltiere. Dr. Friedrich Pfeil, München, 672 pp.

Nessov, L. A. 1981. Cretaceous salamanders and frogs of Kyzylkum Desert. Proceedings of the Zoological Institute of Academy of Sciences of the USSR 101:57-88.

Nickerson, M. A., and C. E. Mays. 1973. The Hellbenders: Northe American "Giant salamanders". Milwaukee Public Museum, California University, 106 pp.

Pyron, A. R., and J. J. Wiens. 2011. A large-scale phylogeny of Amphibia including over 2800 species, and a revised classification of extant frogs, salamanders, and caecilians. Molecular Phylogenetics and Evolution 61:543-583.

Reese, A. M. 1906. Anatomy of Cryptobranchus allegheniensis. The American Naturalist 40:287-326.

Rose, C. S. 2003. The developmental morphology of salamander skulls; pp. 1684-1781 in H. Heatwole and D. Margaret (eds.), Amphibian Biology. Davis M. Surrey Beatty & Son, Chipping Norton.

Scheuchzer, J. J. 1726. Homo diluvii testis.

Sever, D. M. ed 2003. Reproductive biology and phylogeny of Urodela. Science Publishers, Enfield, 624 pp.

Siebold, P. F. 1838. Fauna Japonica: reptilia elaborantibus C.J. Temmink et H. Schlegel, Volume 3. La Lau, 144 pp.

Skutschas, P. P. 2009. Re-evaluation of Mynbulakia Nesov, 1981 (Lissamphibia: Caudata) and description of a new salamander genus from the Late Cretaceous of Uzbekistan. Journal of Vertebrate Paleontology 29:659-664.

Sonnini, C. S., and P. A. Latreille. 1802. Histoire naturelle des reptiles : avec figures dessinées d'apres nature, Volume An X. Imprimerie de Crapelet, Paris, 280 pp.

Temminck, C. J. 1836. Coup d'Oeil sur la Fauna des Îles de la Sonde et de l'Empire du Japon. Discours Préléminaire Destiné à Servir d'Introduction à la Faune du Japon. Müller, Amsterdam, 144 pp.

Tleuberdina, P. A. 2005. Main stages of development of vertebrates fauna in Cenozoic of Kazakhstan. Transactions of Institute of Zoology 49:12-37.

Tschudi, I. J. 1837. Über Homo diluvii testis, Andrias Scheuchzeri. Nees Jhrbuch für Mieralogie, Geognosie, Geologie und Petrefaktenkunde 1837:545-547.

Vitt, L. J., and J. P. Caldwell. 2009. Herpetology: An introductory biology of amphibians and reptiles. 3. ed. Edition. Academic Press Elsevier, London, XIV, 697 pp.

Westphal, F. 1958. Die Tertiären und Rezenten Eurasiatischen Riesensalamander (Genus Andrias, Urodela, Amphibia). Palaeontographica A 110:20-92.

Westphal, F. 1967. Erster Nachweis des Riesensalamanders (Andrias, Urodela, Amphibia) im europäischen Jungpliozän. Neues Jahrbuch für Geologie und Paläontologie - Monatshefte 1967.

Westphal, F. 1970. Neue Riesensalamander-Funde (Andrias, Amphibia) aus der Oberen Süßwassermolasse von Wartenberg in Bayern. Mitteilungen der Bayerischen Staatssammlung für Paläontologie und historische Geologie 10:253-260.

Zerova, G. A. 1985: Preliminary results of studies on the Middle Sarmatian herpetofauna of Ukraine. Sixth herpteological conference, Tashkent, 1985.